National Library of Canada

Cataloguing Branch
Canadian Theses Division

Ottawa, Canada
K1A 0N4

Bibliothèque nationale du Canada

Direction du catalogage
Division des thèses canadiennes

NOTICE

The quality of this microfiche is heavily dependent upon the quality of the original thesis submitted for microfilming. Every effort has been made to ensure the highest quality of reproduction possible.

If pages are missing, contact the university which granted the degree.

Some pages may have indistinct print especially if the original pages were typed with a poor typewriter ribbon or if the university sent us a poor photocopy.

Previously copyrighted materials (journal articles, published tests, etc.) are not filmed.

Reproduction in full or in part of this film is governed by the Canadian Copyright Act, R.S.C. 1970, c. C-30. Please read the authorization forms which accompany this thesis.

THIS DISSERTATION
HAS BEEN MICROFILMED
EXACTLY AS RECEIVED

AVIS

La qualité de cette microfiche dépend grandement de la qualité de la thèse soumise au microfilmage. Nous avons tout fait pour assurer une qualité supérieure de reproduction.

S'il manque des pages, veuillez communiquer avec l'université qui a conféré le grade.

La qualité d'impression de certaines pages peut laisser à désirer, surtout si les pages originales ont été dactylographiées à l'aide d'un ruban usé ou si l'université nous a fait parvenir une photocopie de mauvaise qualité.

Les documents qui font déjà l'objet d'un droit d'auteur (articles de revue, examens publiés, etc.) ne sont pas microfilmés.

La reproduction, même partielle, de ce microfilm est soumise à la Loi canadienne sur le droit d'auteur, SRC 1970, c. C-30. Veuillez prendre connaissance des formules d'autorisation qui accompagnent cette thèse.

LA THÈSE A ÉTÉ
MICROFILMÉE TELLE QUE
NOUS L'AVONS REÇUE

UNIVERSITÉ D'OTTAWA
UNIVERSITY OF OTTAWA

THE OFF-SHELL BEHAVIOUR AND CONSTRAINTS ON THE $^1S_0$ TWO-NUCLEON TRANSITION MATRIX

by

Jennifer Tan

Submitted to the School of Graduate Studies
in partial fulfilment of the requirements
of the degree of Doctor of Philosophy.

Department of Physics
Faculty of Science and Engineering
University of Ottawa
Ottawa, Canada
1976.

.. to the memory of my Father

ABSTRACT

The complete off-shell T-matrix can be constructed from a real symmetric function $\sigma(k,k')$. Off-shell variations are generated by directly distorting the σ-function, or by parametrizing the two-body wave function in the interaction interior. The σ-function can then be obtained from a knowledge of this interior wave function. The resulting T-matrices for the ^1S_o channel are utilized to calculate the binding energies of nuclear matter, ^{16}O and ^{40}Ca. The sensitivity of the results to off-shell behaviour is studied. The variations are found to be appreciable, especially for nuclear matter. The interior wave function method produces a larger range of variation than the direct distortions. The wave function seems to be strongly correlated to the binding energies through the 'difference Integral'. By limiting the wave function to physically acceptable forms, the σ-functions can be restricted. The range of allowed wave functions and corresponding σ-functions is dependent on the assumptions made for the boundary conditions.

ACKNOWLEDGEMENTS

I would like to express my deepest gratitude to Professor R.J.W. Hodgson for suggesting this problem, and for his collaboration throughout the course of this study. I have been very fortunate in having the opportunity to work under his guidance.

I would like to thank Loretta Leroux and Lise Ménard for typing this thesis and Dr. Hodgson for proof-reading it. I am grateful to my husband for the encouragement and understanding given to me during the work.

Finally, I wish to thank the Ontario Graduate Scholarship and the National Research Council for grants in support of this work.

TABLE OF CONTENTS

LIST OF FIGURES

LIST OF TABLES

CHAPTER I INTRODUCTION

1.1 Purpose of Study

The two-nucleon transition matrix $T(\omega)$ is defined[1] in terms of the two-nucleon potential V as either

$$T(\omega) = V + V(\omega - K)^{-1} T(\omega) \tag{1.1}$$

or

$$T(\omega) = V + V(\omega - K - V)^{-1} V \tag{1.2}$$

where K is the kinetic energy. For an uncoupled partial wave and in the centre-of-mass system a T matrix element $\langle k| T(\omega) |k'\rangle$ is a function of three variables i.e. k, k' which are relative wave numbers (or momenta), and ω, which is a frequency (or energy). When all three variables are equal i.e. $\langle k | T(k^2) | k\rangle$, the T matrix element is said to be 'on the energy shell' or 'on shell'. When two of the variables are equal, i.e. $\langle k' | T(k'^2) | k\rangle$, $\langle k' | T(k^2) | k\rangle$, the T matrix element is 'half on and half off the energy shell' or 'half-shell'. When all these variables are not equal, the T matrix element $\langle k' | T(\omega) | k\rangle$ is completely 'off-shell'.

The T matrix has an established importance in nuclear physics. It is, unlike V, closely related to experiment . Its on-shell matrix elements are given by the scattering phase-shifts $\delta_o(k)$

$$\langle k | T(k^2 + io) | k\rangle = -\left(\frac{2k}{\pi}\right) \sin \delta_o(k) e^{i\delta_o(k)} \tag{1.3}$$

in a representation where the basis states are normalized to be

$$\langle r|k\rangle = (2/\pi)^{\frac{1}{2}} kr j_\ell(kr) \tag{1.4}$$

so that volume elements are simply dr and dk. Units are chosen so that $\hbar^2/m = 1$. $T(k^2 + i\omega)$ indicates that the underlying stationary wave function has an outgoing wave boundary condition.

The half-shell elements of T define the transition probability per unit time W_{fi} for a change in a system from an initial state i to all accessible final states f, i.e.

$$W_{fi} = (2\pi/\hbar)\ \rho(E_f)\,|T_{fi}|^2. \tag{1.5}$$

$$T_{fi} = \langle k_f|T(k_f^2)|ki\rangle\ , \qquad E_f = k_f^2$$

where $\rho(E_f)$ is the density of final states. This expression forms the second of Fermi's 'Golden Rules" and is of wide-ranging importance in nuclear physics. The amplitude for nucleon-nucleon bremsstrahlung is a function of the T matrix. In the simplified case of a thin-target bremsstrahlung process, the differential bremsstrahlung cross section is given by

$$d\sigma_B = \frac{L^3}{V_i}\ W_{fi} \tag{1.6}$$

where L^3 is the volume of a large box and V_i is the initial nucleon velocity.

Calculations of direct reactions such as inelastic scattering of nucleons by nuclei require the off-shell T matrix elements. Again, the differential cross section is given by the squared transition matrix elements.

The Reaction matrix or G matrix of Brueckner Theory may be obtained from the T matrix. It satisfies the Bethe-Goldstone equation

$$G(\omega) = V + VQ(\omega - K)^{-1} G(\omega) \tag{1.7}$$

where Q is the Pauli operator forbidding the scattering of two particles into the occupied states below the Fermi sea. Equations (1.7) and (1.1) are very similar except for Q, indicating that the reaction matrix is very closely related to the T matrix[1]. When the off-shell matrix element of $T(\omega)$ in equation (1.1) has the ω equivalent to the sum of the true self-consistent energies of the particles considered, not just the kinetic energies, then it would correspond to the G matrix element. The differences between the G matrix and the T matrix are the effect of the Pauli exclusion principle due to the presence of the other nucleon's and spectral corrections. The T matrix is therefore identical to the 'reference G matrix' from which the G matrix is calculated. The reaction matrix is vital in that it allows for the calculation of binding energies of nuclear matter as well as finite nuclei.

Properties of the three-nucleon system are determined by the T matrix which is used in the solution of the three-body problem via the Fadeev equations[3]. In this formulation, the expectation value of an operator $T(\omega - K)^{-1} F(\omega - K)^{-1} T$ is calculated. Here, T is a transition matrix involving two of the three particles and F is another transition matrix when one of those two particles watches as a spectator. Both transition matrices are therefore usually off the energy shell.

As one can see, the T matrix is a convenient, and at times necessary starting point for certain important calculations in nuclear physics. This natural course has not been attempted until the last few years. The common practice has been to do the calculations in terms of the potential V. The parameters of an assumed potential function are adjusted so that phase-shifts extracted from nucleon-nucleon elastic scattering experiments are fitted by a complicated process. By retracing this process backwards, the T matrix is then calculated from the potential model built. This roundabout method is wasteful of time and effort but popular. The reason is that V has a great virtue: it is very simple to decide what properties V must have in order to be acceptable. It must be hermitean. The direct approach has been avoided since it is not obvious at all to decide what type of T matrices are acceptable.

It has already been shown (equation (1.3)) that the on-shell T matrix elements are given by experimental phase-shifts directly. The pole of the T matrix is also given by the deuteron. The half-shell T matrix element is a measureable quantity, in principle[4,5]. In the three-body problem, the T matrix is a direct and transparent link between experimental two-nucleon data and the three-nucleon observables. The T matrix is therefore closely related to experiment whereas the potential is not.

Potentials which have identical fits to two-body data (or on-shell data) can disagree completely in many body calculations. This is because in the many-body situation, conservation of energy and momentum must be obeyed overall, but not necessarily in every two-body interaction.

The T matrix elements are much more closely related to many-body applications than the potential.

Once the off-shell transition matrix is determined experimentally, the complete T is known with no arbitrariness. This is only possible through a process having an interaction with known off-shell behaviour, in addition to the strong interaction. Proton-proton bremsstrahlung experiments ($p + p \rightarrow p + p + \gamma$) provide such a possibility, since the protons interact also with the electromagnetic field so that a photon is produced. Experimental information about the off-shell T-matrix elements can then be extracted since the off-shell amplitude of the electromagnetic interaction is known unambiguously. At the present stage, proton-proton bremsstrahlung experiments are not capable of delivering reliable information about off-shell transition matrix elements The off-shell part of T must then be parametrized. When one uses the potential, a particular off-shell behaviour has to be assumed first. This assumption is unclear because its nature is not made explicit. On the other hand, the T matrix can have its off-shell arbitrariness neatly isolated and the assumptions are clear right from the beginning. By using the T matrix instead of the potential, one can control and measure the off-shell behaviour more directly.

Phase-shift equivalent potentials can be generated by unitary transformations. They are equivalent in the sense that they all have the theoretically required one-pion-exchange tail and all fit the experimental data equally well. Off-shell behaviour has been studied using these phase-shift equivalent potentials[6,7,8]. Most of these potentials have been found to violate the charge-symmetry constraint with respect

to the effective range parameters and should therefore be rejected[9,10]. In this study, as shown later, generating the T matrix directly involves using nuclear effective range parameters which, by construction, are those of the Reid potential. The T matrix is then in sufficient agreement with charge symmetry and approximates charge independence.

The above arguments serve to stress the advantages of working with the T matrix over potentials which are only equivalent in their on-shell behaviour, but which have uncontrolled off-shell behaviour. The T matrix presents a logical and useful tool to study off-shell effects which in turn enable us to examine the physical constraints that must be applied to the parametrization of the unknown parts of the nuclear force.

1.2 Background

The aim of performing direct calculations of nuclear structure in terms of two-nucleon phase-shifts has long attracted theorists. It became one of the motivating ideas behind Brueckner theory[11], and later, behind the work of Bég and Peierls[12]. Practical methods for achieving this aim were developed by Kallio[13], Elliott et al[14] and Koltun[15]. In 1968, Elliott et al[16] used an auxiliary potential together with the two-body data to generate harmonic-oscillator matrix elements of a potential which need never be defined. The assumption that the on-shell T-matrix elements determine the entire T was generally accepted. Additional freedom associated with the half-shell and off-shell T were exploited by

Cromer and Sobel[17] in their study of proton-proton bremsstrahlung, and Kahana and Tomusiak[18] in their study of finite nuclei. In another approach, dispersion relations involving the scattering amplitude were employed by Razavy and Hodgson[19] to yield matrix elements similar to those used by Elliot et al. A similar approach was employed by Reiner[20] to generate off-shell T-matrices.

In yet another approach, Baranger et al.[1] and Haftel[21] constructed the fully off-shell T matrix from a symmetric function $\sigma(k',k)$ which contained the phase shift information in its diagonal elements. σ was a real but arbitrary function to be parametrized. Constraints which should be imposed on the σ function were examined by Van Dijk and Razavy[22]. The approach of Baranger et al. was generalized to include bound states. A further discussion was found in the work of Kowalski et al.[23]. It has been shown that the range and non-locality of the interaction place restrictive conditions on the off-diagonal elements of σ. Sauer[24] extended the approach of Baranger et al. to include tensor forces. In a subsequent study, Sauer[25] suggested a wide variety of parametrization of σ, and examined possible constraints to be imposed on its form. Shell model calculations for O^{18} and calculations of binding energies of nuclear matter and O^{16} exhibited a sensitivity to reasonable variations of the off-diagonal σ function.

Picker, Redish and Stephenson[26] advocated an alternative to Sauer's scheme of parametrizing the form of $\sigma(k',k)$ directly. The well-known aspects of the two-body interaction, i.e. the on-shell T matrix and the long-range tail of the potential are still retained.

Variations in the half-shell T matrix were investigated through a parametrization of the scattering wave function in the interaction region.

Running parallel to the investigations of practical methods to construct the T matrix directly are extensive studies[6-8, 27-43] into the parametrization of the unknown parts of the nuclear force by fitting a potential model to the experimental two-nucleon data. Off-shell changes in the interaction can be generated by means of unitary transformations which produce phase-shift equivalent potentials. These potentials are equivalent to each other in that they all have the theoretically required local one-pion exchange tail and must all account, together with the Coulomb force, for the experimental phase shifts in exactly the same way. The form of the unitary operator is parametrized to control the range of transformation and to generate off-shell variations. Phase-shift equivalent potentials of different types and varying non-locality (hard core, soft core, non-local and non-local separable) have been generated to study the off-shell behaviour of the S-state N-N interaction[28,29,30]. Short-range unitary transformations have also been used for the three nucleon bound state[34,35,38,39].

There are many possible forms for the unitary transformation (U) - the only condition being that $U \to 1$ faster than $1/r$ as $r \to \infty$. The main consideration for choosing a form of the transformation is that numerical calculations can be carried out easily. These transformations usually produce exotic structures in the contour pattern of the σ function used in the approach of Baranger et al.[25], implying arbitrarily complicated and hard to control off-shell behaviour. This disadvantage is avoided

using the σ function to control off-shell changes. Constraints such as charge symmetry can be violated by phase-shift equivalent potentials[9,10] whereas they are imposed on the σ function by construction since the effective range parameters are made to be those of the Reid potential.

There is extensive evidence in either approach, i.e. T-matrix or phase-shift equivalent potentials to demonstrate the sensitivity of nuclear structure properties to off-shell changes. This sensitivity is apparent for nuclear matter[6,7,8,25], the ground state of nuclei[25,33] and the shell model spectra[25,36]. The deuteron photodisintegration cross section was found to be sensitive to the off-shell T matrix[44]. In studies of the three nucleon system, the off-shell effects are much smaller[34,38,45]. Purely off-shell changes bring about a variation of around 8 MeV in the triton binding energy[38]. Studies discussed so far have dealt with the effects of various S-wave off-shell extrapolations on nuclear structure results. The $\ell = 0$ case is certainly most important and the effects most substantial but there are certain features, such as the spin-orbit splitting in finite nuclei, where P-waves are important. Recently, off-shell behaviour in P-waves has also been examined[42].

Nuclear structure results that are dependent on the choice of parametrization of the off-shell behaviour are important but not useful yet to determine the unknown nuclear force parameters. The basic many-body theory underlying the results - with the exception of the three-body system - is not completely reliable yet. The nuclear force, whose potential representation can become non-local at small distances, contains

many degrees of freedom to be determined from the results. Since the nucleon-nucleon interaction remains largely unknown, its parametrization demands constraints which are simple to implement and have solid physical meaning. More recent investigations have been devoted to this subject. Charge symmetry of the nuclear force has been employed as an off-shell constraint[9,10]. It was deduced that nuclear effective range parameters from proton-proton scattering data in the ^1S_o state without Coulomb interaction depend strongly on the unknown potential at small distances. Assuming that charge symmetry holds exactly, one may use the knowledge of the n-n and p-p scattering lengths (a_{nn} and a_{pp} respectively) to restrict the off-shell behaviour in the ^1S_o amplitude. Unitarily transformed potentials which are unable to yield the correct experimental value of the neutron-neutron scattering length while preserving the fit to proton-proton data have to be rejected. Transformed potentials which produce the correct neutron-neutron scattering length but are unable to account for the experimental proton-proton data have to be rejected as well. Charge symmetry as a constraint on off-shell effects in the three-nucleon system has also been investigated[43]. Off-shell variations are restricted to the extent that the binding energy of the triton (E_T) and the neutron-deuteron doublet scattering length (^2a) should lie on the Phillips line. Without any constraint on the off-shell behaviour of the ^1S_o T-matrix, there is a variation of about (2-3) MeV in E_T and 1.5 fm in ^2a. Imposing this constraint of the Phillips line does not significantly alter the amount of variation in E_T or ^2a.[43].

By tracing the interests in and developments of studies in off-shell effects, hopefully, the motivation of this study is brought into view.

1.3 Program of Dissertation

In the present study, Sauer's approach is followed in constructing the fully off-shell T matrix from the function $\sigma(k',k)$ and in parametrizing the form of σ. An alternative scheme to restrict σ is also studied, adapting from the work of Picker, Redish and Stephenson[26], hereafter referred to as PRS. Only the ^1S_o channel is investigated here. This one parameter model allows one to limit the form of σ inherently. Both approaches are compared in the calculations of binding energies of finite nuclei i.e. ^{16}O, ^{40}Ca and nuclear matter, as well as in nuclear structure results. Off-shell behaviour is examined in all cases and some insights into possible constraints are scrutinized.

Chapter 2 presents a general formalism in which the T-matrix is expressed in terms of the half-shell T,ϕ. ϕ is in turn determined by the σ-function. The Reaction G-matrix, being the input in nuclear structure calculations, is derived from the T-matrix. The theory of the σ-function is developed more fully in Chapter 3. The parametrization of σ and the uniform transformations that can be applied directly to it are discussed. Chapter 4 describes the theoretical formulation of the

interior wave function method in which the σ-function is obtained from a knowledge of the two-body wave function in the interaction interior. Uniform transformations are obtained by parametrizing the interior wave function. A step-by-step description of the calculational procedures involved is presented in Chapter V, from the construction of the σ-functions right up to the calculation of the binding energies of nuclear matter, ^{16}O and ^{40}Ca. Chapter VI gives a detailed analysis of the results obtained. Conclusions on the effects of the off-shell variations and on the plausible constraints are discussed. Finally, Chapter VII deals with the general conclusions that can be extracted from the entire study. Other ideas leading to a better control of the off-shell behaviour and to further restrictions on the form of σ are mentioned.

CHAPTER II GENERAL FORMALISM

In this study, a formalism based on a model, which is more or less the viewpoint of nuclear structure physics, is followed. In this model, the nucleons are considered as non-relativistic point particles interacting by a force which can be described by a non-relativistic potential. The formalism is therefore restricted to a non-relativistic, quantum mechanical description of the system. Since high energy phase shifts are unimportant for low energy calculations, meson thresholds are not considered. Therefore, the existence of mesons can be ignored except insofar as they are responsible for generating the NN force.

In the formalism used in the calculations of this study the two-nucleon partial wave being considered is assumed to have no bound state The bound state case requires a completely different treatment.

2.1 Transition Matrix T

The definition of T has already been given in section 1.1. T should obey two types of restrictions, i.e. restrictions based on meson theory, such as suitable range, one-pion exchange behaviour at large distances; and restrictions of the quantum mechanical nature with the assumption that a potential V exists. Restrictions of the latter type must be considered in this formalism while the former type, being less stringent, can be added on later. Therefore, relativistic effects,

nucleon form factors, and meson currents can all be invoked later on as corrections in specific circumstances where they show up.

The T matrix is given in the centre of mass system and in the momentum-space representation. To define the T matrix, the two-body scattering problem must be examined.

Starting from the two-body Schrödinger equation of the centre-of-mass system, we have:

$$(H - k^2)|\phi_k\rangle = 0 \tag{2.1}$$

or

$$\begin{aligned}(\nabla^2 + k^2)|\psi_k\rangle &= (k^2 - K)|\psi_k\rangle \\ &= V|\psi_k\rangle \quad ,\end{aligned} \tag{2.2}$$

where $k^2 = E$ is the relative energy in fm^{-2} and $K = -\nabla^2$ is the kinetic energy operator. Again, units are chosen such that $\hbar^2/m = 1$. The potential is assumed to have a finite range. $|\phi_k\rangle$ and $|\psi_k\rangle$ are scattering states.

The usual definition[46] of the transition matrix is then

$$\begin{aligned}\langle k'|T|k\rangle &= \langle k'|V|\psi_k^+\rangle \\ &= \langle k'|V|k\rangle + \langle k'|V(k^2 - K + i\varepsilon)^{-1}V|\psi_k^+\rangle\end{aligned} \tag{2.3}$$

where $|\psi_k^+\rangle$ is the wavefunction with an outgoing scattered wave. The off-shell continuation of equation (2.3) is

$$\langle k'|T(\omega)|k\rangle = \langle k'|V|k\rangle + \langle k'|V(\omega - K)^{-1}V|\psi_k^+\rangle \tag{2.4}$$

or

$$T(\omega) = V + V(\omega - K)^{-1} T(\omega) ,$$

and $$T(\omega) = V + V(\omega - K - V)^{-1} V$$

which are equations (1.1) and (1.2) in section 1.1 of Chapter I. Here, the Moller wave operator Ω is introduced to be:

$$|\psi_k^+\rangle = \Omega(k^2 + i\varepsilon)|k\rangle \tag{2.5}$$

Corresponding to equations (1.1) and (1.2) Ω has the following relations:

$$\begin{aligned} \Omega(\omega) &= 1 + (\omega - K)^{-1} V\Omega(\omega) \\ &= 1 + (\omega - K)^{-1} T(\omega) \\ &= 1 + (\omega - K - V)^{-1} V \end{aligned} \tag{2.6}$$

By taking the potential as composed of two parts V_1 and V_2, equations (2.6) lead to the useful two-potential formula

$$\begin{aligned} T(\omega) &= (V_1 + V_2)\Omega(\omega) \\ &= T_1(\omega) + \Omega_1^\dagger(\omega^*) V_2 \Omega(\omega) \end{aligned} \tag{2.7}$$

where $T_1(\omega)$ is the transition operator and $\Omega_1^\dagger(\omega^*)$ is the Hermitian conjugate of the wave operator for the interaction V_1 alone.

By carrying out the partial wave decomposition in the coordinate space representation, the Lippmann-Schwinger equation

$$|\psi_k^+\rangle = |k\rangle + (k^2 - K + i\varepsilon)^{-1} V|\psi_k^+\rangle \tag{2.8}$$

becomes[47] for any partial wave

$$\psi_k^+(r) = (2/\pi)^{\frac{1}{2}}\{ \hat{\jmath}_\ell (kr) + \int_0^\infty \frac{\hat{\jmath}_\ell(kr)\langle k'|T_\ell(k^2 + io)|k\rangle}{k^2 - k'^2 + io} k'^2 dk' \tag{2.9}$$

where $\hat{\jmath}_\ell(x) = xj_\ell(x)$ is the Ricatti Bessel function of the first kind. $\psi_k^+(r)$ satisfies the boundary condition that at large distances the wave function consists of a plane wave plus an outgoing spherical wave, i.e.

$$\psi_k^+(\vec{r}) \to \exp(i\vec{k}.\vec{r}) + f_E(\theta, \phi)\frac{e^{ikr}}{r}$$

where $f_E(\theta, \phi)$ is the elastic scattering amplitude. The potential in the ℓ^{th} partial wave is

$$\langle r|V_\ell|r'\rangle = \int\langle r|V|r'\rangle P_\ell(\cos\theta_{r,r'})d\Omega \tag{2.10}$$

The T_ℓ-matrix element satisfies the integral equation

$$\langle p|T_\ell(\omega)|q\rangle = \langle p|V_\ell|q\rangle + \int_0^\infty \frac{\langle p|V_\ell|k\rangle\langle k|T_\ell(\omega)|q\rangle k^2 dk}{\omega - k^2 + i0} \tag{2.11}$$

The phase shift $\delta_\ell(k)$ is determined by the asymptotic behaviour of $\psi_k^+(r)$:

$$\psi_k^+(r) \to (\frac{2}{\pi})^{\frac{1}{2}} e^{i\delta_\ell(k)} \sin\{kr - \tfrac{1}{2}\ell\pi + \delta_\ell(k)\} \tag{2.12}$$

which depends on the singularities of the integrand in eq. (2.9). At large distances, the pole at $k' = k + i0$ dominates, giving:

$$\psi_k^+(r) \to (\frac{2}{\pi})^{\frac{1}{2}}\hat{\jmath}_\ell(kr) - (\frac{\pi}{2})^{\frac{1}{2}}\langle k|T_\ell(k^2 + i0)|k\rangle e^{i(kr - \ell\pi/2)}/k$$

$$= (\frac{2}{\pi})^{\frac{1}{2}}\sin(kr - \ell\pi/2) - (\frac{\pi}{2})^{\frac{1}{2}}\langle k|T_\ell(k^2 + i0)|k\rangle e^{i(kr - \ell\pi/2)}/k, \tag{2.13}$$

where $\mathcal{H}^+_\ell(x) = x h^+_\ell(x)$ is the Riccati Hankel function for outgoing waves.

From equations (2.12) and (2.13), we can now see that

$$\langle k|T_\ell(k^2 + io)|k\rangle = -\left(\frac{2k}{\pi}\right) e^{i\delta_\ell(k)} \sin\delta_\ell(k) \tag{2.14}$$

which is the equivalent to equation (1.3) exactly.

Thus, the on-shell T matrix elements are given by the experimental phase shifts. The complete off-shell T matrix elements are given by the half-shell T matrix elements, which are equivalent to a complete knowledge of the wave function at energy k^2, through equation (2.9). This will be shown later.

The off-shell T matrix elements are not completely arbitrary. They are, for any Hermitian interaction, time-reversal invariant and satisfy off-shell two-body elastic unitarity[48]

$$\mathrm{Im}\langle k'|T(k^2 + io)|k''\rangle = -\frac{\pi}{2k}\langle k'|T(k^2 + io)|k\rangle \langle k''|T^*(k^2 + io)|k\rangle, \quad k^2 > 0 \tag{2.15}$$

Bound states and the unitary cut indicated by equation (2.15) provide the only singularities in the complex energy variable ($= k^2$) that lie on the physical sheet. The off-shell T elements must also obey these constraints, i.e. the completeness and orthonormality of the scattering states.

$$\int |\psi^+_k\rangle\, dk\, \langle\psi^+_k| = 1 \tag{2.16}$$

and

$$\langle\psi^+_k \mid \psi^+_{k'}\rangle = \delta(k - k'), \tag{2.17}$$

where δ denotes a delta function here.

This implies that the scattering, both on- and off-shell, is generated by a Hermitian Hamiltonian with scattering states satisfying

the Bethe-Goldstone equation[49].

$$(\nabla^2 + \omega)\,|\psi_k^+\rangle = Q V |\psi_k^+\rangle + (\omega - k^2)\,|k\rangle. \tag{2.18}$$

The complete off-shell T matrix elements are given by the half-shell T matrix elements which are denoted by $\phi(k, k')$. These are defined by Baranger et al.[1] to be:

$$\phi(k,k') = \langle k'|T(k^2 + i\varepsilon)|k\rangle\, e^{-i\delta_o(k)} \tag{2.19}$$

A real wave function is also defined

$$\langle k'|\psi_k^o\rangle = e^{-i\delta(k)} \langle k'|\psi_k^+\rangle$$

$$= \delta(k - k') \cos\delta(k) + \frac{P}{k^2 - k'^2}\, \phi(k,k') \tag{2.20}$$

where P indicates the principal value to be taken at the singularity. By this choice, the conditions of completeness and orthogonality ((2.16) and (2.17)) are further restricted to be:

$$WW^+ = 1$$
$$W^+W = 1 \tag{2.21}$$

where W is a real operator with matrix elements given by

$$\langle k'|W|k\rangle = \langle k'|\psi_k^o\rangle \tag{2.22}$$

If the exact stationary states ψ_q^o are used as intermediate states and the operator

$$\int dq\, |\psi_q^o\rangle \langle\psi_q^o| = 1$$

is placed between the V operators in the righthand side of equation (1.2), we get an expression for T.

$$\langle k'|T(\omega)|k\rangle = \langle k'|V|k\rangle + \int_0^\infty dq(\omega - q^2)^{-1} \phi(q,k') \phi(q,k) \tag{2.23}$$

or

$$\langle k'|T(\omega)|k\rangle = \langle k'|T(k^2 + io)|k\rangle + \int_0^\infty dq \{(\omega - q^2)^{-1} - (k^2 - q^2 + io)^{-1}\} \phi(q,k') \phi(q,k) \tag{2.24}$$

Equation (2.24) is derived from equation (2.23) by subtracting the same equation with ω replaced by $k^2 + io$. The complete off-shell T is now given by known quantities, since $\phi(q,k')$ and $\phi(q,k)$ can be calculated from the σ-function as the following section will demonstrate.

The Low equation can now be written as

$$\langle k'|T(\omega)|k\rangle = \phi(k,k') \cos \delta_o(k) + \int_0^\infty dq \{(\omega - q^2)^{-1} - P(k^2 - q^2)^{-1}\} \phi(q,k') \phi(q,k) \tag{2.25}$$

where ω can have any complex value.

To calculate potential matrix elements, ω is allowed to go to ∞ in equation (2.25).

$$\langle k'|V|k\rangle = \langle k'|T(\infty)|k\rangle = \phi(k,k') \cos \delta_o(k) - P \int_0^\infty dq(k^2 - q^2)^{-1} \phi(q,k') \phi(q,k) \tag{2.26}$$

Analytically, $\langle k'|T(\omega)|k\rangle$ has a cut along the positive real axis in the ω-plane[50]. This discontinuity is $-i\pi\omega^{-\frac{1}{2}}\phi(\omega^{\frac{1}{2}}, k')\phi(\omega^{\frac{1}{2}}, k)$

2.2 Half-Shell T Matrix

In the preceding section, the off-shell T matrix is shown to be determined by the half-shell T matrix ϕ, which is closely related to the scattering wave functions. ϕ then gives T more visible physical meaning by relating it to the scattering wave functions.

In the present formalism, $|\psi_k^o\rangle$ is the exact stationary state, $|\psi_k^+\rangle$ is a scattering state with an outgoing scattered wave and $|\psi_k^-\rangle$ is a scattering state with ingoing scattered wave. The normalization of $|\psi_k^o\rangle$ is the same as that of $|k\rangle$, namely,

$$\langle\psi_k^o \mid \psi_{k'}^o\rangle = \langle k|k'\rangle = \delta(k - k') \tag{2.27}$$

The scattering matrix element can be determined from elastic scattering by

$$\delta_{kk'} = \langle\psi_k^-| \psi_{k'}^+\rangle = e^{2i\delta_o(k)} \delta(k - k') \tag{2.28}$$

This vanishes unless $k = k'$ and gives the on-shell T matrix elements only in that case. It is now obvious why elastic scattering does not provide any information about the off-shell T-matrix.

In this study where only the ^1s_o partial wave is examined, the ^1s_o scattering wave functions are required to be orthogonal and complete; thus placing constraints on ϕ. $|\psi_k^+\rangle$ has the following asymptotic form in the coordinate representation

$$\langle r|\psi_k^+\rangle \sim (2/\pi)^{\frac{1}{2}} \sin\{kr + \delta_o(k)\} e^{i\delta_o(k)} \tag{2.29}$$

As seen from this expression, the scattering wave function has the form of the free particle wave function beyond the potential range, with a displacement given by the phase shift $\delta_o(k)$. $\langle r|\psi_k^-\rangle$ by time reversal is the complex conjugate of $\langle r|\psi_k^+\rangle$ and is therefore

$$\langle r|\psi_k^-\rangle = e^{-2i\delta_o(k)} \langle r|\psi_k^+\rangle \tag{2.30}$$

The wave functions are related by

$$\langle r|\psi_k^o\rangle = e^{-i\delta_o(k)} \langle r|\psi_k^+\rangle = e^{i\delta_o(k)} \langle r|\psi_k^-\rangle \tag{2.31}$$

real for all r.

Multiplying equation (2.8) by $\langle k'|V$ to the left, we get

$$\langle k'|V|\psi_k^+\rangle = \langle k'|V|k\rangle + \langle k'|V(k^2 - k + i0)^{-1} V|\psi_k^+\rangle \tag{2.32}$$

Comparing this equation with equation (1.1), it is immediately seen that:

$$\langle k'|V|\psi_k^+\rangle = \langle k'|T(k^2 + i0)|k\rangle \tag{2.33}$$

and similarly,

$$\langle k'|V|\psi_k^-\rangle = \langle k'|T(k^2 - i0)|k\rangle, \tag{2.34}$$

$$\langle \psi_k^-|V|k'\rangle = \langle k|T(k^2 + i0)|k'\rangle \tag{2.35}$$

The half-shell T matrix element is defined now as

$$\phi(k,k') = \langle k'|V|\psi_k^o\rangle = \langle \psi_k^o|V|k'\rangle \tag{2.36}$$

By equations ((2.31) - (2.36)):

$$\phi(k,k') = \langle k'|T(k^2 + i0)|k\rangle e^{-i\delta_o(k)}$$

$$= e^{-i\delta_o(k)} \langle k|T(k^2 + io)|k'\rangle$$

$$= \langle k'|T(k^2 - io)|k\rangle \; e^{i\delta_o(k)}$$

$$= e^{i\delta_o(k)} \langle k|T(k^2 - io)|k'\rangle \qquad (2.37)$$

So far, the off-shell ϕ has been defined. According to equation (1.3) and (2.37) the on-shell ϕ is given by

$$\phi(k,k) = -(2k/\pi) \sin \delta_o(k) \qquad (2.38)$$

To show how ϕ is related to the scattering states in momentum space, the following is presented. Equation (2.33) is substituted into equation (2.8) which is multiplied by $\langle k'|$ to give

$$\langle k'|\psi_k^+\rangle = \langle k'|k\rangle + (k^2 - k'^2 + io)^{-1} \langle k'|T(k^2 + io)|k\rangle \qquad (2.39)$$

This is then multiplied by $e^{-i\delta_o(k)}$ and $(k^2 - k'^2 + io)^{-1}$ is expressed as a sum of a principal value and a delta function. This yields:

$$\langle k'|\psi_k^+\rangle = \delta(k - k') \cos \delta_o(k) + P(k^2 - k'^2)^{-1} \phi(k,k') \qquad (2.40)$$

Because of this relationship, being given ϕ is the same as being given all the wave functions. ϕ is not arbitrary because the wave functions are not arbitrary. They must form an orthonormal and complete set since there are no bound states. However, it can be shown[65], with ϕ not being a symmetric function, that its symmetric part is arbitrary and determines its antisymmetric part.

The orthogonal operator in (2.22) is written as a sum of a

symmetric part and an antisymmetric part, i.e.

$$W = W_S + W_A \tag{2.41}$$

If we consider an n-dimensional vector space, W has n^2 matrix elements. Since there are $\frac{1}{2}n(n+1)$ orthonormality conditions, $\frac{1}{2}n(n-1)$ parameters are left. This is exactly the number of matrix elements in W_A.

Bloch and Messiah have shown[75] that any real antisymmetric matrix can be brought by an orthogonal transformation into a canonical form of fig. 2-1. The relationship between W_S and W_A are given by equation (2.21) which can be rewritten as

$$\begin{aligned} W_S^2 - W_A^2 &= 1 \\ W_A W_S - W_S W_A &= 0 \end{aligned} \tag{2.42}$$

If W_A is given arbitrarily then the representation can be changed to bring it into the canonical form (fig. 2-1). Equation (2.42) is satisfied by the symmetric matrix W_S of fig. (2-2). The signs of the two square roots inside the 2 x 2 submatrix must be the same for equation (2.42) to be satisfied. The relative signs in different submatrices are arbitrary. Of course, there is the minor restriction $|m_i| < 1$.

The above has served to prove that W_A can be given arbitrarily and W_S is then determined. If this holds true for n-dimensions, one can extrapolate for the continuous matrix $\langle k'|W|k\rangle$.

The symmetric part of ϕ is σ where

$$\sigma(k,k') = \tfrac{1}{2}\{\phi(k,k') + \phi(k',k)\}. \tag{2.43}$$

The on-shell elements of σ are equal to those of ϕ; hence,

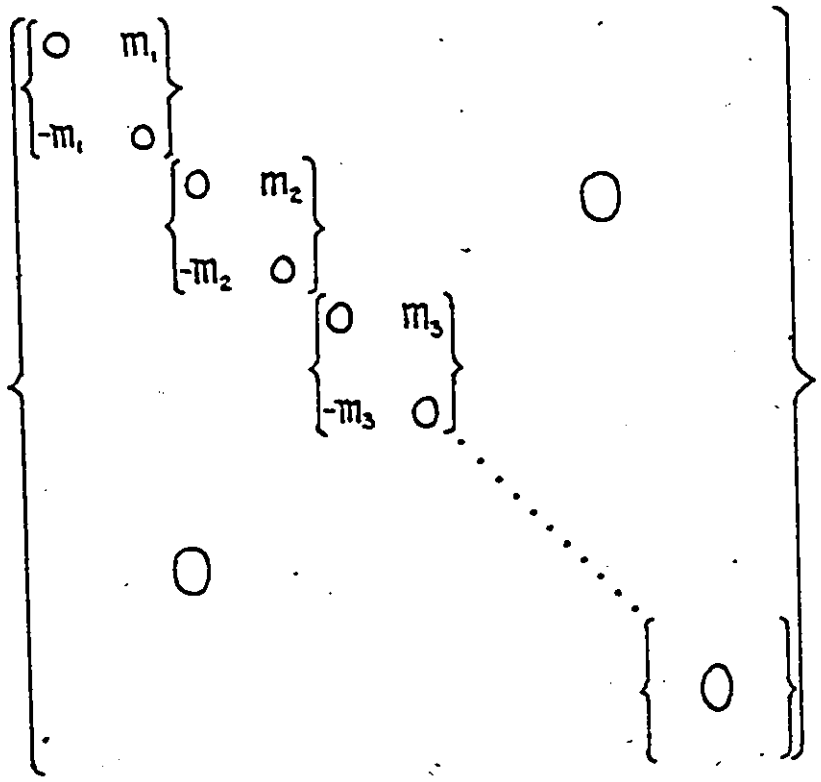

Fig. 2-1 Canonical form of an antisymmetric matrix

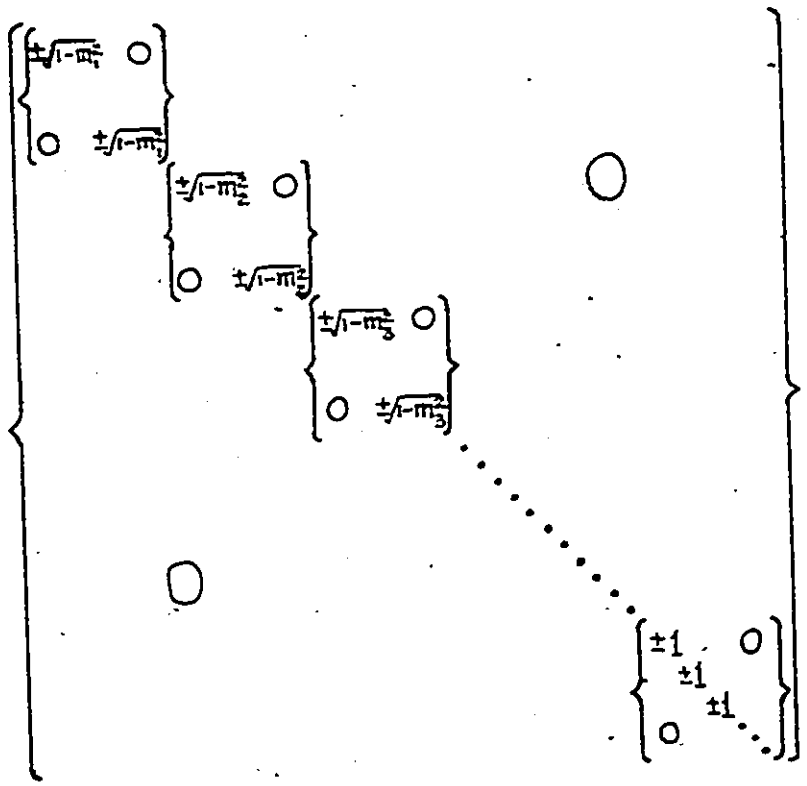

Fig. 2-2 Canonical form of a symmetric matrix

$$\sigma(k,k) = \phi(k,k) = -(2k/\pi)\sin\delta_o(k) \tag{2.44}$$

If ϕ is now written as the sum of a symmetric part σ and an antisymmetric part α i.e.

$$\phi(k,k') = \sigma(k,k') + \alpha(k,k') \tag{2.45}$$

then together with equation (2.42), equations (2.20) and (2.22) become

$$\langle k'|W_S|k\rangle = \delta(k - k')\cos\delta_o(k) + \alpha(k,k')/(k^2 - k'^2) \tag{2.46}$$

$$\langle k'|W_A|k\rangle = \frac{P}{k^2 - k'^2}\,\sigma(k,k') \tag{2.47}$$

W_A therefore contains only σ, which when given, determines α. Then the conditions (2.42), (2.46) and (2.47) completely determine $\phi(k,k')$. Since on-shell data give only $\sigma(k,k)$, the arbitrariness in the continuation of T off-shell is isolated as an arbitrariness in the off-diagonal elements of σ i.e. the symmetric part of T. The isolated form of arbitrariness now eliminates the tedious task of fitting to experimental data. A correct fit to the experimental phase shift is ensured by starting with σ instead of V to determine T. Off-shell variations can be generated by changes or distortions of the off-diagonal elements of σ.

2.3 Reaction Matrix G

The reaction matrix is essential in nuclear matter calculations as well as in the calculations of properties of finite nuclei. To discuss the reaction matrix in nuclear matter or finite nuclei calculations, one must do so in the light of Brueckner theory.

In the Brueckner theory of nuclear matter[51], the ground state is discussed as a Fermi gas with Fermi momentum k_F. The nucleons fill a sphere in momentum space up to k_F which is related to the density ρ of the system by $\rho = 2k_F^3/3\pi^2$. Since the nucleons move in a potential due to all the other nucleons, their energy is of the Hartree-Fock type rather than purely kinetic in character. The interaction between a pair of nucleons is represented by the G-matrix. Since both nucleons must scatter into unoccupied quantum states, the exclusion principle plays a central role. By introducing these considerations, the G-matrix is required to satisfy the Bethe-Goldstone Equation

$$G(\omega) = V + VQ(\omega - H_o)^{-1} G(\omega) \tag{1.7}$$

where ω is the 'starting energy', H_o the unperturbed hamiltonian, V the potential and Q the Pauli operator, which ensures the exclusion of scattering into occupied states. This equation is derived from the Schrödinger equation for a two-body system which is solved using the method of Green's functions[52]. The perturbation solution to equation (1.7) is easily obtained by successive approximation and is

$$G(\omega) = V + V \frac{Q}{(\omega - H_o)} V + V \frac{Q}{(\omega - H_o)} V \frac{Q}{(\omega - H_o)} V + \ldots\ldots \tag{2.48}$$

This series describes a succession of scattering by the potential V, the particles being propagated from interaction to interaction by the Green's function or propagation function $Q\{(\omega - H_o)^{-1}\}$.

In the Brueckner-Goldstone Theory, use is made of the Goldstone expansion[53], which is a linked-cluster perturbation series for the ground-state energy of a many-body system such as nuclear matter or a finite nucleus. The expression is:

$$E = E_o + \frac{\langle \Phi | H' | \Psi \rangle}{\langle \Phi | \Psi \rangle} \tag{2.49}$$

where E, the ground-state energy is the eigenvalue of the perturbation H'. E_o is the eigenvalue of the unperturbed Hamiltonian H_o. Φ is the ground-state eigenfunction of H_o and Ψ is that of the overall Hamiltonian H. $(H = H_o + H')$

The treatment of expression (2.49) is accomplished with the aid of Feynman type particle/hole diagrams. The perturbation calculation involves the summation of these diagrams. The sum is given for each pair of particles by the solution of an equation of the type

$$|\psi\rangle = |\phi\rangle - \frac{Q}{e} V|\psi\rangle \qquad \text{where } e = \omega - H_o \tag{2.50}$$

with

$$G(\omega)|\phi\rangle = V|\psi\rangle \tag{2.51}$$

where $|\phi\rangle$ is the unperturbed two-particle wave function and $|\psi\rangle$ the perturbed wave function.

The main term in the expansion of the binding energy of nuclear matter is the two particle cluster. Its Feynman-Goldstone diagram is shown in Fig. 2-3 and its value is

$$\tfrac{1}{2} \sum_{AB} \langle AB|G(\omega)|AB\rangle$$

where the G matrix includes exchange. A and B are two particles below the Fermi surface and the summation is over the entire Fermi sea. The factor of ½ takes into account the double counting.

The Brueckner theory of finite nuclei is in a much more 'fluid state' than that of nuclear matter. In nuclear matter calculations, one can rely on translational invariance to simplify matters. The single-particle wave functions are known a priori to be plane waves; the single-particle potential is only a function of momentum. In addition, momentum conservation eliminates many diagrams and greatly simplifies the calculations. In the case of finite nuclei, all this is not found. The form of the potential is unknown. In the calculation of the G matrix elements of nuclear matter, ω is calculated by a process of self-consistency. In finite nuclei, this problem is compounded by a self-consistency requirement of the single-particle potential. More of this will be discussed in a later chapter. In this study, the Brueckner self-consistent calculation is performed on ^{16}O and ^{40}Ca. The Bethe-Goldstone diagrams are shown in fig. 2-4.

The reaction matrix is obtained from the T matrix which differs from the G matrix by the Pauli correction (see Chapter 1)[54].

$$G(\omega) = T(\omega_{c.m.}) + T(\omega_{c.m.}) \{Q/[\omega - H_o(1) - H_o(2)] - 1/[\omega_{c.m.} - K_{rel}]\} G(\omega) \qquad (2.52)$$

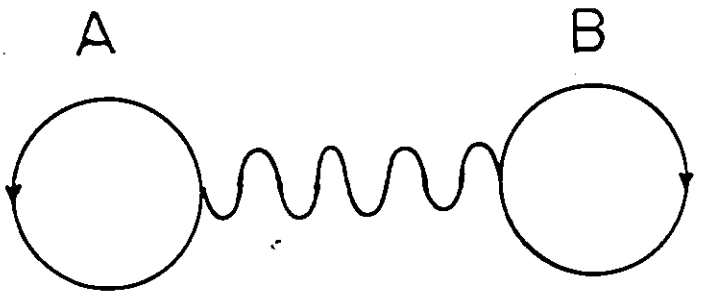

Fig. 2-3 Feynman-Goldstone diagram of binding energy of nuclear matter

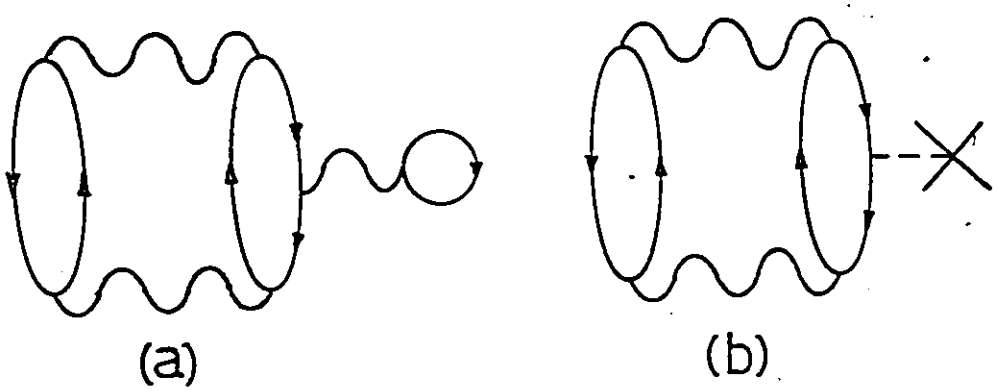

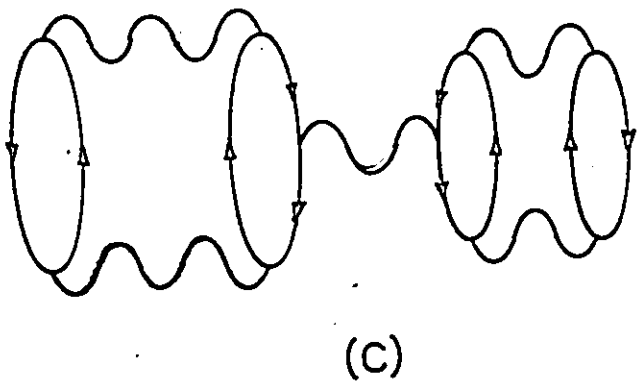

Fig. 2-4 Bethe-Goldstone diagrams of ^{16}O and ^{40}Ca

The single-particle Hamiltonian H_o is given by K + U where K denotes the single-particle kinetic energy (K_{rel} the kinetic energy of relative motion) and U the one-body potential. U is usually put to zero for particle states because the three-body clusters are assumed to be very small. This choice i.e. QUQ = 0 is also used in this calculation.

The transition matrix T ($\omega_{c.m.}$) is obtained as a one-body operator related to the relative motion of two nucleons. $\omega_{c.m.}$ represents any centre of mass dependence there is and is chosen to minimize the correction kernel in (2.52) stepping from $T(\omega_{c.m.})$ to $G(\omega)$. In contrast to T, $G(\omega)$ is a genuine two-body operator which is usually truncated to that of relative motion for computational convenience. It then retains a parametrical c.m. dependence only, just as T.

At this point, it is interesting to note that there is an analog to eq. (2.9) for the K-matrix elements, i.e.[47]

$$\psi_k^o(r) = \left(\frac{2}{\pi}\right)^{\frac{1}{2}} \{j_\ell(kr) + P\int_0^\infty \frac{j_\ell(k'r)\langle k'|K_\ell(k^2)|k\rangle}{k^2 - k'^2} k'^2 dk' \tag{2.53}$$

The K_ℓ matrix element is given by

$$\langle p|K_\ell(\omega)|q\rangle = \langle p|V_\ell|q\rangle + P\int_0^\infty \frac{\langle p|V_\ell|k\rangle\langle k|K_\ell(\omega)|q\rangle}{\omega - k^2} k^2 dk \tag{2.54}$$

The K-matrix which is real, is given by

$$K(\omega) = V - V\frac{P}{H_o - \omega}K(\omega), \qquad \omega = \text{real} \tag{2.55}$$

$$\langle k|K_\ell(k^2 + i0)|k\rangle = -\left(\frac{2k}{\pi}\right)\tan\delta_\ell(k) \tag{2.56}$$

K_ℓ has no cut from 0 to ∞ along the real axis in the ω-plane. It has poles in ω at the position of resonances and not on the unphysical sheet as is the case with $T_\ell(k)$[55].

In the method of Baranger et al. the partial wave channel without a bound state is the only case considered. The formalism does not hold for the case of a channel with a bound state because the bound state is a member of a complete set of scattering wave functions which do not form a complete set by themselves. The binding energy of the bound state plays a role equivalent to the phase shift in the asymptotic wave function of a scattering state.

Chapter III FORMALISM OF THE FUNCTION $\sigma(k, k')$

As we have seen in the previous chapter and in equation (2.44), the real symmetric function $\sigma(k, k')$ contains the phase-shift information as its diagonal part. Elastic experiments determine the diagonal elements up to about 400 MeV, i.e. 2.2 fm^{-1}. The Reid potential which is used in this study gives a fit up to 350 MeV. The off-diagonal parts of σ remain completely arbitrary. The problem then lies in imposing physical constraints to restrict its form. It is also recognised that there should be an intimate connection between the diagonal elements and off-diagonal parts of σ if the underlying interaction is purely local. What are then the physically acceptable forms of $\sigma(k, k')$? This problem was first examined by Sauer[24,25] who started from field theoretic considerations.

3.1 Field Theoretic Constraints on σ and subsequent Parametrization.

From field theory, two definite constraints must be imposed; (i) the nucleon-nucleon interaction is of short range, (ii) the tail of the interaction outside R = 3 fm is described by the local one-pion-exchange (OPE) potential[26].

With the theoretical information on the interaction known and the experimental phase-shifts provided, the two-body wave functions out-

side R can be calculated. Sauer[54] derived an analytic expression for the scattering wave functions of relative motion in the ^1S_o channel to be

$$\langle r|\psi_k\rangle = \left(\frac{2}{\pi}\right)^{\frac{1}{2}} \{\sin[kr + \delta(k)]$$

$$[1 + C(\mu)\int_{\mu}^{2\mu} d\alpha\ (\alpha^2 + 4k^2)^{-1} e^{-\alpha r}]$$

$$+ \cos[kr + \delta(k)]\ 2k\ C(\mu)$$

$$\int_{\mu}^{2\mu} d\alpha\ (\alpha^2 + 4k^2)^{-1}\ \alpha^{-1}\ e^{-\alpha r}\} \qquad (3.1)$$

where $r > R$ and μ is the inverse Compton wave length of the pion. $C(\mu)$ is a constant given by the strength of the OPE potential. The form (3.1) is valid to terms of the order $e^{-2\mu r}$. Any complete and orthogonal set of wave functions chosen to give a fit to the phase shifts must therefore have the required tail (3.1). However, Sauer[24,25] has shown that the OPE tail is insignificant for the ^1So σ function. The tail becomes completely masked by the full interior of the interaction which dominates the behavior of the σ function. There is no need to match the details of the wave function in the OPE region for the S waves. For higher partial waves, this has to be reassessed.

Field theoretic constraints can be more directly imposed on the half-shell T matrix element $\phi(k, k')$. In turn, conditions on the parametrization of σ can be worked out. Condition (3.1) disallows $\phi(k, k')$ in the complex k' plane to possess any pole at k' with $|\mathrm{Im}\ k'| < \mu$. The purpose of this is to avoid having admixtures to the asymptotic wave decaying slower than $e^{-\mu r}$. From field theory, it is known that σ must be

chosen to give an interaction range of the order μ^{-1} for the ^1S_o interaction. $\phi(k, k')$, according to Sauer, should not even contain complex singularities k' within the vicinity of less than μ from the real k' axis. These singularities can cause rapid variations in the real function values of $\phi(k, k')$. A sufficient but not necessary condition for $\sigma(k, k')$ over a short range is that it should vary smoothly over a distance μ everywhere.

There are two relations between ϕ and the wave functions. These are the Lippman-Schwinger equation:

$$\langle r|\psi_k\rangle = \langle r|k\rangle \cos\delta(k) + P \int_0^\infty dk' \langle r|k'\rangle (k^2 - k'^2)^{-1} \phi(k, k') \tag{3.2}$$

and the equation containing the momentum-space component of the free-scattering defect with respect to its asymptotic wave function[57],

$$\phi(k, k') = -\frac{2k'}{\pi} \sin\delta(k) + (k^2 - k'^2) \times \int_0^\infty dr \langle k'|r\rangle \{\langle r|\psi_k\rangle - (\frac{2}{\pi})^{\frac{1}{2}} \sin[kr + \delta(k)]\} \tag{3.3}$$

One can now incorporate the required properties of the symmetric part of an acceptable ϕ or σ. By choosing smooth parametrization for the remaining arbitrariness in σ, the antisymmetric part of ϕ (i.e. $\alpha(k, k')$) can also be made to comply with the above conditions. We have also seen that smooth off-shell extrapolations of σ can also keep the interaction range short.

Since in eq. (3.3) the contribution from the defect integral

increases with the interaction strength and decreases with the narrowing of the interaction range, Sauer estimated the free scattering defect at low energies to be

$$\langle r|\psi(k)\rangle - \left(\frac{2}{\pi}\right)^{\frac{1}{2}} \sin\left[kr + \delta(k)\right] = -\left(\frac{2}{\pi}\right)^{\frac{1}{2}} \sin\delta(k)\, e^{-\beta r} \tag{3.4}$$

with β^{-1} being of the order of the range μ^{-1}. After calculating the defect integral and $\phi(k, k')$ from eq. (3.3), the low-energy σ function is given by $\sigma(k, k') = 1/2\ (\phi(k, k') + \phi(k', k))$ and becomes:

$$\sigma_{ER}(k, k') = -\left(\frac{k}{\pi}\right) \sin\delta(k') \frac{(\beta^2 + k'^2)}{(\beta^2 + k^2)} - \left(\frac{k'}{\pi}\right) \sin\delta(k) \frac{(\beta^2 + k^2)}{(\beta^2 + k'^2)} \tag{3.5}$$

Sauer has shown that very different potentials with the same scattering length a and effective range r_o produce σ functions which are almost identical in the low energy region i.e. for k and k' less than μ (or 2.08fm^{-1}). Furthermore, if the potentials are local, the σ functions have very similar forms over a larger range. The low energy contours of σ's of these potentials are very similar to the zero-range limit of eq. (3.5) i.e. σ_o

$$\sigma_o(k, k') = -\left(\frac{k}{\pi}\right) \sin\delta(k') - \left(\frac{k'}{\pi}\right) \sin\delta(k) \tag{3.6}$$

in the limit $k, k' \ll \mu$.

In Fig. 3-1.5 standard ^1S_o potentials which reproduce the same low-energy form of σ are shown. The σ function (3.5) is similar to the effective range off-shell expansion of the T matrix given by Fuda[58] and Srivastava and Sprung[28]. It is in the low energy domain where the effec-

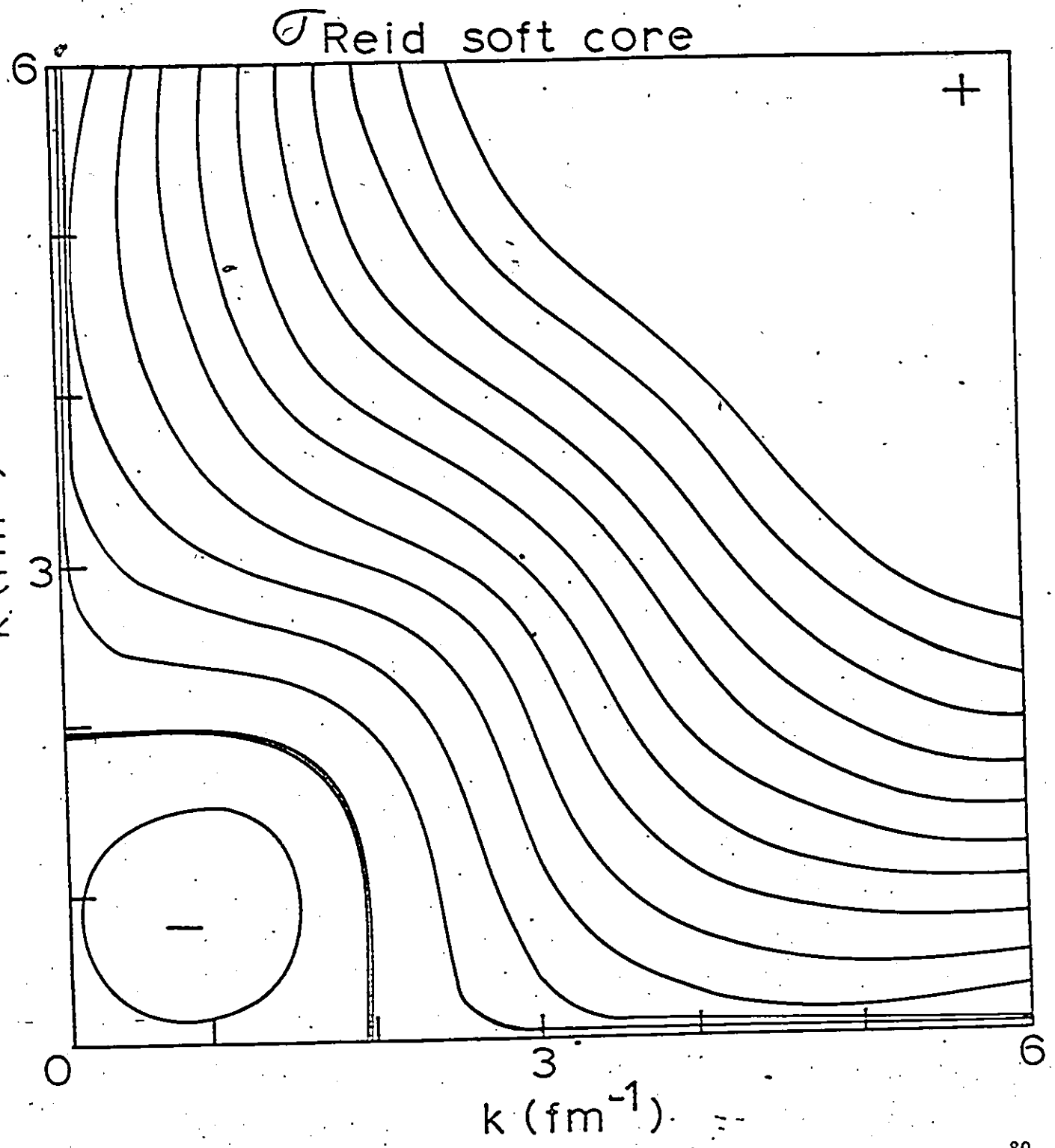

Fig. 3-1 (a) $\sigma(k,k')$ of the $^1S_0$ Reid Soft Core potential[80]. Equal-value contours are drawn in steps of 0.2 fm^{-1}. Heavy line denote zero-value contour. - and + denote the minimum and the maximum.

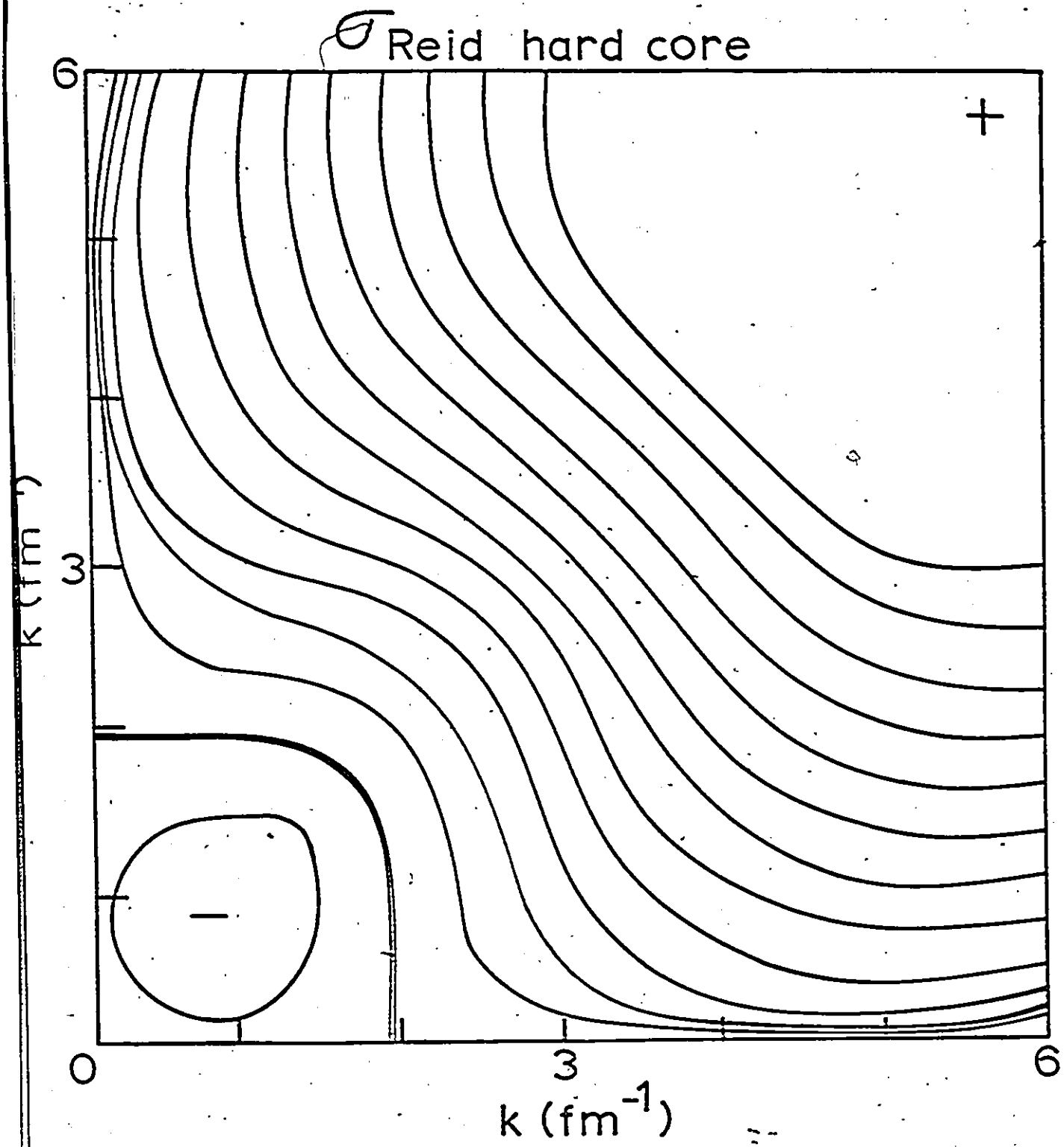

Fig. 3-1 (b) $\sigma(k,k')$ of the $^1S_0$ Reid Hard Core potential[80].

See fig. 3-1 (a) caption.

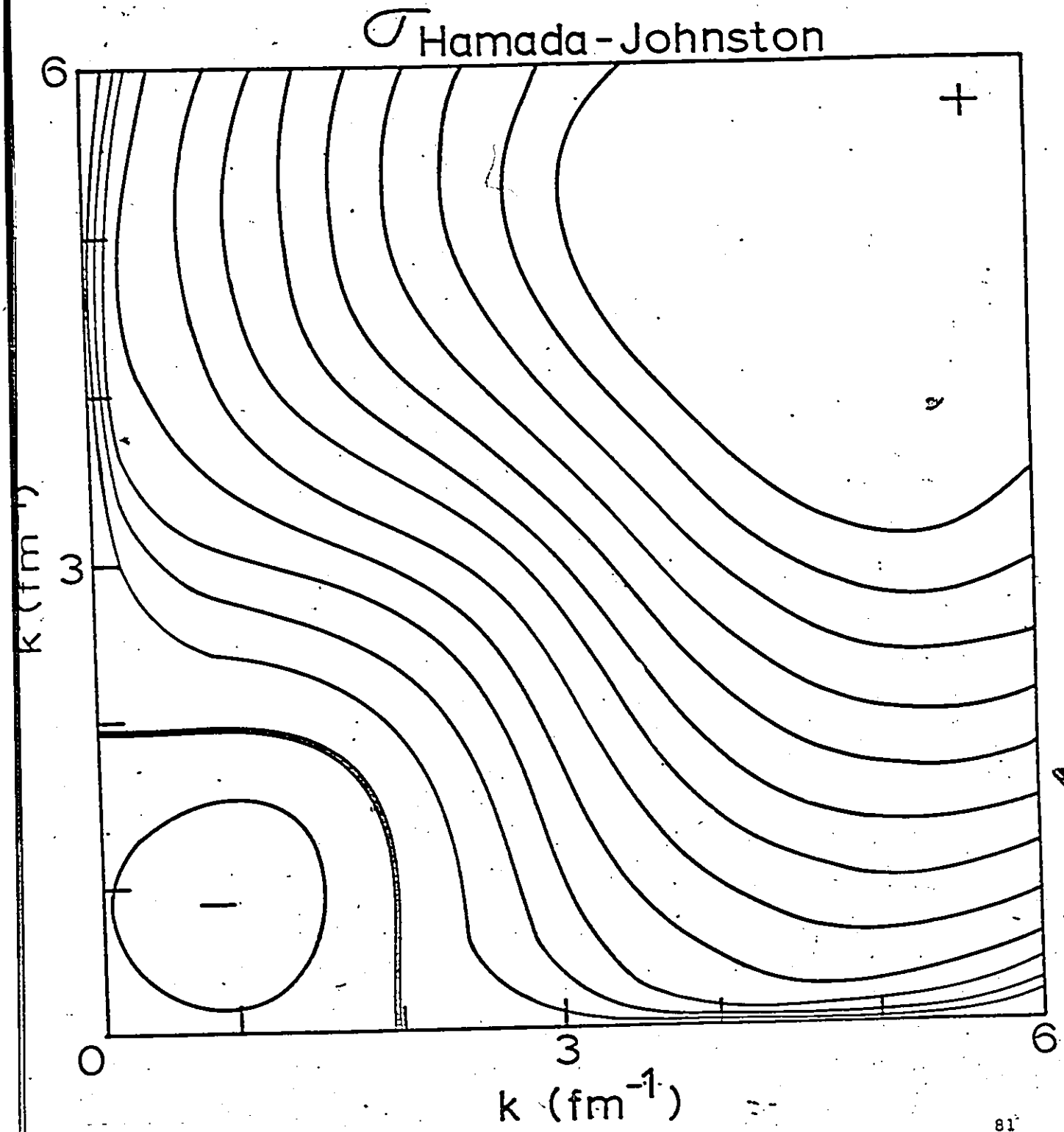

Fig. 3-1 (c). $\sigma(k,k')$ of the $^1S_0$ Hamada Johnston potential.[81]

See fig. 3-1 (a) caption.

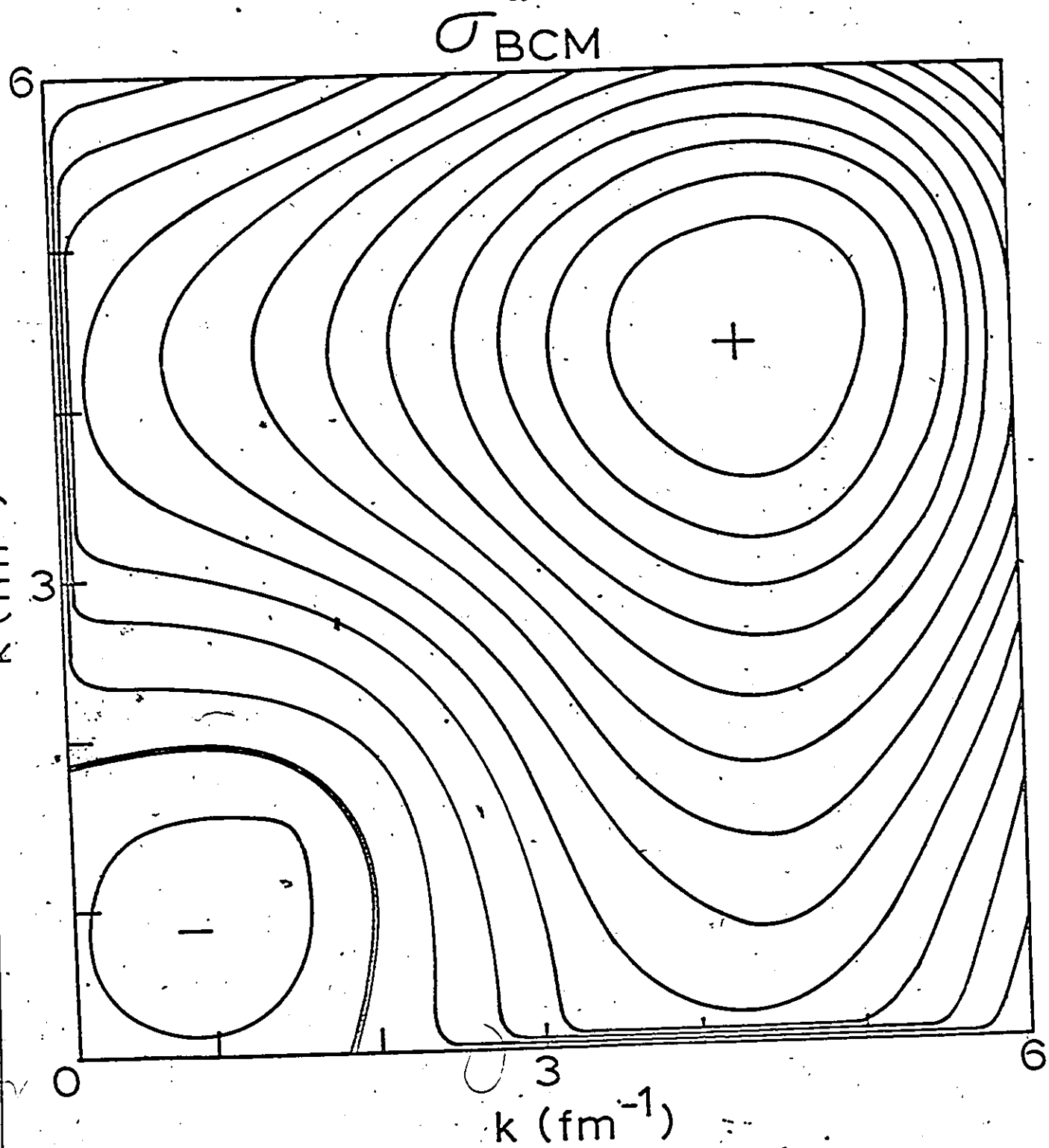

Fig. 3-1 (d) $\sigma(k,k')$ of the $^1S_0$ Boundary-condition model.[82] See fig. 3-1 (a) caption.

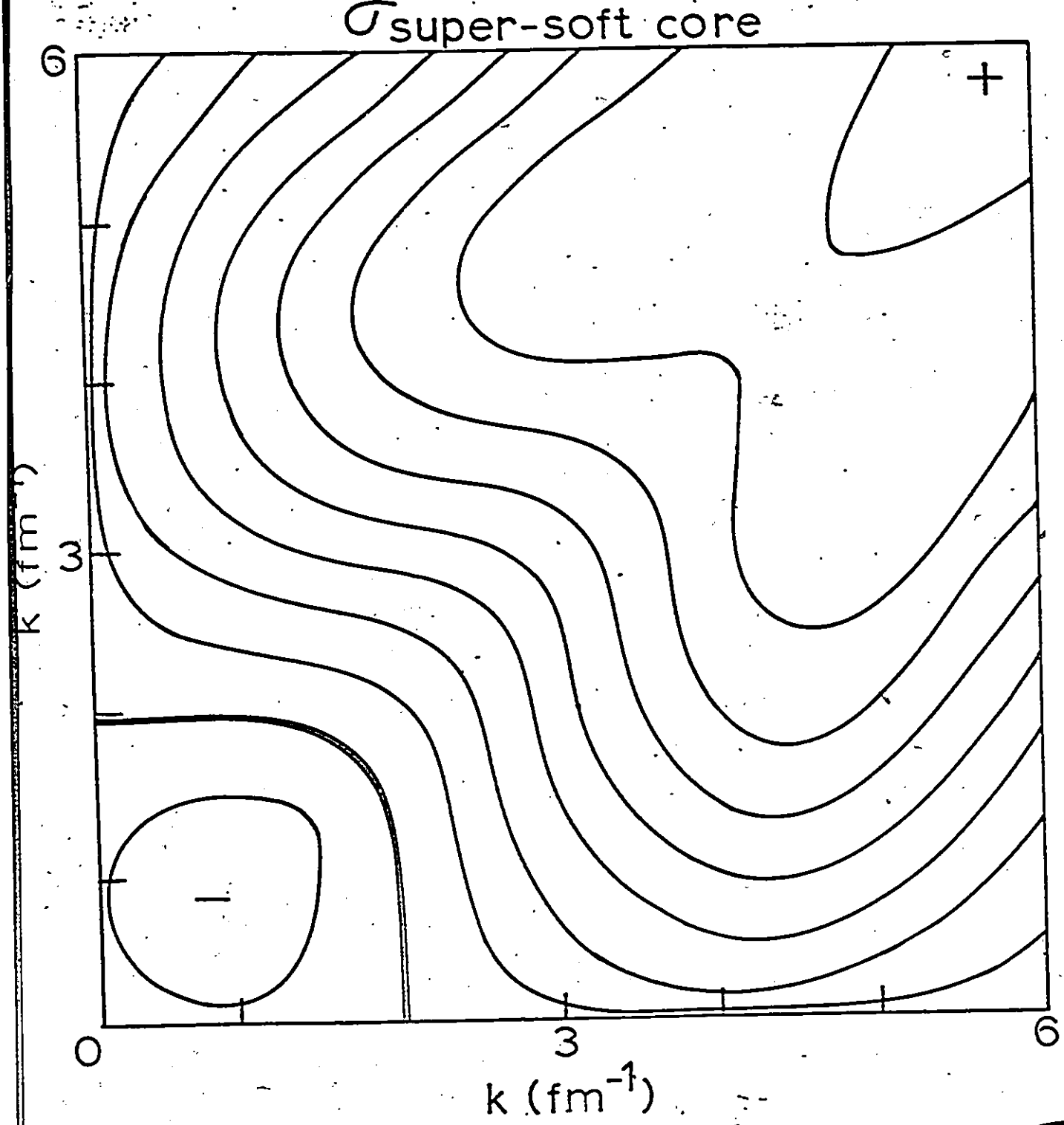

Fig. 3-1 (e). $\sigma(k,k')$ of the $^1S_0$ Super-soft-core potential.[83] See fig. 3-1 (a) caption.

tive-range expansion holds for the phase shift. In the ^1S_o partial wave, the effective-range expansion works well up to about 100 MeV below which the resonance is dominating. The resonance in ^1S_o occurs at almost zero energy as seen in Fig. 3-2. It seems to determine the σ function in the low-energy region, which is then uniquely given by the effective-range parameters. The resonance also imposes the constraint on any distortions of the σ function that they should not alter the contour of the low-energy region. Any σ parametrization in the ^1So partial wave should therefore contain σ_{ER} for low energies and σ_o for $k, k' \ll \mu$. Otherwise, the resonance may be treated in an arbitrary fashion, and the range of the interaction can turn out to be far too large.

In view of the fact that the low-energy σ functions of short-ranged interactions corresponding to the same effective-range phase-shift are approximately unique, Sauer has chosen the σ function of the Yamaguchi potential as a low-energy parametrization. It is convenient because it is the σ function of eq. (3.5) i.e. σ_{ER}, given completely by the effective-range parameters:

$$k \cot \delta_{ER}(k) = 1/a + 1/2\, r_o k^2 - \rho\, r_o^3\, k^4 \tag{3.7}$$

$$\beta^{-1} = (3/8)\, a \left[1 - (1 - (16/9) r_o/a)^{1/2}\right] \tag{3.8}$$

$$\rho r_o^3 = (1/6\beta^3)\left[(2/a\beta) - r_o\beta\right] \tag{3.9}$$

where β^{-1} is approximately $1/3\, r_o$. σ_{ER} decreases rapidly for large energies allowing the σ function to be easily corrected on-shell and off-shell when the actual phase-shift δ deviates from δ_{ER}. σ_{ER} also contains the resonating part of the σ function. One type of σ parametrization

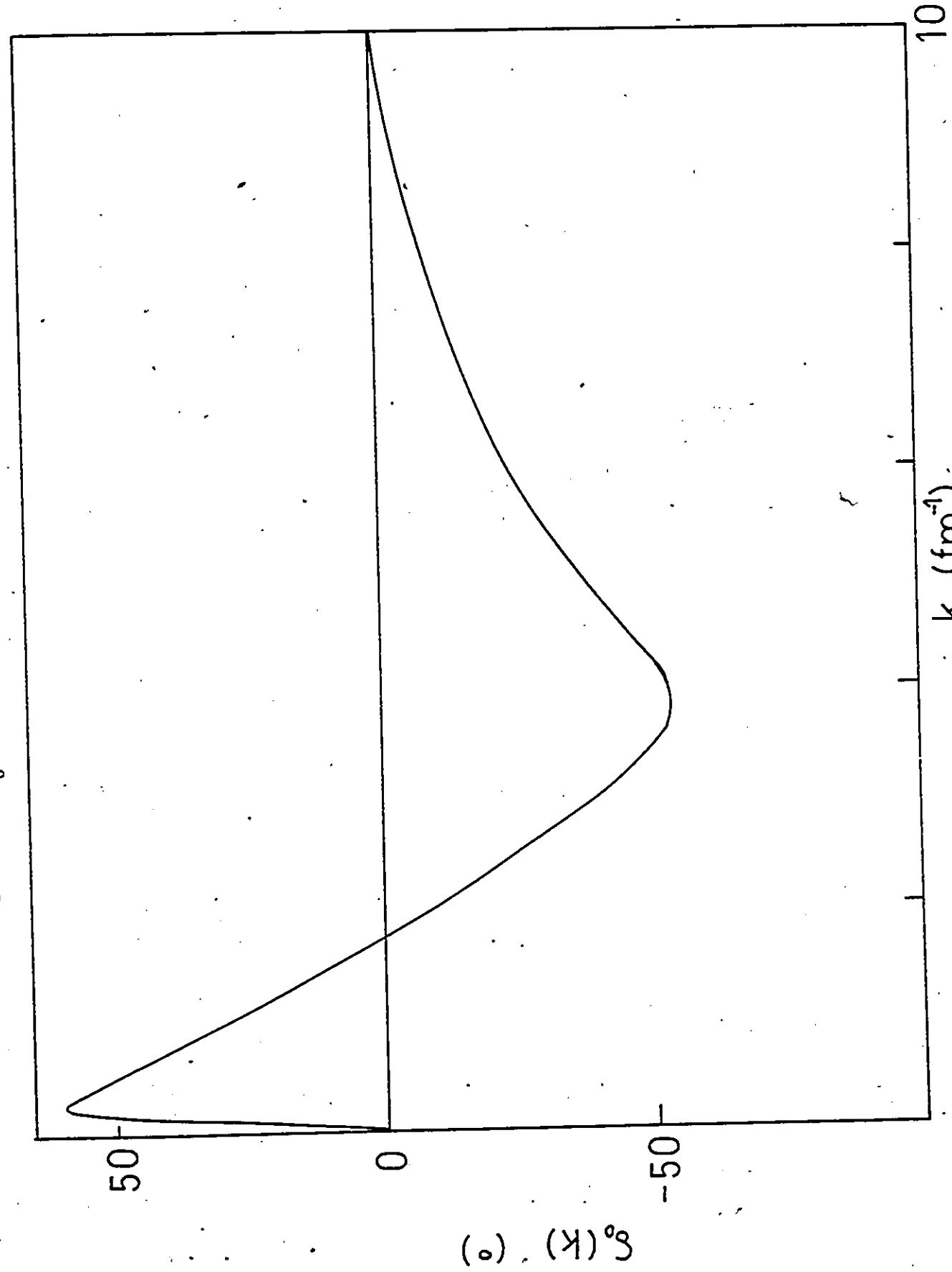

Fig. 3-2 $^1S_0$ phase shift $\delta_0(k)$

that is suitable is

$$\sigma(k, k') = \sigma_{ER}(k, k') - (2kk'/\pi)\, R(k, k')^{-1} \{\sin \delta[R(k, k')] - \sin \delta_{ER}[R(k, k')]\} \tag{3.10}$$

where any smooth contour $R(k, k')$ for continuing the difference of the phase-shifts i.e. $\sin \delta(k) - \sin \delta_{ER}(k)$ off shell gives the desired 2-3 fm. interaction range and yields small matrix elements for the non-resonating, off-diagonal part of σ.

3.2 Unitary Transformations on σ.

Phase-shift equivalent potentials are potentials with exactly equivalent phase shifts and therefore identical on-shell behavior. These can be generated from an original potential V which satisfies

$$H\psi = (H_o + V)\,\psi = E\psi \tag{3.11}$$

by a unitary operator of finite range U i.e.

$$U\psi = \tilde{\psi} \to \psi \tag{3.12}$$

Then with $\tilde{H} = UHU^{\dagger}$, we have

$$\tilde{H}\tilde{\psi} = E\tilde{\psi} \tag{3.13}$$

So we can see that $\tilde{\psi}$ has the same phase shift as ψ at all energies and the energy spectrum of $\tilde{H}$ is identical to that of H. The transformed potential is given by

$$\tilde{V} = \tilde{H} - H_o = U[H_o, U^{\dagger}] + UVU^{\dagger}, \tag{3.14}$$

and its form is determined by the choice of U which has always been for the purpose of calculational ease only. Some unitary transformations which have been used in the study of off-shell effects of phase-equivalent potentials[6,7,8] produce quite violent distortions in the contours of σ. When these unitary transformations are performed on the σ function of the Reid potential, the low-energy σ function remains unchanged but the transformations produce dramatic structures into the higher energy σ contour. These unsmooth structures can be the consequence of a strong-state-dependence of the scattering wave function causing $\phi(k, k')$ to vary rapidly with respect to k. The σ function of Reid's potential does not exhibit any complicated structure, so it seems more reasonable to assume that the phase equivalent potentials should have σ functions with simple contours.

Since the condition that the long-range part of the interaction be local, and that any non-locality be confined to the short-range interaction is a reasonable one, any wild variations of σ which affect the region $k, k' < 2.0$ fm^{-1} should then be excluded. Sauer has found that most unitarily transformed potentials are unable to yield the correct experimental value of the neutron-neutron scattering length and have to be rejected.[10]

A simple, convenient alternative of inducing a unitary transformation without pitfalls associated with the transformed potentials is to distort a given σ function directly. Any distorting function which disappears on the diagonal elements of σ can be added to it. Since the phase shifts remain unchanged, the distorted σ function belongs to a potential differing from the original potential by a finite-range unitary

transformation. The σ contour of low-energy momenta, k, k' < 1.5 fm^{-1} is required to remain undistorted, confining to the constraint discussed in the preceding section.

Sauer has demonstrated the use of two unitary transformations on the σ function (3.10). The first one, adds large off-shell elements to σ. The distorting function has the form:

$$\sigma_{D1}(k, k') = (2kk'/\pi)\, \Gamma_{D1}(k, k')(k^2 - k'^2)^2 \times [d^6 + (k^2 + k'^2)^3]^{-1} \qquad (3.15)$$

The second distorting function decreases the off-shell elements of σ.

$$\sigma_{D2}(k, k') = \sigma(k, k')\, \{[1 + (k^2 - k'^2)^2 \times \Gamma_{D2}(k, k')]^{-1} - 1\} \qquad (3.16)$$

In both cases, the parameter function $\Gamma_{D1(2)}$ is given by

$$\Gamma_{D1(2)}(k, k') = \gamma_{D1(2)}\, \{1 - \exp[-(k^2 - k'^2)/(2d^2)]\} \qquad (3.17)$$

The parameters γ and d are chosen such that the low-energy σ pattern up to k = 1.5 m^{-1} is preserved approximately and the transformed σ functions do not contain complicated structures. At k = k', σ_{D1}, σ_{D2} and $\Gamma_{D1(2)}$ all vanish.

3.3 Properties and behaviour of σ.

When various contours of distortions of circles are used for the off-diagonal parametrizations (3.10) of σ which meet all essential field-theoretical constraints, and distorting functions are added, certain

trends and behavior patterns of σ surface.[54]

Nuclear structure results exhibit negligible variations even when contours are radically changed. They appear to be sensitive to the off-diagonal σ elements in the two momentum strips closest to the axes, about 1.0 fm^{-1} wide. Large off-diagonal elements of σ of either sign yield a more repulsive interaction while small elements yield a more attractive interaction. Correspondingly, large elements produce a decrease in the binding energies of finite nuclei and nuclear matter. It has been demonstrated that the theoretical binding energy of many-nucleon systems can be manipulated in a transparent way[45]. By decreasing or increasing the σ-elements in the momentum strips, the binding energy can become larger or smaller within bounds.

On-shell parametrization of σ can be studied by keeping a certain smooth off-shell parametrization fixed. However, any resulting change in nuclear structure results will be due to the combined effect of on-shell as well as subsequent off-shell variations in σ. The dependence of nuclear structure results on the details of a chosen set of phase shifts can still be traced. Sauer studied nuclear structure sensitivity to (i) high-energy phase shift, (ii) charge dependence of the ^1S_o phase shift, and (iii) the existing experimental uncertainties in phase-shifts.

Ordinary nuclear structure calculations are insensitive to high energy ^1S_o phase-shifts. Only the reaction matrix of highly excited states can become affected. The charge dependence of the ^1S_o scattering length is well established[59]. The proton-proton and proton-neutron scattering lenghts differ by 6 fm. indicating that the proton-neutron interaction is slightly more attractive. To test this charge dependence of

the ^1S_o phase, the difference between the Reid proton-proton phase-shift corrected for Coulomb effects and the experimental proton-neutron phase shift is taken to be an upper bound on the charge splitting of the ^1S_o phase. Nuclear structure results display a weak dependence on the possible charge splitting. However, nuclear properties other than those tested (e.g. binding energy) can be more sensitive to the charge dependence of the interaction and cannot be conclusive. Experimental uncertainties in the phase shift have only little effect on the nuclear structure calculations.

All changes associated with on-shell parametrization of σ are minimal compared with those obtained from off-shell variations. The insignificant effects are consistent with the observation that the smaller the off-shell σ elements are the more attractive the resulting reaction matrix becomes. Small (large) off-shell σ elements for high momenta are associated with small (large) negative high-energy phases and more (less) attractive phases between 250 and 400 MeV. The more attractive (repulsive) phase shifts yield slightly less (more) binding in nuclear matter. With the most of low-energy σ fixed and the off-shell part of σ smooth., variations in nuclear structure results are in consequence not dramatic. Smooth off-shell changes can bring about variations of up to 20%.

3.4 Evaluation of the σ function Method.

Sauer's method of using the σ function as another tool for creating off-shell changes in the two-nucleon interaction is advantageous over the short-range unitary transformations of a given potential. The

form of the transformation is usually chosen for the purpose of facilitating numerical calculations and the resulting σ function displays exotic structures in the contour pattern. Such arbitrarily complicated off-shell behaviour is avoided when using the σ function directly. σ is then a convenient starting point for calculations of off-shell variations. Physical constraints which can be directly imposed on σ are sometimes violated in unitary transformations. One example is charge symmetry of the nuclear force. As we have seen, the theoretical binding energy of many nucleon systems can be manipulated in a transparent manner. Off-shell changes can be well controlled using the σ function.

There are certain drawbacks in the method of Sauer. First of all, σ is a quantity for which one does not have much physical meaning yet. Off-shell changes initiated in σ do not affect T in a linear way. As we have seen in a single partial wave channel with no bound states, the phase shifts at all energies (i.e. $\sigma(k, k)$ for all k) determine the potential (providing it being local and energy-independent) and, hence, $\sigma(k, k')$ uniquely. The σ functions for various potentials (Fig. 3-1) are very similar since these potentials yield very similar phase shifts up to quite high energies. Similarly, if $\sigma(k,k)$ is fixed for all k, any resulting variation in $\sigma(k, k')$ in Sauer's method is due to differing degrees of non-locality in the underlying interaction. Field-theoretic models suggest that the NN interaction is approximately local at large distances. These suggestions are substantiated by the NN peripheral phase shifts. It is therefore essential to be able to control explicitly the degree and range of non-locality implied by a specific choice of $\sigma(k, k')$. The Sauer scheme does not allow this control as yet. The

parametrization of σ as described in this chapter still contains too many free parameters and allows far too much freedom. Further constraints are essential.

Variations in σ are related to variations in the two-body scattering wave function. The on-energy-shell part of T is determined by the scattering wave function beyond the potential range. The off-shell part of T controls the interior wave function. Additional constraints resulting from the behavior of the interior wave function should be imposed on σ. The NN potential is well determined at large distances, and this information should be incorporated in the construction of σ.

Chapter IV FORMALISM OF THE INTERIOR WAVE FUNCTION

As we have seen, the on-energy-shell part of T is given by the exterior scattering wave function i.e. wave function outside of the potential range. The off-shell part of T controls the interior wave function i.e. wave function in the interaction region. The two-body interaction at large distances is described by a specific, well determined local potential. It is also known that the two-nucleon wave function is suppressed at short distances. All this information should be incorporated into the construction of the T matrix. Following this reasoning, Picker, Redish and Stevenson (1971), (from now on referred to as PRS in this study) have established an alternative procedure to generate the half-shell T matrix. It is a simple and direct approach in which a half-shell element is expressed in terms of the on-shell element plus a term depending on the Fourier-Bessel transform of the difference between the actual wave function and its asymptotic form. PRS make use of the lack of information about the short-range, interior part of the interaction. The wave function can be varied arbitrarily but must obey certain constraints such as boundary condition at the origin, smoothness and a known asymptotic form. The wave function generated by the well-determined external part of the interaction provides a matching point.

4.1 The Difference Function $\Delta_o(k,r)$ and the Half-Shell T

PRS define a real 'Difference Function' $\Delta_o(k, r)$ for the ^1S_o

state, which is proportional to the difference between the outgoing scattering wave function $\psi_o^{(+)}$ and the phase-shifted free wave function V_o,

$$\Delta_o(k, r) = kre^{-i\delta_o(k)}[\psi_o^{(+)}(k, r) - V_o(k, r)] \qquad (4.1)$$

where $\psi_o^{(+)}$ is normalized to

$$\psi_o^{(+)}(k, r) \underset{r\to\infty}{\sim} \frac{1}{kr} e^{i\delta_o(k)} \sin [kr + \delta_o(k)] \qquad (4.2)$$

and

$$V_o(k, r) = e^{i\delta_o(k)}[\cos \delta_o(k) j_o(kr) + \sin \delta_o(k) n_o(kr)] \qquad (4.3)$$

$j_o(kr) = \sin(kr)/kr$ is the zeroth spherical Bessel function and $n_o(kr) = -\cos(kr)/kr$ is the zero-order spherical Hankel function. The half-shell T-matrix can be expressed in terms of Δ_o using the following reasoning.

The S-wave half-shell T in which the initial momentum is on shell and the final momentum off shell is given by[60]

$$t_o(p, k; k^2) = -\int_0^\infty dr\, r^2\, j_o(pr) \int_0^\infty dr' r'^2 U(r, r') \psi_o^{(+)}(k, r') \qquad (4.4)$$

where $U(r, r')$ is the S-wave projection of the potential. The on-shell limit comes to

$$\begin{aligned} t_o(k) &\equiv t_o(k, k; k^2) \\ &= \int_0^\infty dr\, r^2\, j_o(kr) \int_0^\infty dr' r'^2 U(r, r') \psi_o^{(+)}(k, r') \\ &= -\frac{1}{k} e^{i\delta_o(k)} \sin \delta_o(k), \end{aligned} \qquad (4.5)$$

which is completely determined by the phase shift. The S-wave non-relativistic Schrödinger equation at centre-of-mass energy k^2 is

$$\left[\frac{1}{r^2}\frac{d}{dr}\left(r^2\frac{d}{dr}\right) + k^2\right]\psi_o^{(+)}(k,r)$$

$$= \int_0^\infty U(r, r')\psi_o^{(+)}(k, r')\, r'^2\, dr' \qquad (4.6)$$

The potential in eq. (4.4) can now be eliminated by replacing the integral $\int_0^\infty dr'\, r'^2\, U(r, r')\psi_o^{(+)}(k,r')$ with $\left[\frac{1}{r^2}\frac{d}{dr}\left(r^2\frac{d}{dr}\right) + k^2\right]\psi_o^{(+)}(k, r)$. Since $\left[\frac{1}{r^2}\frac{d}{dr}\left(r^2\frac{d}{dr}\right) + k^2\right]V_o(k, r) = 0$, we may write finally

$$t_o(p, k; k^2) = \int_0^\infty dr\, r^2 j_o(p, r)\left[\frac{1}{r^2}\frac{d}{dr}\left(r^2\frac{d}{dr}\right) + k^2\right]\left[\psi_o^{(+)}(k, r) - V_o(k, r)\right] \qquad (4.7)$$

In so doing, $\psi_o^{(+)}(k, r)$ which oscillates undamped for large r, is now replaced by a function which disappears for large r. In terms of $\Delta_o^{\psi}(k,r)$ and $u_o(p; r)$ where $u_o(p, r) = prj_o(p, r) = \sin pr$, we have

$$t_o(p, k; k^2) = \frac{e^{i\delta_o(k)}}{pk}\int_0^\infty dr\, u_o(p, r)\left[\frac{d^2}{dr^2} + k^2\right]\Delta_o(k, r) \qquad (4.8)$$

Integrating by parts twice gives this as

$$t_o(p, k; k^2) = t_o(k) + (k^2 - p^2)\frac{e^{i\delta_o(k)}}{pk}\int_0^\infty dr u_o(p, r)\Delta_o(k, r). \qquad (4.9)$$

The half-shell T is now expressed explicitly in terms of the on-shell T and the spherical Bessel transform of the scattering difference function.

4.2 Constraints on $\Delta_o(k, r)$ and its Parametrization

The class of functions which might be used as model difference functions can be limited by three types of constraints imposed by (1) the properties of $\Delta_o(k, r)$, (2) known behaviour of the potential in the

exterior region, and (3) the assumptions and parametrization of $\Delta_o(k, r)$ in the interior region. The exterior region is defined by $r > R$ and the interior region by $0 \leq r \leq R$ where $R = \lambda\!\!\!^{-}_{\pi} = 1.43$fm. $\lambda\!\!\!^{-}_{\pi}$ is the pion Compton wavelength.

There are two properties of $\Delta_o(k, r)$ which can be read directly from its definition eq. (4.1). Since $\psi_o^{(+)}(k, r)$ is practically identical to $V_o(k, r)$ outside the interaction region, one can see that $\Delta_o(k, r)$ is vanishingly small for r greater than the range of interaction. The second property, due to the behavior $kr\ \psi_o^{(+)}(k, r) \underset{r\to 0}{\to} 0$, is

$$\Delta_o(k, r) \underset{r\to 0}{\to} -\sin\delta_o(k)\cos kr \underset{r\to 0}{\to} -\sin\delta_o(k) \tag{4.10}$$

Two boundary conditions result from the above properties. The first is that in the limit that the range becomes very small, $\Delta_o(k, r)$ and $t_o(p, k; k^2)$ are completely determined by the phase-shift as expected. The second is that $\Delta_o(k, r)$ can be expected to vary smoothly with r. The on-shell T and half-shell T for any local or nonlocal short-range force become correlated by these constraints.

In the exterior region i.e. $r \geq \lambda\!\!\!^{-}_{\pi}$, a unique and local potential provides a specific description of the interaction. The effect of this local exterior potential should be incorporated in $\Delta_o(k, r)$ as constraints. Starting from an integral equation for $\psi_o^{(+)}(k, r)$ equivalent to eqs. (4.2) and (4.5), PRS obtained an expression of $\Delta_o(k, r)$ in terms of the nonlocal potential $U(r, r')$. Since it is believed that the nonlocality in the potential (in a given partial wave) is confined to distances shorter than $\lambda\!\!\!^{-}_{\pi}$, $U(r, r')$ can be written as:

$$U(r, r') = N(r, r') + \delta(r - r')L(r)/rr' \tag{4.11}$$

where $N(r, r')$ represents the nonlocality and $L(r)$ the local part of the potential. When $r > R$,

$$|L(r)| \text{ ->> } \int_0^\infty dr'\, r'^2\, |N(r, r')| \tag{4.12}$$

The effect of a local potential on $\Delta_o(k, r)$ in the exterior region can now be isolated and $\Delta_o(k, r)$ can be expressed in terms of $L(r)$ for $r > R$.

$$\Delta_o(k,r) = \Delta_o^{(o)}(k, r) + \frac{1}{k}\int_r^\infty dr'\, g_o(k; r,r')L(r')\Delta_o(k,r') \quad r > R \tag{4.13}$$

with

$$\Delta_o^{(o)}(k,r) = \frac{1}{k}\int_r^\infty dr' g_o(k; r,r')L(r')[\cos\delta_o(k)u_o(kr') + \sin\delta_o(k)\, y_o(kr')], \quad r > R \tag{4.14}$$

where

$$g_o(k; r,r') = y_o(kr)\, u_o(kr') - u_o(kr)y_o(kr') = -\sin k\,(r - r'), \tag{4.15}$$

$$y_o(kr) = kr\, n_o(kr), \tag{4.16}$$

and

$$u_o(kr) = kr\, j_o(kr) \tag{4.17}$$

Eq. (4.14) can be solved by iteration and the iteration series has been shown by PRS to converge rapidly, when the Reid soft core ^1S_o potential was used as the exterior potential. Differentiating eq. (4.14) one obtains two additional conditions i.e. $\Delta_o'(k,r)$ and $\Delta_o''(k,r)$ for $r > R$, as well as two additional matching points at $r = R$, i.e. $\Delta_o'(k, R)$ and $\Delta_o''(k, R)$.

One important constraint that can be imposed on the relativily arbitrary interior region is the hypothesis that $\Delta_o(k,r)$ varies

smoothly enough over the region [0,R] to be represented by a polynomial in r of reasonably low degree for r < R. A 6th degree polynomial form is chosen for $\Delta_o(k,r)$ in that region so that

$$\Delta_o(k, r) = P_5(k,r) + \eta r^3(r - R)^3, \quad 0 \leq r \leq R \tag{4.18}$$

$$= P(k, r) \qquad k << \lambda\!\!\!^{-1}_N$$

where $\lambda\!\!\!^{-}_N$ is the nucleon Compton wave length. The above form of $\Delta_o(k,r)$ permits the use of one free parameter η to specify $\Delta_o(k,r)$ and to include variations which cannot be represented by P_5, the polynomial of lowest degree (smoothest one). From the exterior potential, $\Delta_o(k,R)$, $\Delta_o'(k,R)$ and $\Delta_o''(k,R)$ are known. $\Delta_o(k,0)$ is given by eq. (4.10) while $\Delta_o'(k,0)$ and $\Delta_o''(k,0)$ are regarded as free parameters. $\Delta_o(k,r)$, its slope and curvature are then specified at the two end points of [0,R], imposing important constraints on $\Delta_o(k,r)$. The six conditions satisfied by P(k,r) are:

$$\begin{aligned} P(k,R) &= \Delta_o(k,R) \\ P'(k,R) &= \Delta_o'(k,R) \\ P''(k,R) &= \Delta_o''(k,R) \end{aligned} \tag{4.19}$$

and

$$\begin{aligned} P(k,0) &= \Delta_o(k,0) = -\sin\delta_o(k) \\ P'(k,0) &= \Delta_o'(k,0) \\ P''(k,0) &= \Delta_o''(k,0). \end{aligned}$$

These then become the parametrization of $\Delta_o(k,r)$ over the interior region.

By assuming that the wave function is very small at short distances, the last two conditions become

$$\begin{aligned} P'(k,0) &= \Delta_o'(k,0) = -k\cos\delta_o(k) \\ P''(k,0) &= \Delta_o''(k,0) = k^2\sin\delta_o(k) \end{aligned} \tag{4.20}$$

thus giving a one-parameter model of $\Delta_o(k,r)$. If the interaction is purely local, the first derivative of $\Delta_o(k,0)$ in eq. (4.20) is more completely given by

$$\Delta_o'(k,0) = k/|f_o(k)| - k \cos \delta_o(k), \tag{4.21}$$

$$= w_o'(k,0) - k \cos \delta_o(k)$$

where $$f_o(k) = \exp\left(-\frac{2}{\pi}\int_0^\infty dq \frac{\delta_o(q)}{q - k + i\varepsilon}\right), \tag{4.22}$$

is the S-wave Jost function, and

$$w_o(k,r) = e^{-i\delta_o(k)} kr\, \psi_o^{(+)}(k,r) \tag{4.23}$$

$\Delta_o'(k,0)$ can be a measure of the effect of high energy phase-shifts on $\Delta_o(k,0)$. The complete expression for the second derivative of $\Delta_o(k,0)$ for a non-local interaction is given by

$$\Delta_o''(k,0) = k^2 \sin \delta_o(k) + \lim_{r \to 0} r \int_0^\infty dr' r' U(r,r') w_o(k,r') \tag{4.24}$$

For a purely local potential, the above is reduced to eq. (4.20) i.e.

$$\Delta_o''(k,0) = k^2 \sin \delta_o(k), \tag{4.20}$$

when it is assumed further that the local potential is finite at the origin, or that the wave function goes to zero at the origin more rapidly than the potential diverges there. In these cases, $w_o''(k,0) = 0$, giving eq. (4.20). Eq. (4.24) indicates that Δ_o'' is a measure of the effect of short range nonlocality in a potential. For eq. (4.21) to hold, it is also required that the potential be less singular than r^{-2} near $r = 0$.

4.3 Evaluation and Application of the Interior wave function Approach

As one can see, the interior wave function approach offers

many advantages with some drawbacks, as compared to Sauer's approach. It is the purpose of this study to incorporate the best points of both approaches, and to apply them to the generation of the fully off-shell T matrix.

PRS have given a simple and direct approach in which a one-parameter model can be used to calculate the half-shell T. The parametrization of the difference function has fewer free parameters as compared to that of the σ function. The half-shell T, which is measureable, is calculated directly giving the PRS approach more physical meaning. The information carried by the fixed local exterior potential is incorporated in the models of $\Delta_o(k,r)$. The lack of information about the part of the interaction in the interior region is exploited to parametrize the arbitrariness in $\Delta_o(k,r)$. Sauer's approach is specialized to study the purely local potential whereas in the interior wave function approach, non-local interaction can be included in the more generalized formalism.

A drawback of the PRS method is that the model wave functions $\psi_o^{(+)}(k,r)$ do not form a complete orthonormal set. Hence one cannot go completely off-shell by using the Low equation.

In this study, we propose an incorporation of the σ function method and the difference function method. In this approach, the half-shell T-matrix from PRS can be used to construct the σ function of Baranger et al, and then their approach used to generate an off-shell T-matrix. The connection is given by

$$\phi(p,k) = \left(\frac{2}{\pi}\right) pk\, t_o(p, k; k^2) e^{-i\delta_o(k)} \tag{4.25}$$

and

$$\sigma(p,k) = \left(\frac{1}{2}\right) [\phi(p,k) + \phi(k,p)] \tag{4.26}$$

This approach allows us to incorporate all the advantages of the σ

function and the PRS procedure, with the drawbacks eliminated. The simplicity and ease of control of the σ function are made use of. The half-shell T, a measurable and physically meaningful quantity is the starting point and the hurdle in going off-shell is circumvented by means of the σ function. Low energy constraints which are a part of the long-range potential and which are well justified by field theoretic models of the potential, are now automatically incorporated into the construction of σ. One can therefore further limit the freedom of σ. By varying the η values of the one parameter model described in the preceding section, we have an alternate way to generate distortions on σ. The σ functions for a few η values are shown in Fig. 5-5. These σ's belong to phase-shift equivalent potentials with identical effective range parameters.

In the current study, we have imposed the additional constraint on σ that the interior wave function be well behaved, possess no extra nodes, and have an amplitude less than that of the external free wave function.

The condition of no extra nodes is an imposed one, and may not be entirely realistic. For a purely local interaction, extra nodes imply the existence of bound states at negative energy in the ^1S_o state. This is not observed. For a non-local interaction, the existence of bound states in the continuum is possible. However, the accidental degeneracy which gives rise to bound states in the continuum is not physical since any slight perturbation would change them into narrow resonances[61]. Additional nodes have been introduced into wave functions generated by unitary transformations[33]. However, no additional bound states can be created since completeness is preserved in these transformations. These extra nodes

then should not be associated with bound states. Neudatchin et al[62] have demonstrated that an extra node in the exterior wave function may be due to a composite structure of nucleons. For our present calculations, no additional nodes are assumed to be created.

According to McVoy, Heller and Bolsterli,[63] the only known mechanism which can cause the amplitude of the wave function inside interaction region to be greater than that of the external phase-shifted free wave function is some sort of resonance trapping of the wave function. Since there is no evidence to suggest considering these resonance effects here, we exclude such wave functions. With these conditions, the arbitrariness in σ is further reduced.

By studying the half-shell T matrices as functions of the wave function in the interaction region, PRS found that when $\eta > 1$, the model wave function developed extra nodes in the interaction region. When $\eta < -1$, the maximum amplitude of the wave function inside this region became greater than that of the phase-shifted free wave function. They were then able to impose the constraint $|\eta| < 1$. Later work in 1973 indicated that this constraint on η was k-dependent[26].

CHAPTER V CALCULATIONAL PROCEDURES

Calculations in this study can be divided into four sections:

1) construction of the σ function;

2) computation of the fully-off-shell T-matrix;

3) nuclear matter calculations;

and 4) finite nuclei calculations.

In each of these areas, procedures are listed and described in details.

5.1 The σ-matrix

In this section, the construction of the σ function $\sigma(k, k')$ following Sauer's approach, and from the real difference function $\Delta_o(k,r)$ will be described. Before doing so, the phase shift used should be discussed.

(a) Phase Shift

In equation (2.44) i.e.

$$\sigma(k, k) = -(2k/\pi) \sin \delta_o (k) \qquad (2.44)$$

the phase shift $\delta_o(k)$ is assumed to refer to the nuclear part only of the nucleon-nucleon interaction. In this context, the experimental phase shift preferred is the proton-neutron phase. Unfortunately, this is not determined accurately yet. The more reliably known proton-proton phase can be used but a model-dependent correction for Coulomb interaction

must be included. The ^1S_o phase shift used to generate $\sigma(k,k')$ is that obtained from Reid's soft-core interaction at low energies. This is taken as the experimental proton-proton phase-shift corrected for Coulomb effects. This low-energy phase-shift is properly matched to a high-energy form given by

$$\delta_o(k) = \frac{[\delta_o(k_c) + C(k - k_c)] \exp[-\alpha(k - k_c)]}{1 + m(k - k_c)^n} \qquad (5.1)$$

for $k > k_c$.

At $k = k_c$, the values and the slope of $\delta_o(k)$ are matched to the value and slope of Reid's phase shift $\delta_o(k_c)$. The parameter C is fixed by the value of $\delta_o'(k_c)$, leaving α, m and n as free parameters. Two distinct high energy forms for $\delta_o(k)$ have been used for this study, and are shown in fig. 5-1. Eq. (2.19) i.e.

$$\phi(k, k') = \langle k' | T(k^2 + i0) | k \rangle \exp[-i\,\delta_o(k)] \qquad (2.19)$$

requires the phase shift $\delta_o(k)$ to remain in the range between $+\pi/2$ and $-\pi/2$. The high-energy phase shift obtained from Reid's soft-core potential becomes more repulsive than $-\pi/2$ so that the mathematical procedure to calculate $\phi(k, k')$ from $\sigma(k, k')$ which will be described in Section 5.2 fails. The phase-shift with high energy form (5-1) gives almost identical results to the $\delta_o(k)$ with high-energy Reid's phase[54] and can be safely substituted.

(b) Generation of the σ-function (following Sauer's Method)

The σ-function computed is the so-called 'Reid Approximate' (RA) form given by Sauer[54]. This is an analytic σ-function approximating features of the ~~proper~~ σ_R, Reid σ, which is obtained numerically. The phase shifts of σ_R gets more repulsive than $-\pi/2$ at high energies.

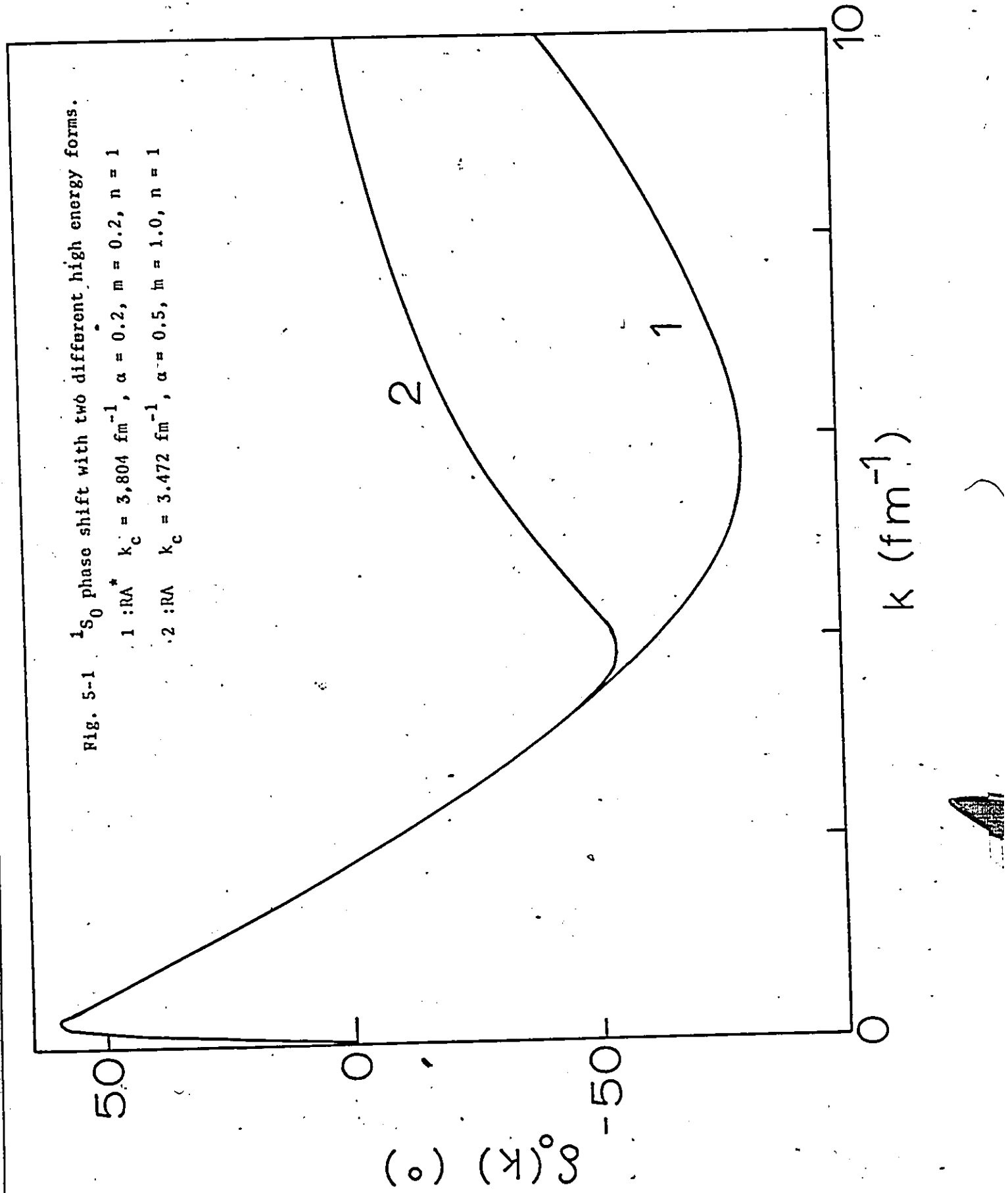

Fig. 5-1 $^1S_0$ phase shift with two different high energy forms.
1 :RA* k_c = 3,804 fm^{-1}, α = 0.2, m = 0.2, n = 1
2 :RA k_c = 3.472 fm^{-1}, α = 0.5, m = 1.0, n = 1

σ_{RA} is given by

$$\sigma_{RA}(k, k') = \sigma_1(k, k') + \{-R_3(k,k')R_2(k,k')\sin\delta_o[R_2(k,k')] - \sigma_1(k, k')\} R_4(k, k') \quad (5.2)$$

Here

$$\sigma_1(k,k') = \sigma_{ER}(k, k') - (2kk'/\pi)R_1(k,k')^{-1}\{\sin\delta_o[R_1(k,k')] - \sin\delta_{ER}[R_1(k,k')]\}, \quad (5.3)$$

$$R_1(k,k') = \{1/2\ (k^2 + k'^2) + 2(k^2 - k'^2)^2(k^2 + k'^2)^{-1}\}^{\frac{1}{2}} \quad (5.4)$$

$$R_2(k,k') = [(k - r_1)^2 + (k' - r_1)^2]^{\frac{1}{2}} + r_1 \quad (5.5)$$

$$R_3(k,k') = (2kk'/\pi)[kk' + r_2(k + k') + r_3^2]^{-1} \quad (5.6)$$

$$R_4(k,k') = \{1 + 2(1 + \exp([k/r_4 - k'/r_4]^2))^{-1}\} \times \exp[-R_1(k,k')/r_5]. \quad (5.7)$$

δ_{ER} is given by equations (3.7), (3.8) and (3.9), i.e.

$$k \cot\delta_{ER}(k) = -(1/a) + 1/2\ r_o k^2 - \rho r_o^3 k^4, \quad (3.7)$$

$$\beta^{-1} = (3/8)\ a\ [1 - (1 - (16/9)\ r_o/a)^{\frac{1}{2}}] \quad (3.8)$$

and

$$\rho r_o^3 = (1/6\beta^3)\ [(2/a\beta) - r_o\beta] \quad (3.9)$$

σ_{ER} is given by equation (3.5) i.e.

$$\sigma_{er}(k,k') = (-k'/\pi)\sin\delta_{ER}(k)\ (\beta^2 + k^2)\ (\beta^2 + k'^2)^{-1} - (k/\pi)\sin\delta_{ER}(k')\ (\beta^2 + k'^2)\ (\beta^2 + k^2)^{-1} \quad (3.5)$$

At very low momenta for which $\delta_{ER}(k) \simeq \delta_o(k)$, $\sigma_{RA}(k,k') = \sigma_{ER}(k,k')$.

The parameter values used were $r_1 = 0.9$ fm^{-1}, $r_2 = 0.1$ fm^{-1}, $r_3 = \sqrt{10} \times 10^{-2}$ fm^{-1}, $r_4 = 1.5$ fm^{-1}, $r_5 = 5.0$ fm^{-1}, $a = -17.163$ fm and $r_o = 2.80$ fm.

Two unitary transformations discussed in Chapter III, section

3.2 have been used to generate three distortions which are added to σ_{RA}. These are described by equations (3.15), (3.16) and (3.17), i.e.

$$\sigma_{D1\pm}(k,k') = (2kk'/\pi)\Gamma_{D1\pm}(k,k')(k^2 - k'^2)^2[d^6 + (k^2 + k'^2)^3]^{-1} \tag{3.15}$$

$$\sigma_{D2}(k,k') = \sigma_{RA}(k,k')\{[1 + (k^2 - k'^2)^2\,\Gamma_{D2}(k,k')]^{-1} - 1\} \tag{3.16}$$

$$\Gamma_{D1\pm(2)}(k,k') = \gamma_{D1\pm(2)}\{1 - \exp[-(k^2 + k'^2)/(2d^2)]\} \tag{3.17}$$

Eq. (3.15) describes two distortions σ_{D1+} and σ_{D1-}, the former having the parameter $\gamma_{D1} = 6\ fm^{-1}$ and the latter having $\gamma_{D1} = -6\ fm^{-1}$. The third distortion σ_{D2} has $\gamma_{D2} = (2/3)^4\ fm^4$. In all cases, d is assigned the value 2.0 fm^{-1}. Contour plots of these functions are shown in Figs. 5-2 and 5-3. σ_{D1+} increases the off-shell elements of σ_{RA}, while σ_{D1-} decreases them. σ_{D2} reduces even further the off-shell elements.

In this study, the σ_{RA} function with two different forms for the high-energy phase shift has been generated. To each of these i.e. σ_{RA} and σ_{RA}* three distortions σ_{D1+}, σ_{D1-} and σ_{D2} have been added.

(c) Generation of σ-function from $\Delta_o(k,r)$

We have also generated σ(k, k') from the real difference function Δ_o (k, r) defined by equations (4.1) and (4.3), i.e.

$$\Delta_o(k,r) = kr\, e^{-i\delta_o(k)}[\psi_o^{(+)}(k,r) - V_o(kr)] \tag{4.1}$$

where $$V_o(kr) = e^{i\delta_o(kr)}[\cos\delta_o(k)\, j_o(kr) + \sin\delta_o(k)\, n_o(kr)] \tag{4.3}$$

In chapter IV, $\Delta_o(k,r)$ is shown to be given by eq. (4.18) in the interaction range $r \leq R = 1.43$ fm, i.e.

$$\Delta_o(k,r) = P_5(k,r) + \eta\, r^3\,(r - R)^3, \qquad 0 \leq r \leq R \tag{4.18}$$

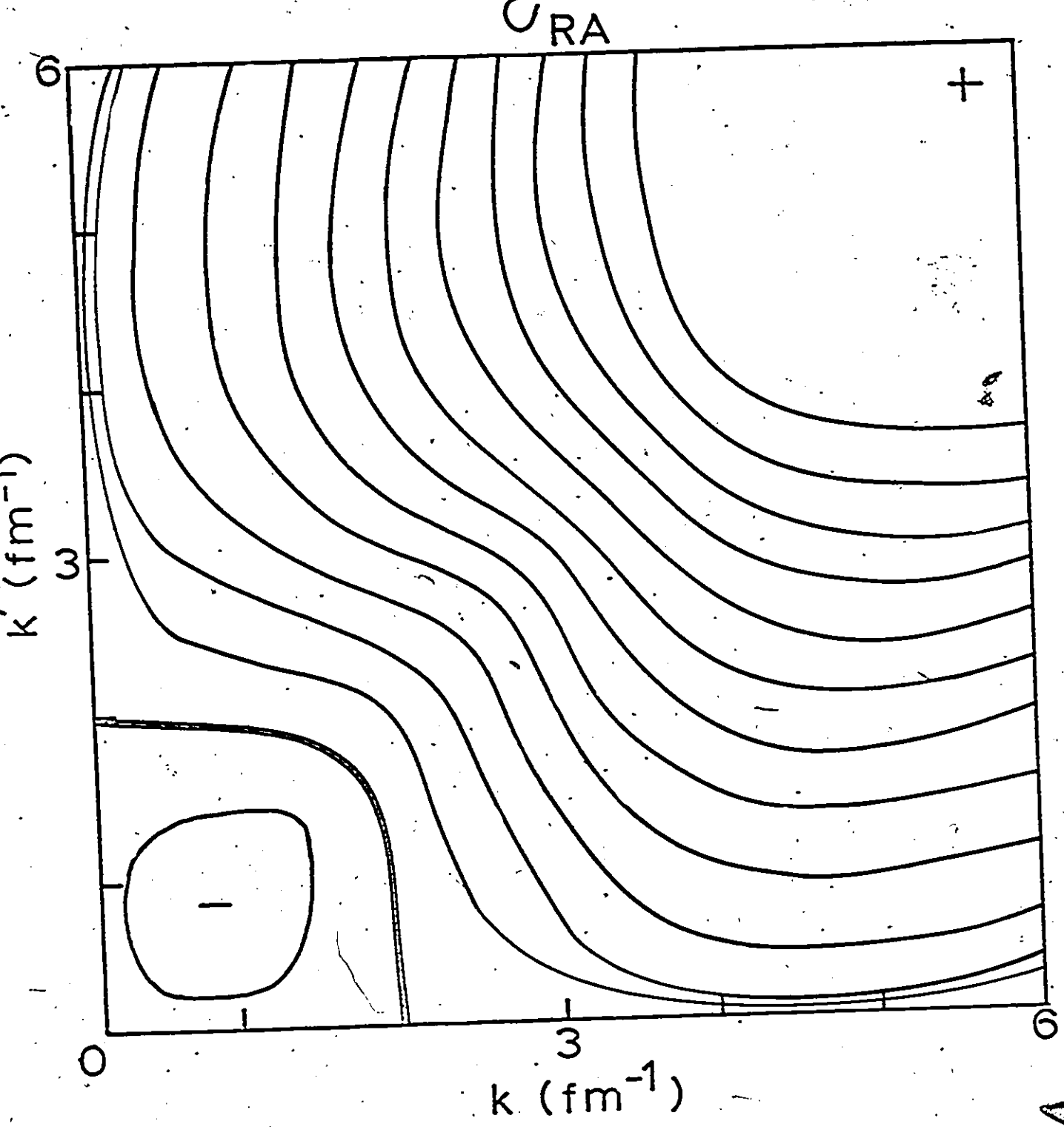

Fig. 5-2 (a) Equal-value contours of σ_{RA}. The contours are drawn in steps of 0.2 fm^{-1}, with the heavy line denoting the zero-value contour. - and + denote the minimum and the maximum.

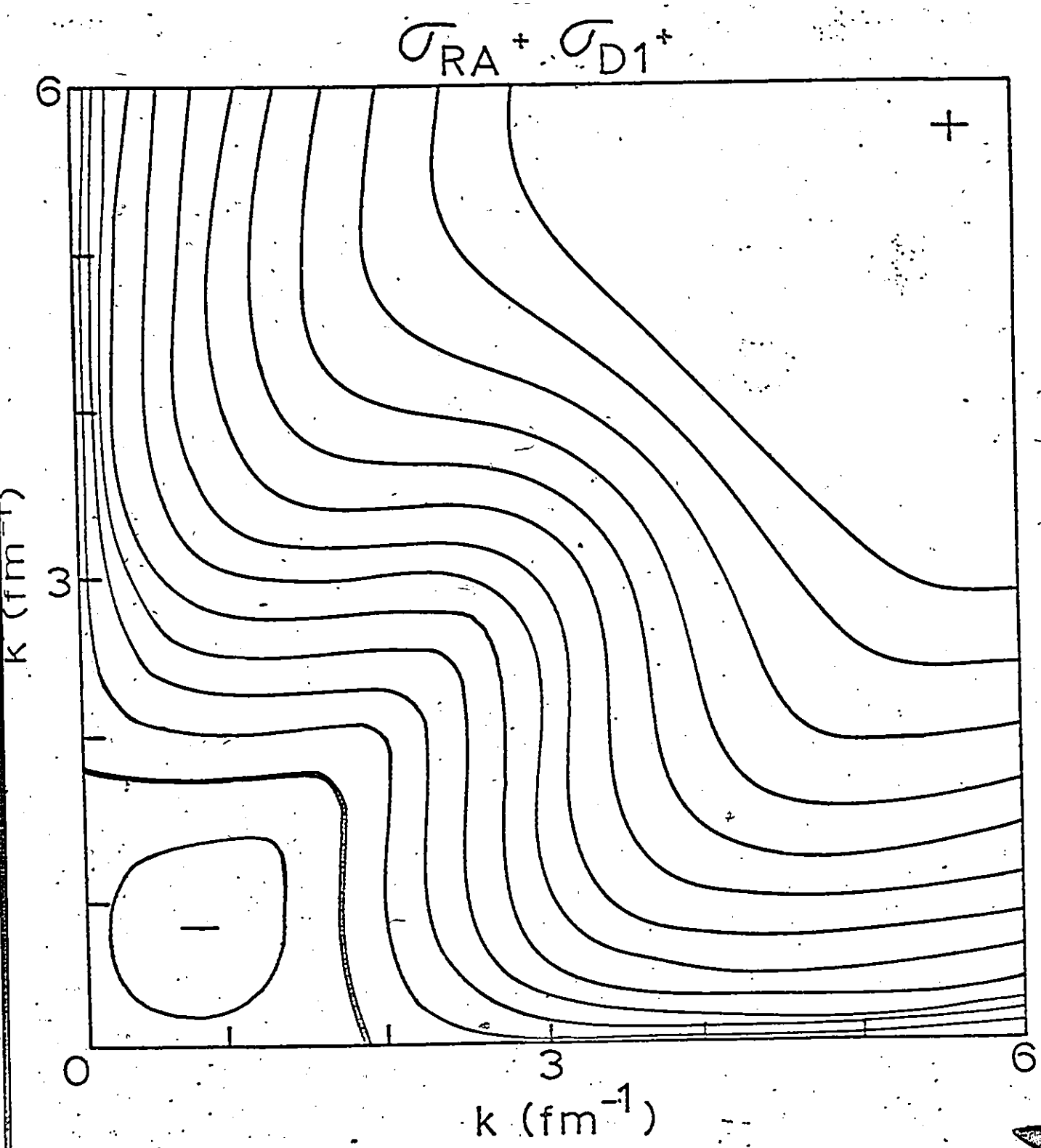

Fig. 5-2 (b) Equal-value contours of $\sigma_{RA^+} \cdot \sigma_{D1^+}$.

See fig. 5-2 (a) caption.

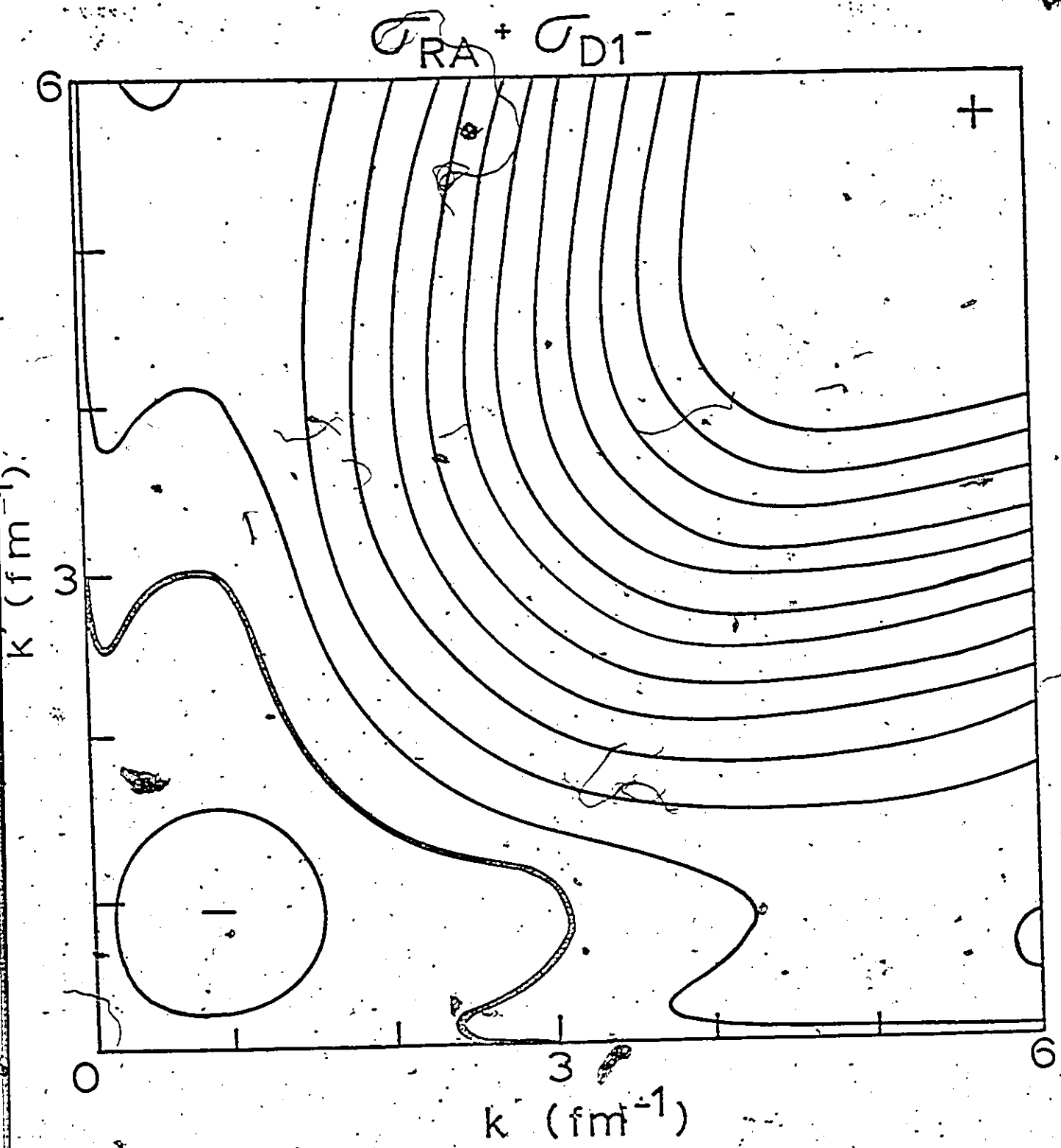

Fig. 5-2 (c) Equal-value contours of $\sigma_{RA}+\sigma_{D1-}$.

See fig. 5-2 (a) caption.

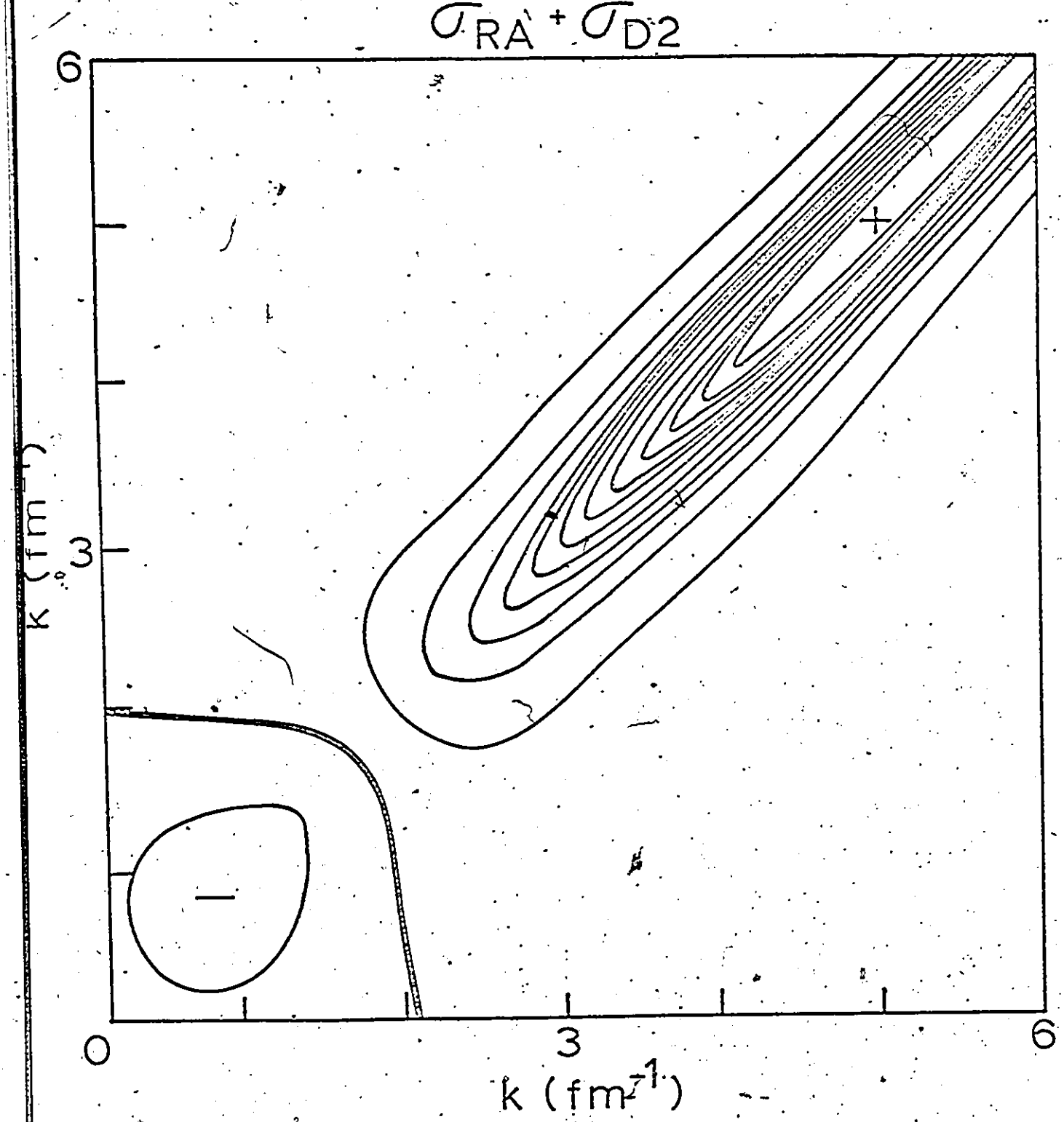

Fig. 5-2 (d). Equal-value contours of $\sigma_{RA}+\sigma_{D2}$.

See fig. 5-2 (a) caption.

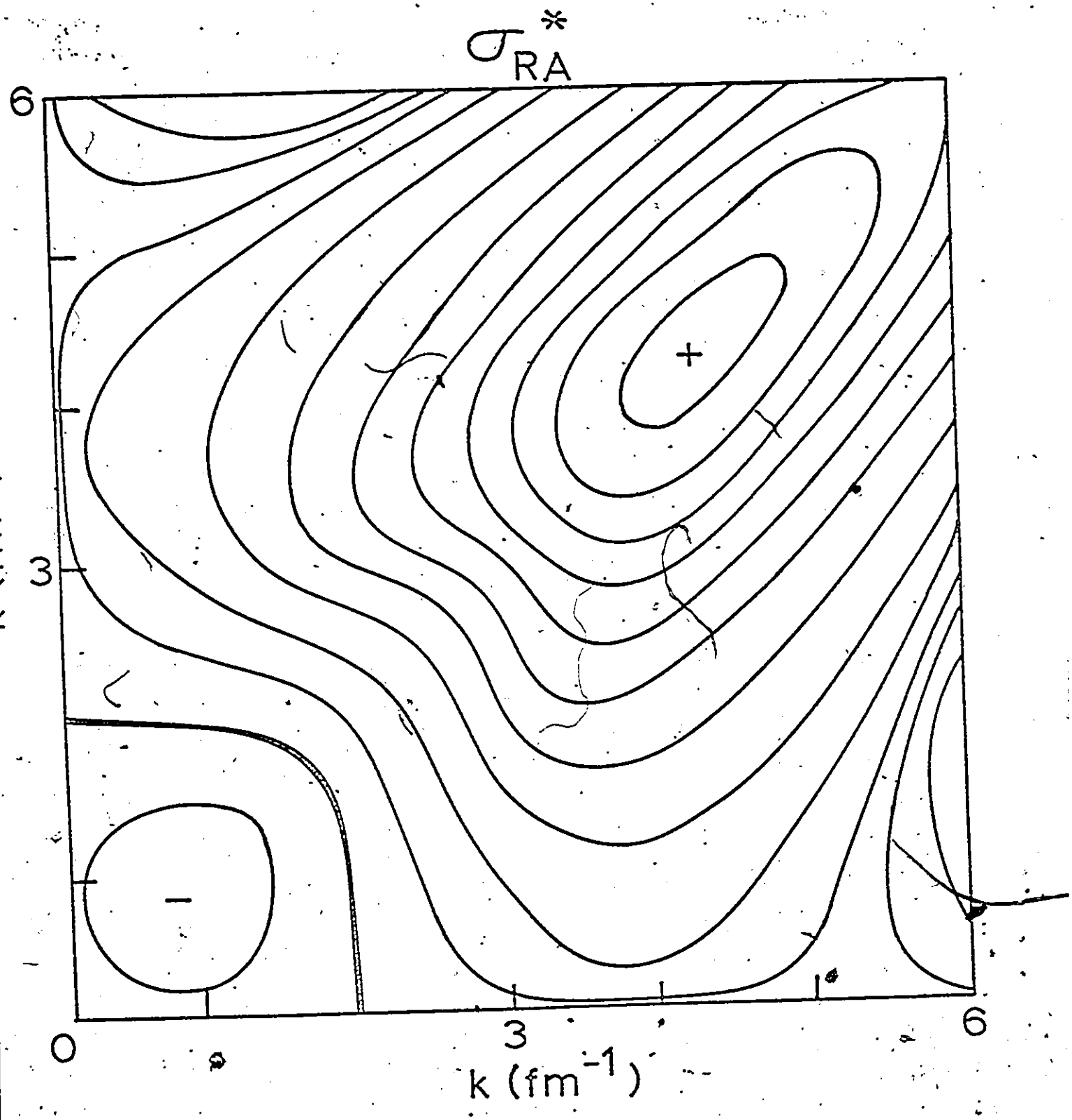

Fig. 5-3 Equal-value contours of σ_{RA}^*. The contours are drawn in steps of 0.2 fm^{-1}, with the heavy line denoting the zero-value contour. - and + denote the minimum and the maximum.

$$= P(k, r).$$

Since $P(k,r)$ and hence $P_5(k, r)$ satisfies the six conditions (4.19), the determination of P_5 can be regarded as a six-point interpolation problem in the limit that three of the points coincide at $r = 0$ and another three at $r = R$. Therefore one can write the fifth-degree polynomial as

$$\begin{aligned} P_5(k,r) &= p_o(k) + p_1(k)(r - R) + p_2(k)(r - R)^2 \\ &\quad + p_3(k)\, r\,(r - R)^2 + p_4(k)\, r^2\,(r - R)^2 \\ &\quad + p_5(k)\, r^2\,(r - R)^3 \end{aligned} \tag{5.8}$$

These six conditions i.e.

$$\begin{aligned} P(k,R) &= \Delta_o(k,R) \\ P'(k,R) &= \Delta_o'(k,R) \\ P''(k,R) &= \Delta_o''(k,R), \end{aligned} \tag{4.19}$$

and

$$\begin{aligned} P(k,0) &= \Delta_o(k,0) \\ P'(k,0) &= \Delta_o'(k,0) \\ P''(k,0) &= \Delta_o''(k,0), \end{aligned}$$

then give

$$\begin{aligned} p_o(k) &= \Delta_o(k, R), \\ p_1(k) &= \Delta_o'(k, R), \\ p_2(k) &= \frac{\Delta_o(k,0) - \Delta_o(k,R) + R\Delta_o'(k,R)}{R^2} \\ p_3(k) &= \frac{\Delta_o(k,0) - \Delta_o'(k,R) + 2Rp_2(k)}{R^2} \end{aligned}$$

$$p_4(k) = \frac{\Delta_o''(k,R) - 2p_2(k) - 2Rp_3(k)}{2R^2}$$

$$p_5(k) = -\frac{[\Delta_o''(k,0) - 2p_2(k) + 4Rp_3(k) - 2R^2p_4(k)]}{2R^3}$$

$\Delta_o(k,R)$ and hence the first three of the six conditions can be obtained from the Reid soft-core (RSC) wave function. We have used the RSC to represent the exterior potential for $r > \lambda\!\!\!^{-}_{\pi}$. PRS have shown that once $\delta_o(k)$ has been fixed, $\Delta_o(k,r)$ and $t_o(p,k;k^2)$ are not sensitive to the exterior potential. The RSC potential in units of fm^{-2} is

$$V(r) = G_1 \frac{e^{-\mu r}}{\mu r} + G_4 \frac{e^{-4\mu r}}{\mu r} + G_7 \frac{e^{-7\mu r}}{\mu r}, \qquad (5.10)$$

where $\mu = 0.7\ fm^{-1}$, and

$$G_1 = -10.463/41.47\ fm^{-2},$$

$$G_4 = -1650.6/41.47\ fm^{-2},$$

$$G_7 = 6484.2/41.47\ fm^{-2}.$$

We have employed the approximation used by PRS and replaced $\Delta_o(k,r)$ in the region $r < R$ by

$$\Delta_o^{(o)}(k,r) = [\cos kr \sum_{\beta=1,4,7} G_\beta I_\beta(k,r) - \sin kr \sum_{\beta=1,4,7} G_\beta \tilde{I}_\beta(k,r)]/k, \qquad (5.11)$$

where

$$I_\beta(k,r) = \{\cos\delta_o(k)[E_1(\beta\mu r) - \mathrm{Re}E_1((\beta\mu - 2ik)r)] + \sin\delta_o(k)\ \mathrm{Im}E_1((\beta\mu - 2ik)r)\}/2\mu \qquad (5.12)$$

and

$$\tilde{I}_\beta(k,r) = \{\sin\delta_o(k)[E_1(\beta\mu r) + \mathrm{Re}E_1((\beta\mu - 2ik)r)] + \cos\delta_o(k)\ \mathrm{Im}E_1((\beta\mu - 2ik)r)\}/2\mu \qquad (5.13)$$

$E_1(z)$ is the exponential integral

$$E_1(z) = \int_1^\infty dt\, e^{-zt}/t \tag{5.14}$$

This approximation then allows us to calculate the first and second derivatives at r = R, of $\Delta_o(k,r)$, i.e.

$$\Delta_o'(k,r) = - \sum_{\beta=1,4,7} G_\beta [\sin kr\, I_\beta(k,r) + \cos kr\, \tilde{I}_\beta(k,r)], \tag{5.15}$$

and

$$\Delta_o''(k,r) = V(r) \sin [kr + \delta_o(k)] - k^2 \Delta_o(k,r). \tag{5.16}$$

The remaining $p_i(k)$ coefficients in equation (5.9) which are not given by the three conditions at r = R can be extracted from the other three at r = 0. The assumption that the wave function is very small at short distances is used here, so that $w_o(k,0) = w_o'(k,0) = w_o''(k,0) = 0$. $w_o(k,r)$ is given by equation (4.23) i.e.

$$w_o(k,r) = e^{i\delta_o(k)}\, kr\, \psi_o^{(+)}(k,r). \tag{4.23}$$

The last two conditions become

$$\begin{aligned} \Delta_o'(k,0) &= -k \cos \delta_o(k), \\ \Delta_o''(k,0) &= k^2 \sin \delta_o(k), \end{aligned} \tag{4.20}$$

with $\Delta_o(k,0) = -\sin \delta_o(k)$.

η is the only free parameter, enabling us to use the one-parameter model. From the values of $\Delta_o(k,R)$, $\Delta_o'(k,R)$ and $\Delta_o''(k,R)$ given by equations (5.11), (5.12), (5.13), (5.15) and (5.16), as well as from values of $\Delta_o(k,0)$, $\Delta_o'(k,0)$ and $\Delta_o''(k,0)$ given by equation (4.20), the coefficients $p_i(k)$ are computed from equation (5.9). This gives us the fifth-degree polynomial $P_5(k,r)$, to which is added $\eta r^3 (r - R)^3$ to get the sixth-degree polynomial $P(k,r)$, and hence $\Delta_o(k,r)$, from equation (4.18). $w_o(k,r)$

corresponding to different η values are obtained by adding sin [kr + $\delta_o(k)$] to P(k,r) since

$$w_o(k,r) = \Delta_o(k,r) + \sin [kr + \delta_o(k)] \tag{5.17}$$

The difference function $\Delta_o(k,r)$ for 5 different η values (η = -2, -1, 0, 1, 2) are shown in fig. 5-4.

The next step is the calculation of the half-shell T matrix elements $t_o(p, k;k^2)$ using equation (4.9), i.e.

$$t_o(p,k;k^2) = t_o(k) + (k^2 - p^2) \frac{e^{i\delta_o(k)}}{pk} \int_0^\infty dr u_o(pr) \Delta_o(k,r) \tag{4.9}$$

where $u_o(pr) = \sin pr$.

The only complication lies in the evaluation of the integral in eq. (4.9). It is written as

$$\mathcal{J}(p,k) = \int_0^\infty dr \sin pr \, \Delta_o(k,r) \tag{5.18}$$

which can be divided into two parts $\mathcal{J}$ int and $\mathcal{J}$ ext , so that

$$\mathcal{J}(p,k) = \int_0^R dr \sin pr \, P(k,r) + \int_R^\infty dr \sin pr \, \Delta_o^{ext}(k,r)$$

$$= \mathcal{J}_{int}(p,k) + \mathcal{J}_{ext}(p,k). \tag{5.19}$$

$\Delta_o^{ext}(k,r)$ is the difference function obtained from the exterior potential. We have

$$\mathcal{J}_{int}(p,k) = \sum_{n=0}^{6} C_n(k) In(p), \tag{5.20}$$

where

$$In(p) = -p^{-n-1} \sum_{j=0}^{n} j! \binom{n}{j} [(pr)^{n-j} \cos (pr + 1/2 \, j\pi)] \Big|_{r=0}^{r=R} \tag{5.21}$$

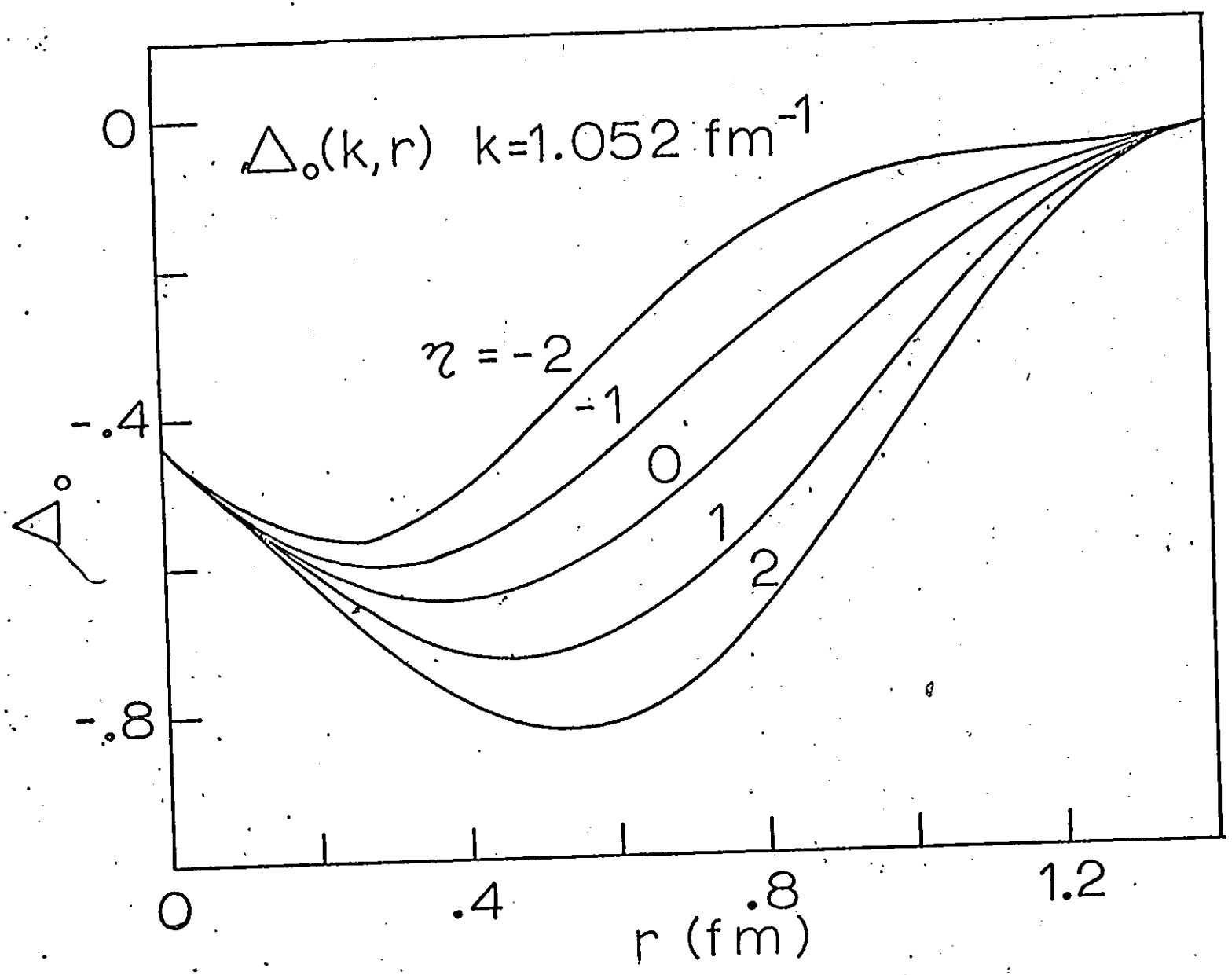

Fig. 5-4 The difference function $\Delta_0(k,r)$ using the polynomial form of PRS.

and

$$C_o(k) = p_o(k) - Rp_1(k) + R^2 p_2(k)$$

$$C_1(k) = p_1(k) - 2Rp_2(k) + R^2 p_3(k)$$

$$C_2(k) = p_2(k) - 2Rp_3(k) + R^2 p_4(k) - R^3 p_5(k) \qquad (5.22)$$

$$C_3(k) = p_3(k) - 2Rp_4(k) + 3R^2 p_5(k) - \eta R^3$$

$$C_4(k) = p_4(k) - 3Rp_5(k) + 3\eta R^2$$

$$C_5(k) = p_5(k) - 3\eta R,$$

$$C_6(k) = \eta.$$

$\mathcal{J}_{ext}(p,k)$ is given by

$$(k^2 - p^2)\mathcal{J}_{ext}(p,k) = \Big[\sum_{\beta=1,4,7} G_\beta I_\beta(p,k;R)\Big] + \sin pR\Delta_o'(k,R) - p\cos pR\,\Delta_o(k,R), \qquad (5.23)$$

where

$$I_\beta(p,k;R) = (2\mu)^{-1}(\cos\delta_o(k)\, R_e\{E_1([\beta\mu - i(p-k)]R) - E_1([\beta\mu - i(p+k)]R)\} + \sin\delta_o(k)\, \mathrm{Im}\{E_1([\beta\mu - i(p-k)]R) + E_1([\beta\mu - i(p+k)]R)\}) \qquad (5.24)$$

From the above results (i.e. equations (5.20)-(5.24)), we can calculate the integral $\mathcal{J}(p,k)$ and hence $t_o(p,k;k^2)$ using equation (4.9). The half-shell T matrix elements for the five η values (η = -2, -1, 0, 1, 2) have been calculated. The corresponding σ-functions have been generated from $t_o(p,k;k^2)$ using equations (4.25) and (4.26), i.e.

$$\phi(p,k) = (2/\pi)\,\rho k\, t_o(p,k;k^2)\, e^{-i\delta_o(k)} \qquad (4.25)$$

and $$\sigma(p,k) = 1/2 \left[\phi(p,k) + \phi(k,p) \right]. \qquad (4.26)$$

The resulting σ functions are shown in fig. 5-5 .

5.2 The off-shell T-matrix.

The numerical procedure of Baranger et al[1] is used to generate the fully-off-shell T-matrix from the σ-matrix. A 48-point Gaussian quadrature is used to construct $\sigma(k,k')$ which becomes a 48 X 48 matrix. The method for the construction of the half-shell T of Baranger et al., $\phi(k,k')$ from $\sigma(k,k')$ is first discussed. $\phi(k,k')$ is related to the half-shell T of PRS $t_o(p,k;k^2)$ through equation (4.25). Then the procedure of computing the fully-off-shell T utilizing $\phi(k,k')$ as input is outlined in this section. $\phi(k,k')$ and the resulting T are both 48 x 48 matrices.

(a) Gaussian Integration Formula

It is clear by now that we have to work on a mesh with 48 mesh points. To evaluate integrals such as equation (2.25), they must be approximated as sums. Gauss' Formula is used here; i.e.

$$\int_{-1}^{1} f(x)\, dx = \sum_{i=1}^{N} w_i f(x_i) \qquad (5.25)$$

with N integration points x_i and corresponding weights w_i. The integrals we encounter here are integrals of regular functions over a momentum k which varies from 0 to ∞. Before the approximation can be made, a transformation from k to the variable x ranging from -1 to +1 must first be performed, using the formula

Fig. 5-5: Equal-value contours of $\sigma(k,k')$ of the ^1S_o potential calculated from the difference function $\Delta_o(k,r)$. Contours are drawn in steps of $0.2 \cdot fm^{-1}$, with the heavy line denoting the zero value contour. - and + denote the minimum and the maximum.

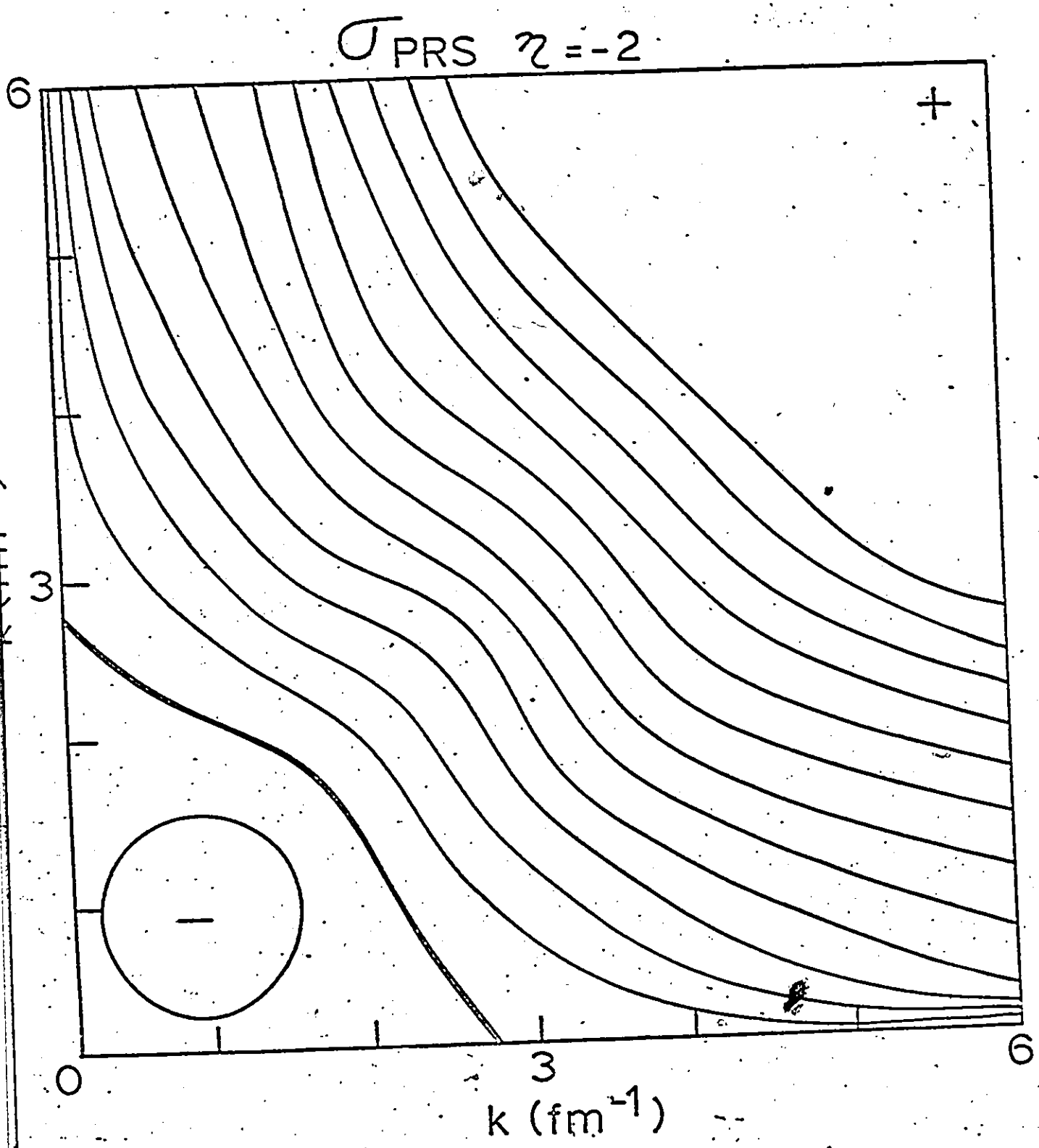

Fig. 5.5 (a) $\eta = -2.0$

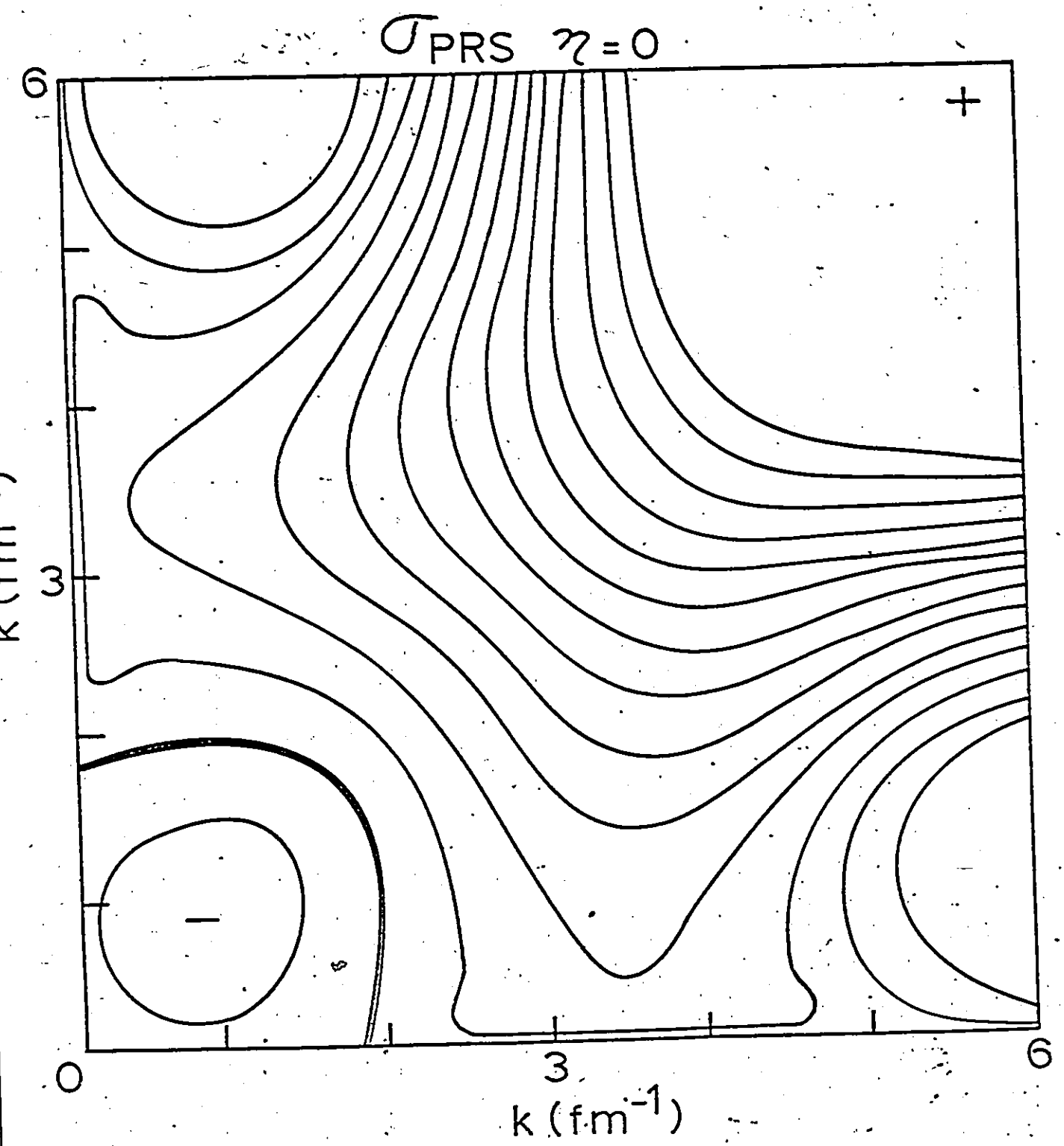

Fig. 5-5 (b) $\eta = 0.0$

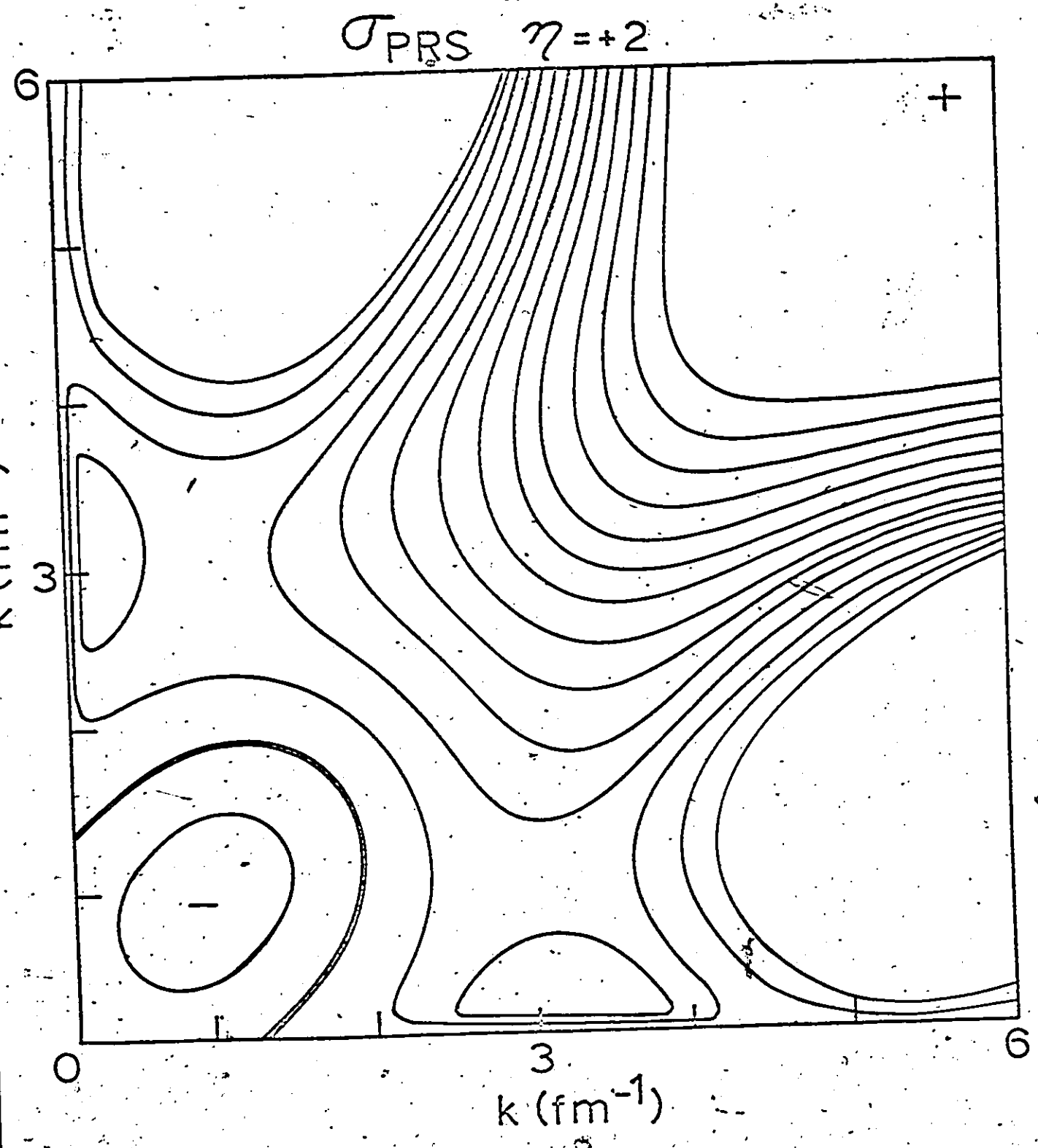

Fig. 5-5 (c) $\eta = 2.0$

$$k = c \tan \pi/4\ (1 + x). \tag{5.26}$$

The approximation (5.25) now becomes, more specifically,

$$\int_0^\infty F(k)\,dk = c\,\frac{\pi}{4}\int_{-1}^{+1} F\left[c \tan \frac{\pi}{4}(1+x)\right]\left[1 + \tan^2 \frac{\pi}{4}(1+x)\right]dx$$

$$= c\,\frac{\pi}{4}\sum_{i=1}^{N} F\left[c \tan \frac{\pi}{4}(1+x_i)\right]\left[1 + \tan^2 \frac{\pi}{4}(1+x_i)\right]w_i \tag{5.27}$$

c is a constant which can be used to alter the range of k-values, and of which the integral should be independent within a reasonable range. In this study, c is taken to be 1 fm^{-1}. The abscissas and weight factors x_i and w_i for N = 48 are taken from ref. 64 and shown in Table 5/1.

By interpolating through phase shift points at regular momentum intervals, the phase shift points at the 48k-values corresponding to the 48 x_i points can be obtained. One can then proceed to calculate $\sigma(k,k')$ and $\phi(k,k')$ at the 48 k points and 48 k' points. Similarly, $\langle k'|T(\omega)|k\rangle$ is determined only at 48 mesh points which are close enough to allow reliable interpolation.

(b) Construction of half-shell T of Baranger et al., i.e. $\phi(k,k')$

In Chapter II, section 2.2., $\phi(k,k')$ is shown to have a symmetric part $\sigma(k,k')$ and an antisymmetric part $\alpha(k,k')$. These can be separated so that the antisymmetric operator W_A contains only σ while the symmetric operator W_s contains α, as seen in equations (2.42), (2.46) and (2.47), i.e.

$$\langle k|W_s|k\rangle = \delta(k - k')\cos\delta(k) + \alpha(k,k')/(k^2 - k'^2), \tag{2.46}$$

Table 5/1

Abscissas and Weight Factors for Gaussian Integration

	Abscissas = $\pm x_i$	Weight Factors = w_i
	$\pm x_i$	w_i
N = 6	0.23861919	0.46791394
	0.66120939	0.36076157
	0.93246951	0.17132449
N = 48	0.03238017	0.06473769
	0.09700470	0.06446616
	0.16122236	0.06392424
	0.22476379	0.06311419
	0.28736249	0.06203942
	0.34875589	0.06070444
	0.40868648	0.05911484
	0.46690291	0.05727729
	0.52316098	0.05519950
	0.57722473	0.05289019
	0.62886740	0.05035904
	0.67787238	0.04761666
	0.72403413	0.04467456
	0.76715903	0.04154508
	0.80706620	0.03824135
	0.84358826	0.03477722
	0.87657202	0.03116723
	0.90587914	0.02742651
	0.93138669	0.02357076
	0.95298770	0.01961616
	0.97059159	0.01557932
	0.98412458	0.01147724
	0.99353017	0.00732755
	0.99877101	0.00315335

$$\langle k'|W_A|k\rangle = P\,(k^2 - k'^2)^{-1}\,\sigma(k,k'). \tag{2.47}$$

W_S and W_A are related by the conditions (2.42);

$$W_S^2 - W_A^2 = 1$$

$$W_A W_S - W_S W_A = 0 \tag{2.42}$$

Since $\sigma(k,k')$ is known, $\langle k'|W_A|k\rangle$ can be determined. $\alpha(k,k')$ can then be calculated from $\langle k'|W_S|k\rangle$. W_S is given as the square root of $(1 + W_A^2)$. The first step then is the calculation of the operator W_A^2. A proper treatment of the P singularity is essential. The singularity of W_A is separated out as

$$\langle k'|W_A|k\rangle = P(k^2 - k'^2)^{-1}\,\sigma(k',k') + r(k,k') \tag{5.28}$$

r is a smooth function given by

$$r\,(k,k') = [\sigma(k,k') - \sigma(k',k')]/(k^2 - k'^2) \tag{5.29}$$

Mukhopadhyay[65] has derived $\langle k'|W_A^2|k\rangle$ to be,

$$\langle k|W_A^2|k\rangle = -\delta(k - k')\,\sin^2\delta_0(k) - g(k,k') \tag{5.30}$$

with
$$g(k,k') = \int_0^\infty dq\,\{\sigma(k',k')[r(q,k) - r(k',k)](q^2 - k'^2)^{-1}$$

$$+ \sigma(k,k)[r(q,k') - r(k,k')](q^2 - k^2)^{-1}$$

$$+ r(q,k')\,r(q,k)\}. \tag{5.31}$$

g is a completely smooth and symmetric function. W_A^2 is also symmetric.

Similarly W_S can be separated as

$$\langle k'|W_S|k\rangle = \delta(k - k')\,\cos\delta_0(k) + p(k,k') \tag{5.32}$$

p is another smooth function given by

$$p(k,k') = \alpha(k,k')/(k^2 - k'^2) \tag{5.33}$$

The first condition of equation (2.42) involves smooth functions only, as we can see now.

Once $\sigma(k,k')$ is given, $g(k,k')$ is known. The next step is to determine $\alpha(k,k')$ or $p(k,k')$. From equation (2.42), we know that W_s must commute with W_A and that W_s is given by $\sqrt{1 + W_A^2}$. The well-known iterative procedure for the square root of a number can then be used. The set of linear equations

$$W_{s_n} W_{s'_n} = 1 + W_A^2 \tag{5.34}$$

is solved for $W_{s'_n}$ with W_{s_n} assumed given. The starting point of the next iteration is

$$W_{s_{n+1}} = \frac{1}{2} (W_{s_n} + W_{s'_n}) \tag{5.35}$$

For the first iteration, we take

$$W_{s_o} = 1 + \frac{1}{2} W_A^2 \tag{5.36}$$

so that all successive W_{s_n} will commute with W_A.

Equation (5.32) can be written as

$$\langle k' | W_{s_n} | k \rangle = \delta(k - k')\ c_n(k) + p_n(k,k'), \tag{5.37}$$

where $c_n(k)$ will converge to $\cos \delta_o(k)$. By using equations (5.30) and (5.37), equation (5.34) becomes

$$\begin{aligned} C_n(k)\, C_{n'}(k) &= 1 - \sin^2 \delta_o(k) = \cos^2 \delta_o(k) \\ g(k,k') &+ p_n(k,k')\, C_{n'}(k') + C_n(k) p_{n'}(k,k') \\ &+ \int_0^\infty dq\ p_n(k,q)\ p_{n'}(q,k') = 0 \end{aligned} \tag{5.38}$$

$C_{n'}$ is first determined from the first expression of (5.38) then the second equation is solved for $p_{n'}$. Gauss approximation is used to transform the integral, and hence the equation into a finite set of linear equations. Putting into matrix form and using 48 mesh points, it becomes

$$\begin{bmatrix} C_n(k_1) + p_n(k_1,k_1)X_1 & p_n(k_1,k_2)X_2 \cdots p_n(k_1,k_{48})X_{48} \\ C_n(k_2) + p_n(k_2,k_1)X_1 & p_n(k_2,k_2)X_2 \cdots p_n(k_2,k_{48})X_{48} \\ \vdots & \vdots \\ C_n(k_{48}) + p_n(k_{48},k_1)X_1 & p_n(k_{48},k_2)X_2 \; p_n(k_{48},k_{48})X_{48} \end{bmatrix} \begin{bmatrix} p_{n'}(k_1,k') \\ p_{n'}(k_2,k') \\ \vdots \\ p_{n'}(k_{48},k') \end{bmatrix}$$

$$= - \begin{bmatrix} g(k_1,k') + p_n(k_1,k')Cn'(k') \\ g(k_2,k') + p_n(k_2,k')C_{n'}(k') \\ \vdots \\ g(k_{48},k') + p_n(k_{48},k')C_{n'}(k') \end{bmatrix} \qquad (5.39)$$

for a fixed k' and for the nth iteration. $X_n = \pi/4(1 + k_n^2)W_n$ is the weight factor. The next iteration begins with.

$$C_{n+1} = \frac{1}{2}(C_n + C_{n'}) \qquad (5.40)$$

$$p_{n+1} = \frac{1}{2}(p_n + p_{n'})$$

For n = 0, the starting values used are

$$c_o(k) = 1 - \frac{1}{2}\sin^2 \delta_o(k) \qquad (5.41)$$

$$p_o(k,k') = -\frac{1}{2} g(k,k')$$

Once p_n is calculated, α is determined by the relation (5.33). α has

been computed not as a continuous function, but at 48 mesh points. The last step is to calculate ϕ from $\phi = \sigma + \alpha$.

In this study, the above numerical proceudre is used to generate $\phi(k,k')$ for each of the σ function calculated. In each case, 3 iterations are found to be sufficient for a desired accuracy. The procedure has been checked by comparing results from it with those computed exactly by other means. In Table 5/2, a few sample values of the function $\phi(k,k')$ of equation (2.37) for the ^1S_o Tabakin potential[66] are listed. The values obtained from the σ-function using the above procedure are compared with those calculated from the exact form (See Appendix A). As can be seen the numerical procedure gives quite good agreement.

(c) Calculation of off-shell T-matrix

$\phi(k,k')$ can now be used as input in equation (2.25) to construct the off-shell T-matrix. For a negative value of ω, the principal value integral is regularized to be

$$P\int_0^\infty dq\, \phi(q,k')\,\phi(q,k)\,(k^2 - q^2)^{-1}$$

$$= \int_0^\infty dq\, [\,\phi(q,k')\,\phi(q,k) - \phi(k,k')\,\phi(k,k)\,](k^2 - q^2)^{-1} \qquad (5.42)$$

Equation (2.25) becomes

$$\langle k'|T(\omega)|k\rangle = \phi(K,k')\cos\delta_o(k)$$

$$+ \int_0^\infty dq\, \{\,\phi(q,k')\,\phi(q,k)\,(\omega - q^2)^{-1}$$

$$-[\,\phi(q,k')\,\phi(q,k) - \phi(k,k')\,\phi(k,k)\,](k^2 - q^2)^{-1}\} \qquad (5.43)$$

TABLE 5/2

Comparison of exact and computed $\phi(k,k')$ and $\langle k|v|k'\rangle$ matrices for Tabakin's $^1S_0$ potential. $k = 0.950$ fm^{-1}.

k' (fm^{-1})	$\phi(k,k')$ (fm^{-1})		$\langle k\|v\|k'\rangle$ (MeV. fm^3)		
	Exact	computed from exact σ	Exact	computed from exact ϕ	computed from exact σ
0.054	-.02894	-.03512	-26.23	-26.02	-31.11
0.220	-.1142	-.1196	-25.38	-25.19	-26.02
0.501	-.2249	-.2280	-22.13	-21.97	-22.00
0.774	-.2772	-.2782	-17.96	-17.82	-17.69
0.950	-.2835	-.2835	-15.25	-15.12	-14.97
1.052	-.2791	-.2786	-13.77	-13.65	-13.50
1.596	-.1993	-.1981	- 7.55	- 7.45	- 7.34
1.996	-.1371	-.1362	- 4.91	- 4.82	- 4.75
3.333	-.06836	-.0690	- 1.87	- 1.82	- 1.82
4.541	-.05520	-.05606	- 1.07	- 1.05	- 1.05
6.549	-.04230	-.04306	- 0.55	- 0.53	- 0.53
10.28	-.02875	-.02930	- 0.23	- 0.22	- 0.22

Using the Gauss approximation for integrals, we got

$$\langle k'|T(\omega)|k\rangle = \phi(k,k') \cos\delta_o(k)$$
$$+ c\frac{\pi}{4}\sum_{i=1}^{N} \phi(q_i,k')\,\phi(q_i,k)(\omega - q_i^2)^{-1}$$
$$- [\,\phi(q_i,k')\,\phi(q_i,k) - \phi(k,k')\,\phi(k,k)\,]\ X$$
$$(k^2 - q_i^2)^{-1}\,(1 + q_i^2/c^2)w_i \qquad (5.44)$$

where $q_i = C \tan\frac{\pi}{4}(1 + x_i)$ and N = 48.

The matrix elements $\langle k|V|k'\rangle$ are obtained from $\langle k|T(\omega)|k'\rangle$ by setting $\omega = \infty$, giving us equation (2.26). In this study, the complete off-shell T matrix has been calculated for 4 ω values for finite nuclei and 6 ω values for nuclear matter. Table 5/2 also gives a comparison of the exact $\langle k|V|k'\rangle$ matrix with that obtained from the σ-function for Tabakin's potential. Again the agreement is close.

5.3 Nuclear Matter

In order to calculate the binding energy of nuclear matter, the reaction or G-matrix must first be constructed from the T-matrix.

(a) G-matrix

The reaction matrix is obtained from the T-matrix by matrix inversion in momentum space. The T-matrix calculated is already in the convenient momentum-space representation. In this study, the reference spectrum method of Bethe, Brandow and Petschek[67] is used. We have

become familiar with the definition of $T(\omega)$, equation (1.1) and the Bethe-Goldstone equation (1.7) i.e.

$$T(\omega) = V + V(\omega - k)^{-1} T(\omega) \tag{1.1}$$

and

$$G(\omega) = V + V\, Q(\omega - k)^{-1} G(\omega) \tag{1.7}$$

with the true energy spectrum $K = E(k_1) + E(k_2)$. In the reference spectrum approximation

$$k = k_R = k_1^2 + k_2^2 = k_{c.m.}{}^2/4 + k^2 \tag{5.45}$$

where k and $k_{c.m.}$ are the relative and centre-of-mass momenta, respectively. Hence.

$$\vec{k}_{c.m.} = \vec{k}_1 + \vec{k}_2$$

$$\vec{k} = (\vec{k}_1 - \vec{k}_2)/2 \tag{5.46}$$

The reference G is given by replacing the Pauli operator Q by 1 in the equation for G, i.e. eq. (1.7)

$$G_r(\omega) = V + V(\omega - k_{c.m.}{}^2/4 - k^2)^{-1} G_r(\omega)$$

$$= V + V(\omega_{c.m.} - k^2)^{-1} G_r(\omega) \tag{5.47}$$

where we have set $\omega_{c.m.} = \omega - k_{c.m.}^2/4$. $\vec{k}_{c.m.}$ commutes with V so that it can be replaced by its eigenvalue. $\omega_{c.m.}$ is therefore just a scalar. As one can see, $T(\omega_{c.m.})$ can be identified with $G_r(\omega)$. It is shown in BBP[67] that G is related to G_r by the integral equation

$$G(\omega) = G_r(\omega) + G_r(\omega) \quad [Q - 1] \quad (\omega - k)^{-1} G(\omega) \tag{5.48}$$

Substituting $T(\omega_{c.m.})$ for $G_r(\omega)$, we obtain equation (2.52) which is used in the matrix inversion process

$$G(\omega) = T(\omega_{c.m.}) + T(\omega_{c.m.}) \quad (Q - 1) \quad (\omega_{c.m.} - k)^{-1} G(\omega) \tag{2.52}$$

In nuclear matter, Q, the Pauli operator is defined to be

$$Q(\underset{\rightarrow}{k}_1,\underset{\rightarrow}{k}_2,k_F) = \begin{matrix} 1 \text{ if } |k_1| > k_F \text{ and } |k_2| > k_F \\ 0 \text{ otherwise} \end{matrix} \qquad (5.49)$$

for a pair of nucleons with momenta $\underset{\rightarrow}{k}_1$ and $\underset{\rightarrow}{k}_2$. k_F is the Fermi momentum. After transformation, Q depends on $|\underset{\rightarrow}{k}_{c.m.}|$, $|\underset{\rightarrow}{k}|$, k_f and the angle between $\underset{\rightarrow}{k}_{c.m.}$ and $\underset{\rightarrow}{k}$. The BG equation can become too complicated to handle. So the angle-averaged Pauli Operator[68] is employed. This involves averaging Q over the angle $(\underset{\rightarrow}{k}_{c.m.}, \underset{\rightarrow}{k})$ giving

$$\text{angle averaged } Q = \begin{matrix} 1 \text{ if } k^2 + k^2_{c.m.}/4 - kk_{c.m.} > k_F^2 \\ 0 \text{ if } k^2 + k^2_{c.m.}/4 < k_F^2 \\ (k^2 + k^2_{c.m.}/4 - k_F^2)/kk_{c.m.} \text{ otherwise} \end{matrix} \qquad (5.50)$$

Alternately, if

$$k^2 + k^2_{c.m.}/4 - kk_{c.m.} > k_F^2,$$

then $k - k_{c.m.}/2 > k_F$;

or when $k \geq k_F + k_{c.m.}/2$, $Q = 1$.

Similarly if $k^2 + k^2_{c.m.}/4 < k_F^2$, then when $k \leq k_F - k_{c.m.}/2$, $Q = 0$. In between, Q is the curve $(k^2 + k^2_{c.m.}/4 - k_F^2/kk_{c.m.})$. This angle-average Q is shown in Fig. 5-6.

Since $T(\omega_{c.m.})$ is a matrix which is known, using the angle-averaged Q, equation (2.52) can be solved as a set of inhomogeneous linear equations by matrix inversion suggested by Kohler and McCarthy[69]. Using equation (2.52), the matrix elements of G are given by

$$\langle k'|G(\omega)|k\rangle = \langle k'|T(\omega_{c.m.})|k\rangle + \frac{2}{\pi}\int dk'' k''^2 \frac{\langle k'|T(\omega_{c.m.})|k''\rangle\langle k''|Q-1|k''\rangle\langle k''|G(\omega)|k\rangle}{\omega_{c.m.} - k''^2} \qquad (5.51)$$

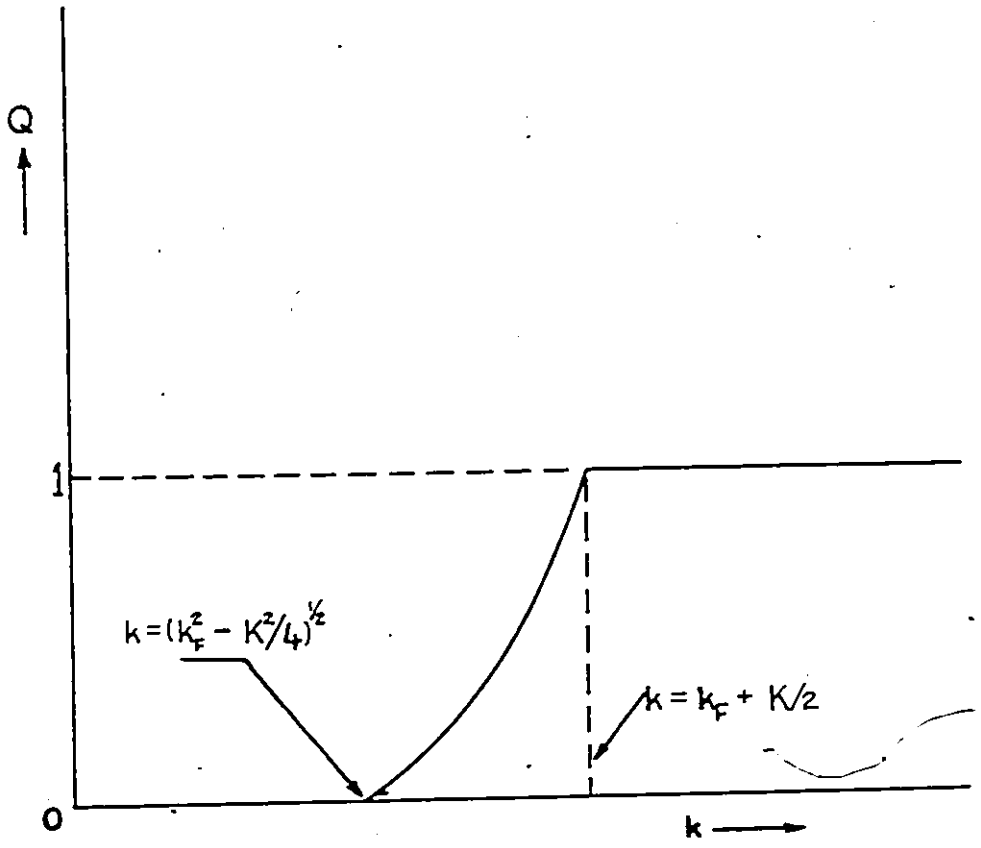

Fig. 5-6 Angle averaged Pauli operator Q

Using the transformation $k_i'' = c \tan \frac{\pi}{4}(1 + x_i)$ and the Gaussian approximation (5.27), matrix inversion allows us to write (5.51) as

$$\langle k_m'|G(\omega)|k\rangle = \langle k_m'|T(\omega_{c.m.})|k\rangle + \frac{c\pi}{4} \sum_{i=1}^{N} F_m(k_i'') \left(1 + \frac{k_i''^2}{c^2}\right) w_i \langle k_i''|G(\omega)|k\rangle \quad (5.52)$$

where

$$F_m(k_i'') = \left(\frac{2}{\pi}\right) k_i''^2 \frac{\langle k_m'|T(\omega_{c.m.})|k_i''\rangle [Q(k_i'') - 1]}{\omega_{c.m.} - k_i''^2} \quad (5.53)$$

for m = 1, 2.....N.

Rearranging, we get

$$\sum_{i=1}^{N} \left[\delta_{k_m', k_i''} - \frac{c\pi}{4} F_m(k_i'')\left(1 + \frac{k_i''^2}{c^2}\right) w_i\right] \langle k_i''|G(\omega)|k\rangle = \langle k_m'|T(\omega_{c.m.})|k\rangle \quad (5.54)$$

For each k, there are N linear equations in $\langle k_i''|G(\omega)|k\rangle$ where i" = 1, ..., N. Getting into matrix form (5.54) becomes

$$\begin{bmatrix} A_{1,1} & A_{1,2} \cdots\cdots\cdots A_{1,48} \\ A_{2,1} & \vdots \\ \vdots & \vdots \\ A_{48,1} \cdots\cdots\cdots\cdots & A_{48,48} \end{bmatrix} \begin{bmatrix} G_1,k \\ G_2,k \\ \vdots \\ G_{48},k \end{bmatrix} = \begin{bmatrix} T_1,k \\ T_2,k \\ \vdots \\ T_{48},k \end{bmatrix} \quad (5.55)$$

for a fixed k-value. Here $A_{m,i}$ is given by

$$A_{m,i} = \left[\delta_{k_m', k_i''} - c\frac{\pi}{4} F_m(k_i'')\left(1 + \frac{k_i''^2}{c^2}\right) w_i\right] \quad (5.56)$$

$$G_{i,k} = \langle k_i''|G(\omega)|k\rangle, \quad (5.57)$$

and $$T_{m,k} = \langle k'_m | T(\omega_{c.m.}) | k \rangle . \qquad (5.58)$$

w_i is of course, the weight factor.

In this study, the above calculations have been carried out using N = 48 points, so equation (5.55) is solved for 48 times. Since saturation properties are not studied, a fixed value is taken for k_F, the Fermi momentum, i.e. $k_F = 1.36\ f_m^{-1}$.

(b) Binding Energy of Nuclear Matter

The total potential energy per particle in the ^1S_o state is obtained from the G-matrix via the equation

$$\frac{PE}{A}\Big|^1 s_o = 6 \int_o^{k_F} dk \left[1 - \frac{3}{2}\frac{k}{k_F} + \frac{1}{2}\left(\frac{k}{k_F}\right)^3\right]$$

$$\times \langle k\ ^1s_o\ k_{c.m.} | G(\omega) | k\ ^1S_o\ k_{c.m.} \rangle \qquad (5.59)$$

with the following averages[70] used,

$$\frac{1}{4} k^2_{c.m.} = \frac{3}{5} k_F^2 \left(1 - \frac{k}{k_F}\right)\left\{1 + \left(\frac{k}{k_F}\right)^2 \left[3\left(2 + \frac{k}{k_F}\right)\right]^{-1}\right\} \qquad (5.60)$$

$$\omega = \left(\frac{m}{m^*}\right)\left(k^2 + \frac{k^2_{c.m.}}{4}\right) - 2U_o \frac{m}{\hbar^2} \qquad (5.61)$$

The hole spectrum is not self consistent, but uses the parameters obtained from a self-consistent calculation with the Reid (1968) potential[70], i.e., $\frac{m^*}{m} = 0.64$, $U_o = 79.05$ MeV at $k_F = 1.36\ f_m^{-1}$. $\frac{\hbar^2}{m}$ is again taken to be 41.47 MeV - fm^2.

Six point Gaussian integration is used in equation (5.59). The 6 abscissas and weight factors are given in Table 5/1. Appendix B

presents details for the Gaussian approximation for the integral between $k = 0$ and $k = k_F$. First, 6 k-values are determined from the six-points x_i using the transformation

$$k_i = c \tan \frac{\pi}{4} [0.596 (1 + x_i)] \tag{5.62}$$

derived in Appendix B. The corresponding 6 $k_{c.m.}$ values and 6 ω-values are then computed from equations (5.60) and (5.61), respectively. For each ω, $\omega_{c.m.}$ is $\omega - k^2_{c.m.}/4$. The matrix elements $\langle k|T(\omega_{c.m.})|k'\rangle$ are calculated for each $\omega_{c.m.}$. From these, the reaction matrix elements $\langle k|G(\omega)|k'\rangle$ are determined by the procedure described in the preceding section. From the 48 diagonal elements $\langle k|G(\omega)|k\rangle$ for each ω, the elements $\langle k_i|G(\omega)|k_i\rangle$ for the 6 k_i values given by equation (5.62) are computed using an interpolation routine. It should be noted that $\phi(k,k')$ has only been claculated once, as a 48 X 48 matrix. From it, 6 T-matrices can be generated. With the reaction matrix elements now available, the integral in equation (5.59) can be approximated into a summation series.

In calculating the binding energy of nuclear matter, only the contribution for the ^1S_o state is computed. The total contribution from the other states is taken from the Reid potential as calculated by Haftel and Tabakin[70] to be +5.71 MeV.

The binding energy is then $\{5.71 + [\frac{PE}{A}|^1S_o]\}$ MeV. For each of the 13 σ-functions shown in Table 6/1, the binding energy of nuclear matter has been calculated. The matrix elements $\langle k_i|G(\omega)|k_i\rangle$ are shown in Table 6/5 while the binding energies are given in Table 6/2.

In this study, the N = 48 mesh point system has been used throughout. A small test was first conducted to compare the efficiency

of a 48 point system and that of a 24 point system. In this test, the binding energy of Nuclear matter has been computed and the discrepancy between the two systems was found to be 4.5% as shown in Table 5/3. Even though a great deal of computing time is reduced by using the 24 Gaussian points, the discrepancy is still too wide; hence the adoption of the 48 point mesh.

5.4 Finite Nuclei

The matrix elements of the reaction matrix of finite nuclei are obtained in the harmonic oscillator representation. The Pauli operator is also represented in terms of oscillator states. The approach of Sauer[24] is followed. The binding energies for ^{16}O and ^{40}Ca have been calculated self-consistently following McCarthy and Davies[71].

(a) Reaction Matrix

In chapter II, section 2.3, the principle of the self-consistency of the single-particle wave functions (the Hartree-Fock self-consistency) for finite nuclei is mentioned. This poses great difficulty in practical calculation. However, self-consistent calculations carried out by Davies et al[72] indicate that the calculated wave functions are similar to the oscillator wave functions. One can therefore, in the first approximation, forget about HF self-consistency and try to solve the Bethe-Goldstone equation in the harmonic oscillator basis. The method of Sauer[24] which assumes QUQ = 0 is employed to calculate the relative-centre-of-mass (RCM) reaction matrix from the T-matrix in momen-

Table 5/3

Nuclear Matter: G-Matrix Elements and Binding Energy

σ_{RA} for N = 24 and N = 48

$k_F = 1.36\ Fm^{-1}$

	$\langle k\|G(\omega)\|k\rangle$ (Mev)	
k (Fm^{-1})	N = 24	N = 48
0.0316	- 4.15	-12.46
0.1599	-41.36	-46.71
0.3723	-38.75	-40.06
0.6549	-28.23	-28.70
0.9845	-15.72	-16.10
1.2721	- 7.82	- 7.76
-BE/A (Mev)	10.82	11.51

tum space, i.e.

$$G(\omega) = T(\omega - \tfrac{1}{2} e_{NL}) + T(\omega - \tfrac{1}{2} e_{NL}) \times \{Q\,[\omega - Q\,(\tfrac{1}{2} e_{NL} + K_{rel})Q]^{-1}\,Q - [\omega - \tfrac{1}{2} e_{NL} - K_{rel}]^{-1}\}G(\omega) \tag{5.63}$$

where $$e_{NL} = (2N + L + \tfrac{3}{2})\,\hbar\Omega \tag{5.64}$$

is the centre-of-mass energy as a function of the oscillator quantum $\hbar\Omega$.

$$\hbar\Omega = \frac{1}{b^2} \tag{5.65}$$

where b is the oscillator parameter. (NL) are quantum numbers of the centre-of-mass motion. Table 5/4 gives their values for ^{16}O and ^{40}Ca.

T-matrix elements of the ^1S_o state and all other (non ^1S_o) partial wave states are calculated separately. The matrix elements of the non ^1S_o states remain the same for different off-shell prescription in the ^1S_o state at the same ω value and (NL) set. The fully off-shell T-matrix for the ^1S_o state is computed from the σ-function in momentum space as described below. For the non-^1S_o states, the matrix elements $\langle k\ell SJ|T(\omega, NL)|k'\ell'SJ\rangle$ are obtained from the momentum-space matrix elements of V by matrix inversion, i.e.

$$T(\omega, NL) = V + V \frac{1}{\omega - \tfrac{1}{2} e_{NL} - K_{rel}} T(\omega, NL) \tag{5.66}$$

The matrix elements of V are given by[73]

$$\langle k|V^{JTS}_{\ell\ell'}|k'\rangle = U^{JTS}_{\ell\ell'}(k,k')\,A^{JS}_{\ell\ell'} \tag{5.67}$$

with

$$U^{JTS}_{\ell\ell'}(k,k') = \int_0^\infty r^2 dr\, j_\ell(kr) V_i^{JTS}(r)\, j_{\ell'}(k'r) \tag{5.68}$$

Table 5/4

Parameters Used in the Calculation of the G-Matrix of ^{16}O and ^{40}Ca

	^{16}O	^{40}Ca
$\hbar\Omega$ (Mev)	14.02	12.50
b (Fm)	1.72	1.82
2N+L	0,1,2,3	0,1,2,3,4,5

for i = central, tensor, or spin-orbit. (n,ℓ) are quantum numbers of the relative motion. S is the total spin and J, the total angular momentum.

$$\left.\begin{aligned}
&\text{For central terms, } A^{JS}_{\ell\ell'} = \delta_{\ell\ell'} \\
&\text{For spin-orbit terms, } A^{JS}_{\ell\ell'} = \frac{J(J+1) - \ell(\ell+1) - S(S+1)}{2}\,\delta_{\ell\ell'} \\
&\text{For tensor terms, } A^{JS}_{\ell\ell'} = 0 \quad \text{if } S = 0 \\
&\qquad = 2 \text{ if } S = 1,\ \ell = \ell' = J \\
&\qquad = \frac{-2(J-1)}{2J+1} \quad \text{if } S = 1,\ \ell = \ell' = J-1 \\
&\qquad = -\frac{2(J+1)}{2J+1} \quad \text{if } S = 1,\ \ell = \ell' = J+1 \\
&\qquad = \frac{6\sqrt{J(J+1)}}{2J+1} \quad \text{if } S = 1 \begin{cases} \ell = J-1,\ \ell' = J+1 \\ \ell = J+1,\ \ell' = J-1 \end{cases}
\end{aligned}\right\} \tag{5.69}$$

The Reid soft-core potential and OPEP is employed in non ^1S_o states, and the integrals involved in the computation of the $U^{JTS}_{\ell\ell'}(k,k')$ can be evaluated analytically, and are expressed in terms of the following ones[74]:

$$I^{(1)}_{\ell\ell'}(m,k,k') = \int_0^\infty r^2 dr\, j_\ell(kr)\,\frac{e^{-mr}}{r}\, j_{\ell'}(k'r), \tag{5.70}$$

$$I^{(2)}_{\ell\ell'}(m,k,k') = \int_0^\infty r^2 dr\, j_\ell(kr)\,\left(\frac{m}{r} + \frac{1}{r^2}\right)\frac{e^{-mr}}{r}\, j_{\ell'}(k'r) \tag{5.71}$$

$$I^{(3)}_{\ell\ell'}(m,k,k') = \int_0^\infty r^2 dr\, j_\ell(kr)\,\left(m^2 + \frac{3m}{r} + \frac{3}{r^2}\right)\frac{e^{-mr}}{r}\, j_{\ell'}(k'r) \tag{5.72}$$

The T-matrix in the harmonic oscillator basis can be calculated from the momentum space T by[73]

$$\langle n\ell,\ SJ|T(\omega,\ NL)|n'\ell',\ SJ\rangle = (-)^{n+n'}\ b_{rel}^3$$

$$\times \int_0^\infty k^2 dk \int_0^\infty k'^2 dk'\ R_{n\ell}(k\ b_{rel})\ \langle k\ell SJ|T(\omega,\ NL)|k'\ell' SJ\rangle$$

$$R_{n'\ell'}\ (k'\ b_{rel}). \tag{5.73}$$

Here,

$$R_{n,\ell}\ (x) = \left[\ \frac{\Gamma(n+\ell+3/2)}{n!\ b^3\ 2^{\ell+1/2}}\ \right]^{1/2}\ \frac{r^\ell\ e^{-r^2/4b^2}}{b^\ell \Gamma(\ell+3/2)}$$

$$\times\ {}_1F_1\ (-n,\ \ell+3/2,\ r^2/2b^2) \tag{5.74}$$

is the radial harmonic-oscillator wave function. b_{rel} is defined to be

$$b_{rel} = b\sqrt{2} \tag{5.75}$$

and is the oscillator parameter of relative motion. The momentum-space wave functions are normalized such that

$$\langle r|k\ell\rangle = (2/\pi)^{1/2}\ j_\ell(kr) \tag{5.76}$$

Again, Gaussian approximation is used in (5.73) to evaluate the integral.

One is now in a position to generate the matrix elements of $G(\omega)$ in the RCM representation from equation (5.63). A set of linear equations for $\langle NLn\ell SJ|G(\omega)|NL\ n'\ell' SJ\rangle$ can be written as[73]:

$$\sum_{n_2\ell_2} \{\delta_{nn_2}\delta_{\ell\ell_2} - \sum_{n_1\ell_1} \langle n\ell,\ SJ|T(\omega,\ NL)\ |n_1\ell_1, SJ\rangle$$

$$\times\ \left[\langle NL,\ n_1\ell_1|Q\ \frac{1}{\omega - Q[\ \tfrac{1}{2}\ e_{NL} + K_{rel}]}\right]Q$$

$$- \frac{1}{\omega - [\ \tfrac{1}{2}\ e_{NL} + K_{rel}]}\ |NL,\ n_2\ell_2\rangle]\}$$

$$\times \langle NL\ n_2\ell_2,\ SJ|G(\omega)|NL\ n'\ell',\ SJ\rangle$$

$$= \langle n\ell,\ SJ|T(\omega,\ NL)|n'\ell',\ SJ\rangle. \qquad (5.77)$$

The finite-nucleus analogue of the angle-average Pauli operator in nuclear matter is used. It is assumed to be diagonal in all relative and centre-of-mass oscillator quantum numbers. Hence,

$$Q(NL,\ n\ell) = \frac{1}{(2L+1)(2\ell+1)} \Sigma(2\lambda+1)\left|\langle n_1\ell_1 n_2\ell_2\lambda|NLn\ell\lambda\rangle\right|^2 \qquad (5.78)$$

where $\langle n_1\ell_1 n_2\ell_2\lambda|NLn\ell\lambda\rangle$ is the Moshinsky transformation bracket[70]. As one can see the G matrix elements off-diagonal in N, L are neglected. The summations over n_1 and n_2 in (5.77) are cut-off at n_{max} which is taken to be 5 in this study. To solve equation (5.77) we have[73]

$$\langle n\ell|\omega - [\tfrac{1}{2}e_{NL} + K_{rel}]|n'\ell'\rangle = (\omega - 1/2e_{NL})A_{n\ell,n'\ell'}(b) - B_{n\ell,n'\ell'}(b) \qquad (5.79)$$

and

$$\langle NLn\ell|\omega - Q[\tfrac{1}{2}e_{NL} + K_{rel}]Q|NLn'\ell'\rangle = \omega A_{n\ell,n'\ell'}(b) - Q(NLn\ell)Q(NLn'\ell')[\tfrac{1}{2}e_{NL}{}^{NL}A_{n\ell,n'\ell'}(b) + B_{n\ell,n'\ell'}(b)] \qquad (5.80)$$

where

$$A_{n\ell,n'\ell'}(b) = (-)^{n+n'}b_{rel}^3 \int_0^\infty dk\ k^2 R_{n\ell}(k\ b_{rel})R_{n'\ell'}(k\ b_{rel})$$

$$= (-)^{n+n'}b_{rel}^3\ C_{n\ell}C_{n'\ell'} \sum_{i=0}^{n}\sum_{j=0}^{n'} \alpha_i^{(n\ell)}\alpha_j^{(n'\ell')}$$

$$\times \int_0^\infty dk\ k^{2m}\ e^{-2k^2b^2} \qquad (5.81)$$

and $$B_{n\ell,n'\ell'}(b) = \frac{n^2}{m} \tilde{A}_{n\ell,n'\ell'} \cdot \tag{5.82}$$

$\tilde{A}_{n\ell,n'\ell'}$ is the same as $A_{n\ell,\, n'\ell'}$ except that the power of k (= 2m) is replaced by 2(m + 1). The expansion coefficients $\alpha_i^{(n\ell)}$ are given by the hypergeometric function

$$ {}_1F_1\,(-n,\ \ell + 3/2,\ 2k^2b^2) = \sum_{i=0}^{n} \alpha_i^{(n\ell)}\ k^{2i} \tag{5.83}$$

$C_{n\ell}$ is defined as

$$C_{n\ell} = \frac{(\sqrt{2}\ b)^{\ell}}{\Gamma(\ell + 3/2)} \left\{ \frac{2\Gamma\ (n + \ell + 3/2)}{n!} \right\}^{1/2} \tag{5.84}$$

Also

$$2m = 2 + \ell + \ell' + 2i + 2j. \tag{5.85}$$

The matrices (5.79) and (5.80) are inverted to give

$$\langle NL\ n_1\ell_1 | \frac{1}{\omega - Q(\sum e_{NL} + K_{rel})Q} | NL\ n_2\ell_2 \rangle$$

and

$$\langle NL\ n_1\ell_1 | \frac{1}{\omega - (\sum e_{NL} + K_{rel})} | NL\ n_2\ell_2 \rangle.$$

The final step is to transform the G(ω) matrix elements in the RCM representation to those in the two-body representation i.e. $\langle abJT|G(\omega)|cdJT\rangle$ where $a = (n_a\ell_a j_a)$ etc., using the usual procedure. These then serve as input in the calculation of binding energy.

(b) Binding Energy and Wound Integral

The self-consistent calculation of McCarthy and Davies[71] is followed to compute the binding energy. The total energy is given by

$$E = \sum_B T_B + \frac{1}{2} \sum_{B,C} \langle BC|G(\omega)|BC\rangle\ P_B P_C + \sum_B (1 - P_B) U_B \tag{5.86}$$

Here,

$$\omega = E_B + E_C \tag{5.87}$$

$$E_B = T_B + U_B \tag{5.88}$$

$$U_B = \sum_C \langle BC|G(\omega)|BC\rangle P_C \tag{5.89}$$

$$P_B = \left[1 - \sum_C \langle BC|\frac{\delta G(\omega)}{\delta \omega}|BC\rangle P_C\right]^{-1} \tag{5.90}$$

T and U are the single particle kinetic energy and potential energy respectively. The occupied single-particle states denoted by $|B\rangle$ or $|C\rangle$ are assumed to be pure oscillator states. Equations (5.86) and (5.90) are evaluated by interpolating on $G(\omega)$ through a third-degree polynomial

$$G(\omega) = G_0 + \omega G_1 + \omega^2 G_2 + \omega^3 G_3 \tag{5.91}$$

Four ω values (ω = -10, -30, -60 and -90 MeV) are employed in this study. The above then becomes a system of four equations enabling us to determine the coefficients G_0, G_1, G_2 and G_3. Differentiating (5.91) gives

$$\frac{\delta G(\omega)}{\delta \omega} = \omega + 2\omega G_2 + 3\omega^2 G_3 \tag{5.92}$$

which can be easily obtained at each of the four ω points.

In addition to the binding energy, the wound integral κ defined by

$$\kappa = -\frac{1}{A}\sum_{B,C}^{A} \langle BC|\frac{\delta G(\omega)}{\delta \omega}|BC\rangle \tag{5.93}$$

has also been calculated for ^{16}O (A = 16) and ^{40}Ca (A = 40). It is the average probability of finding a single-particle state $|B\rangle$ empty. The wound integral is an important quantity since its average value is essentially the expansion parameter of the many-body cluster expansion of the Goldstone series[53] for the ground state energy.

CHAPTER VI RESULTS AND ANALYSIS

In Table 6/1, an attempt is made to present a summary of the lengthy calculations conducted for this study. It may also serve as a quick guide to the diagrams and tables which present the results. In this chapter, these results are discussed and analyzed with two particular intentions in mind: to see how the results are affected by off-shell changes, and to draw out the constraints that should be imposed on the ^1s_o T-matrix and interior wave function. The σ function and Difference Function are starting points for generating these off-shell changes. As a measure of the effects of these variations, the binding energies are examined closely.

6.1 The σ-functions

Comparisons between Fig. 5-2 and Sauer's results show that the form σ_{RA} that we used and the associated distortions are very similar to his. From Fig. 5-5, it is easily observed that for the wave-function generated σ forms, the $\eta = -2$ function has smaller off-diagonal elements in comparison to the $\eta = 0$ result. Larger off-diagonal elements are observed in the $\eta = +2$ case. Checking through Table 6/2 which shows the variation of the binding energies of nuclear matter, ^{16}O and ^{40}Ca with different distortions, an attractive-repulsive effect observed by

Table 6/1

Outline of Calculations and Results

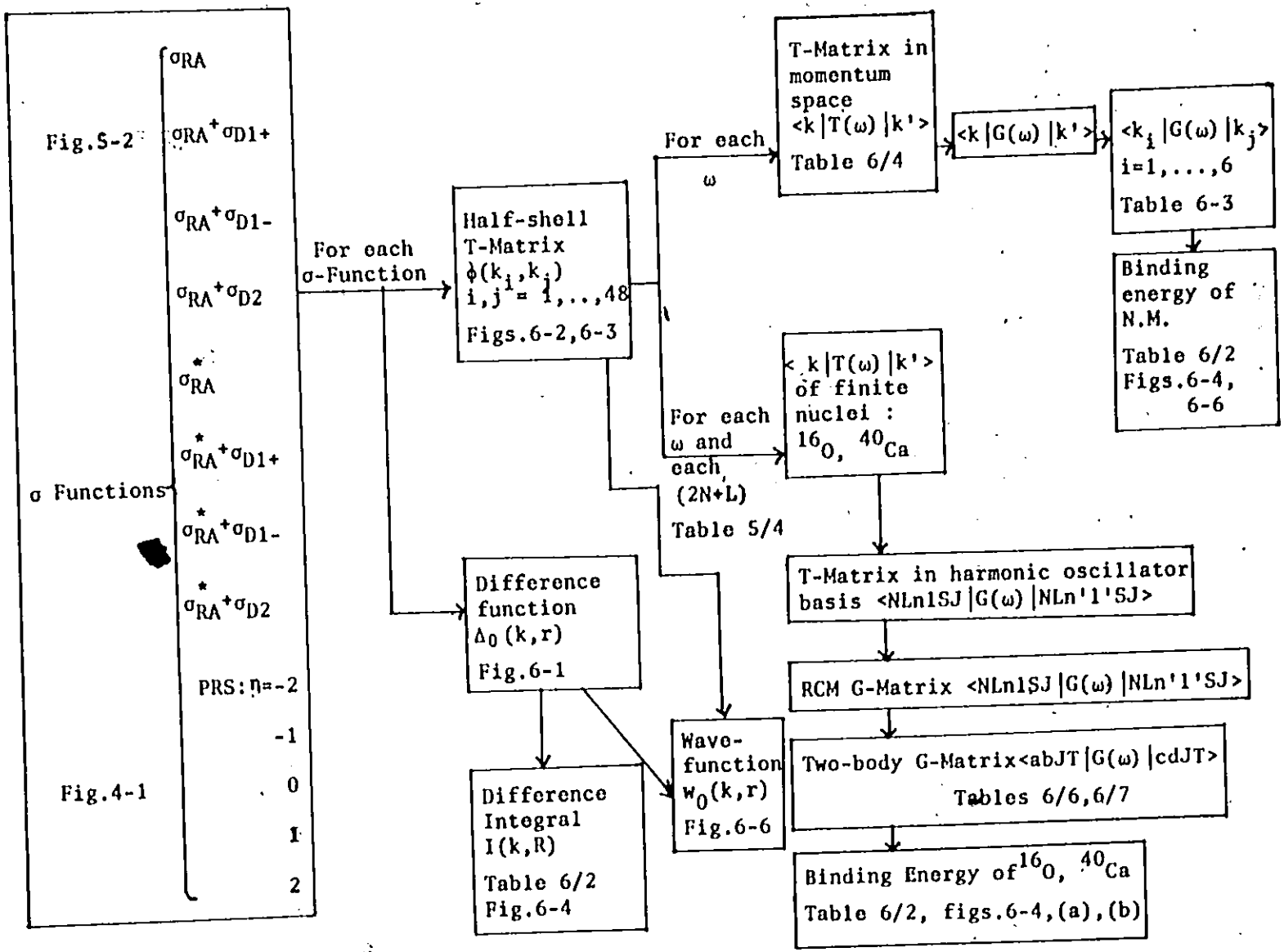

TABLE 6/2

Properties of ^{16}O, ^{40}Ca, and nuclear matter as computed from various $\sigma(k,k')$ functions. The 'difference integral' is defined in eq. (6.7) and is evaluated for $k = 1.052\ fm^{-1}$, $R = 1.43\ fm$.

Case	I(k,R)	^{16}O -BE/A (MeV)	^{16}O κ (%)	^{40}Ca -BE/A (MeV)	^{40}Ca κ (%)	Nuclear Matter -BE/A (MeV)
PRS: η= -2.0	1.82	4.20	10.3	6.91	12.7	12.30
-1.0	2.50	4.06	10.3	6.72	12.8	11.85
0.0	3.39	3.65	11.0	6.12	13.5	10.57
1.0	4.51	2.95	12.5	5.08	15.3	8.31
2.0	5.84	2.01	14.9	3.68	18.2	4.84
σ^*_{RA}	2.33	3.86	10.5	6.45	13.0	11.31
$+\sigma_{D1}{}^+$	3.65	3.57	11.2	5.95	14.0	10.18
$+\sigma_{D1}{}^-$	1.39	3.81	10.6	6.40	13.1	10.49
$+\sigma_{D2}$	1.72	3.94	10.3	6.60	12.6	11.89
σ_{RA}	2.60	3.72	10.9	6.22	13.4	10.89
$+\sigma_{D1}{}^+$	4.08	3.22	12.3	5.39	15.2	8.84
$+\sigma_{D1}{}^-$	1.55	3.84	10.5	6.45	13.0	11.16
$+\sigma_{D2}$	1.72	3.94	10.3	6.60	12.6	11.89

Sauer is present here as well. The results are consistent with the assumption that they depend on off-diagonal changes outside the low-energy region of σ. They are particularly sensitive to changes in the two strips closest to the axes, approximately 1.0 fm^{-1} wide. Large (small) off-diagonal elements there have a repulsive (attractive) effect with a corresponding decrease (increase) in the binding energy of ^{16}O, ^{40}Ca and nuclear matter. $\sigma_{RA} + \sigma_{D1-}$ and $\sigma_{RA} + \sigma_{D2}$ with smaller off-diagonal elements than those of σ_{RA}, have increased binding energies in nuclear matter and the two finite nuclei. The attraction is, of course, stronger for $\sigma_{RA} + \sigma_{D2}$. The direction of changes is reversed for $\sigma_{RA} + \sigma_{D1+}$ with increased off-diagonal elements. Consistent with these qualitative trends, the $\eta = -2$ function yields more attractive wave function and binding energies than the $\eta = 0$ result. As expected, a repulsion is observed for $\eta = +2$. σ_{RA}^{*} has a more complicated form for σ, and it becomes more difficult to trace these trends.

These change patterns are justified further by examining the behaviour of the difference function $\Delta_o(k,r)$ shown in Fig. 6-1. A more negative Δ_o, observed in the D1+ distortions and for increasing η values corresponds to a repulsion. The σ functions in this case show larger off-diagonal elements. The reverse is also observed. Smaller η values and the distortion D1- and D2 yield less negative functions Δ_o, and are more attractive. These observations are reflected in the nuclear matter and finite nuclei binding energies except for $\sigma_{RA}^{*} + \sigma_{D1-}$. It should be noted that the slope of Δ_o at $r = 0$ for this particular distortion is positive. For all the other examples, this slope is negative.

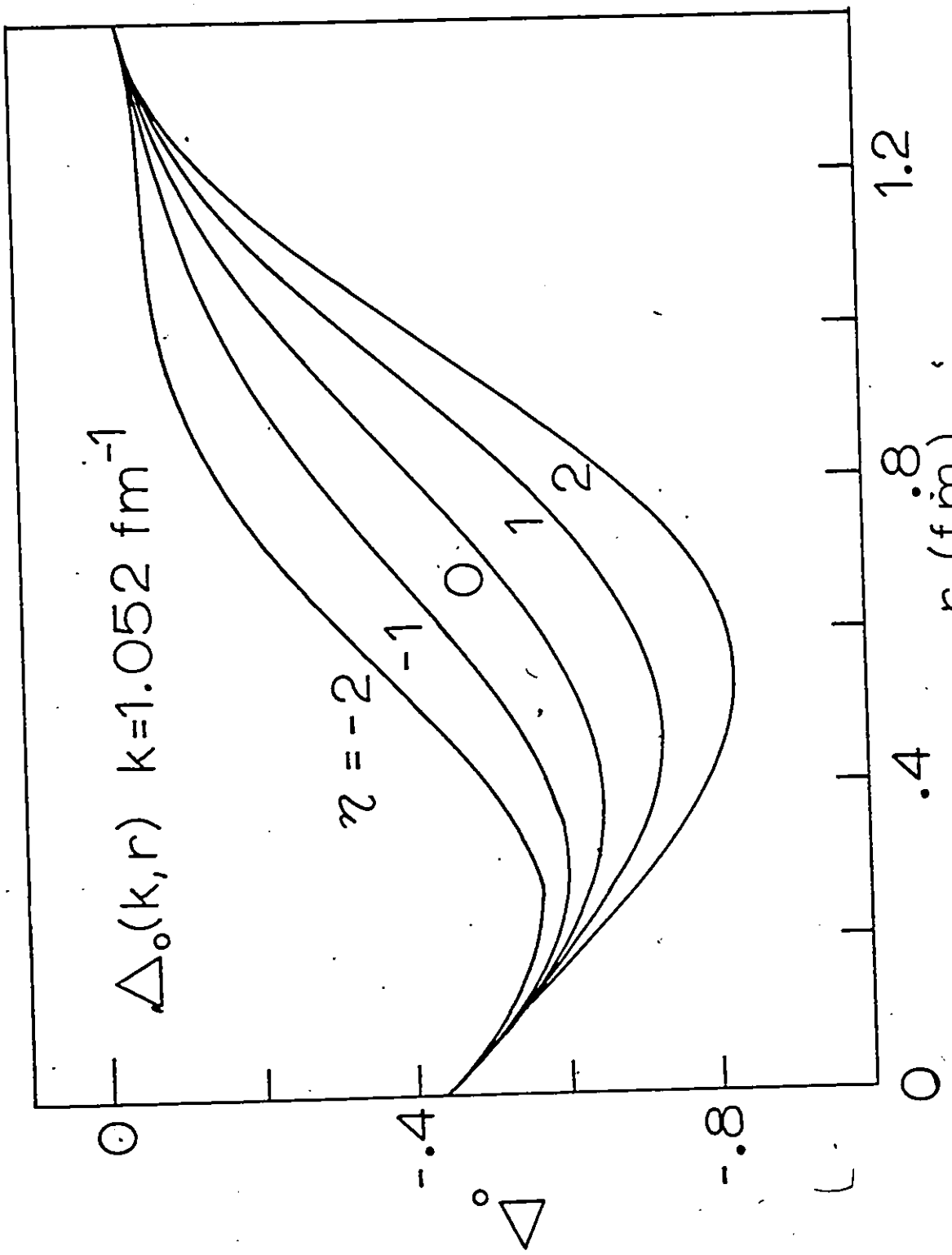

Fig. 6-1 (a) The difference function $\Delta_0(k,r)$ using the polynomial form of PRS.

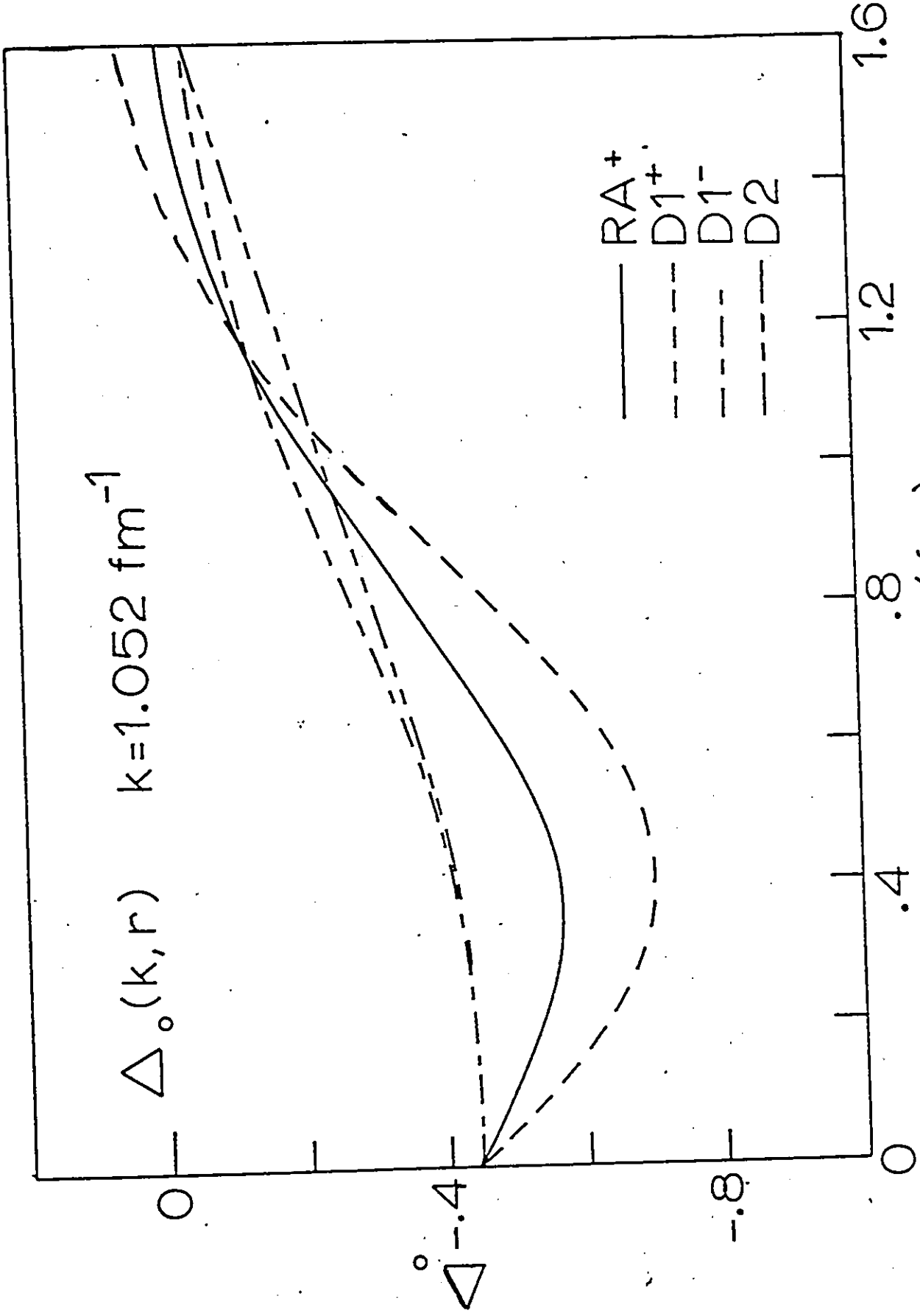

Fig. 6-1 (b) The difference function $\Delta_0(k,r)$ using σ_{RA^+} with distortions.

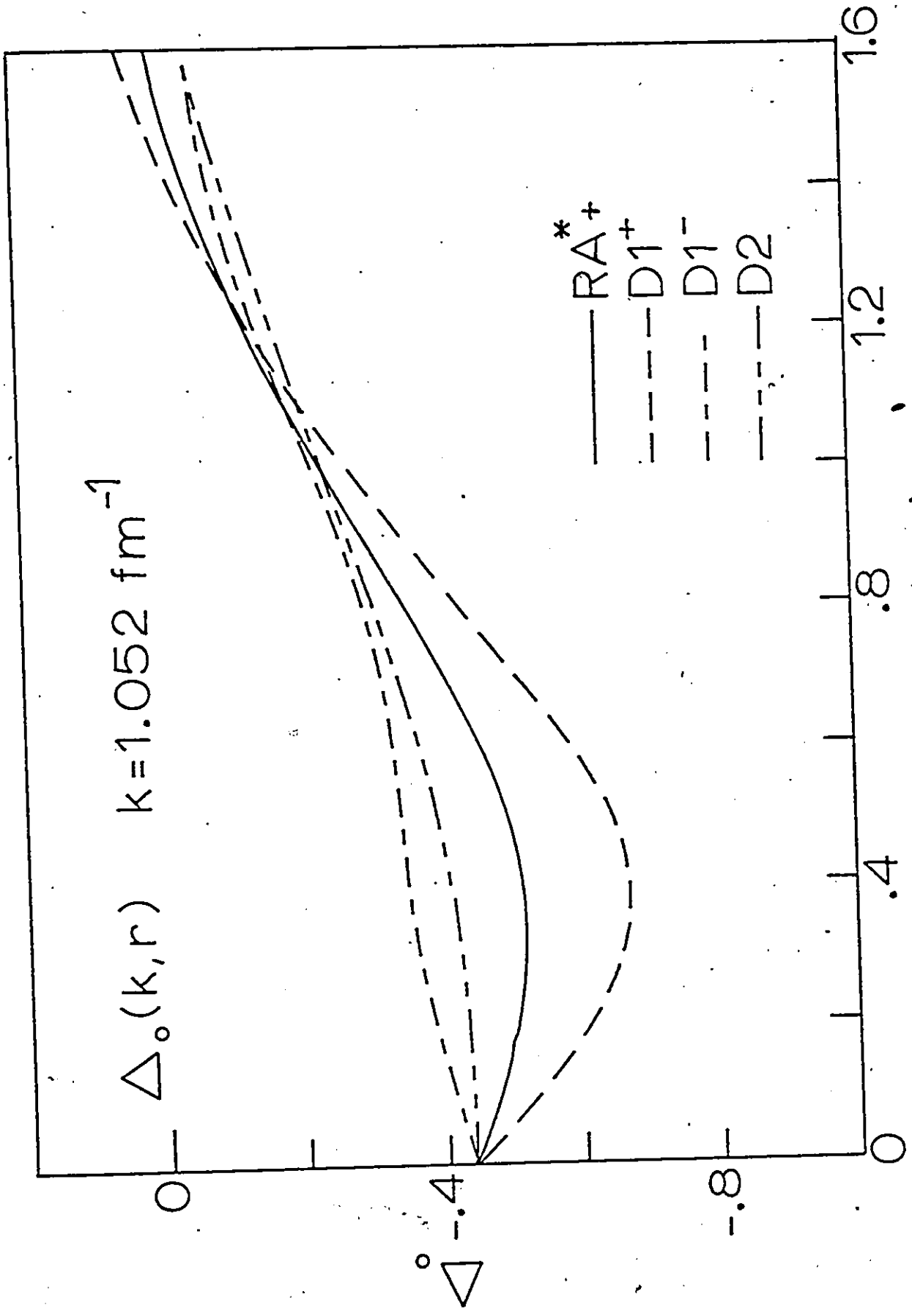

Fig. 6-1 (c) The difference function $\Delta_0(k,r)$ using v_{RA^*} with distortions.

It is of course premature to state that σ functions with positive slope of $\Delta_o(k,o)$ should be rejected. However, the importance of this slope is now surfacing and more will be said about it later.

The single-particle potential energies and occupation probabilities for the neutron states of ^{40}Ca for each of the σ functions are shown in Table 6/3. The attractive and repulsive effects are apparent here as well. The single particle potential energies decrease (increase) with larger (smaller) off-diagonal σ elements, with increasing (decreasing) n values and with more (less) negative Δ_o. Again the exception is the $\sigma_{RA}^* + \sigma_{D1-}$ distortion. The occupation probabilities behave in the same directions, though to a lesser degree.

Examining Table 6/2 reveals that $\sigma_{RA} + \sigma_{D1-}$ and $\sigma_{RA} + \sigma_{D2}$ yield a closer agreement in the results even though their σ functions appear to be quite different (see Fig. 5-2). However, in the relevant momentum region, their σ functions are quite similar. The opposite can be said of σ_{RA} and $\sigma_{RA} + \sigma_{D1+}$ whose σ functions may not look too different from one another, but the binding energies and single-particle potential energies show a wider difference than expected. By decreasing and increasing the σ elements in the momentum strips, one gains and loses binding energy within bounds at will. A larger off-diagonal variation there will result in a more appreciable variation.

The variation of the binding energies with the different distortions is most marked in nuclear matter. This is plausible because the distortions of σ or unitary transformations have been made not to affect the low momenta. In the average, nucleons have smaller momenta in ^{16}O and ^{40}Ca than in nuclear matter. The denser the many-nucleon

TABLE 6.3

Single-particle potential energies (in meV) and occupation probabilities for neutron states in ^{40}Ca.

	PRS: η									
	-2	0	2	σ_{RA}	$+\sigma_{D1+}$	$+\sigma_{D1-}$	$+\sigma_{D2}$	σ^{*}_{RA}	$+\sigma_{D1+}$	$+\sigma_{D1-}$
$V_{os_{1/2}}$	-65.3	-62.8	-53.2	-63.1	-59.8	-63.9	-64.7	-64.1	-62.3	-63.9
$V_{op_{3/2}}$	-52.8	-50.8	-43.7	-51.1	-48.5	-51.7	-52.3	-51.7	-50.3	-51.6
$V_{op_{1/2}}$	-49.0	-47.1	-40.4	-47.4	-45.0	-48.0	-48.5	-48.0	-46.7	-47.9
$V_{od_{5/2}}$	-41.6	-40.1	-35.2	-40.3	-38.4	-40.8	-41.1	-40.7	-39.6	-40.7
$V_{1s_{1/2}}$	-39.0	-38.6	-32.8	-37.7	-36.0	-38.2	-39.6	-38.2	-37.1	-38.2
$V_{od_{3/2}}$	-37.7	-36.3	-31.8	-36.5	-34.8	-37.0	-37.3	-37.0	-35.9	-36.9
$P_{os_{1/2}}$	.87	.86	.82	.86	.85	.86	.87	.87	.86	.86
$P_{op_{3/2}}$	.89	.88	.83	.88	.86	.88	.89	.88	.87	.88
$P_{op_{1/2}}$	.88	.87	.82	.87	.85	.88	.88	.88	.87	.88
$P_{od_{5/2}}$	.87	.87	.82	.87	.85	.87	.88	.87	.86	.87
$P_{1s_{1/2}}$	.86	.86	.81	.86	.84	.86	.87	.86	.85	.86
$P_{od_{3/2}}$	.86	.86	.81	.86	.84	.86	.86	.86	.85	.86

system, the larger its binding energy becomes and vice versa. For example, binding energies for ^{16}O, ^{40}Ca and nuclear matter for σ_{RA} are -3.72, -6.22 and -10.89 MeV, respectively. As the density of the system increases, so does the range of variation of the binding energies with respect to the distortions (2.19 MeV for ^{16}O, 3.23 MeV for ^{40}Ca and 7.46 MeV for nuclear matter). The above ranges are all between the PRS results of $\eta = -2$ and $\eta = +2$. Variations are much smaller in the Sauer type distortions, with a maximum of 3.05 MeV for nuclear matter.

As we can see, the variation of the binding energies with off-shell changes is appreciable, especially in nuclear matter. This is particularly so when we compare with the change resulting from different calculational methods using the same potential. For example, Sprung[76] calculated the binding energy for nuclear matter to be -11.76 MeV, and Kao[77], -14.3 MeV. In both cases, the same Reid soft core potential was used. The difference of 2.5 MeV is lower than the amount of variation generated purely by off-shell effects. We can conclude that off-shell effects are appreciable in many-body calculations and the knowledge of the correct off-shell behaviour is at least as important as the study of higher order diagrams.

Changes in binding energy are accompanied by changes in the respective wound integral κ. The values of κ computed for ^{16}O and ^{40}Ca display the familiar linear relationship with binding energies with a larger (smaller) κ corresponding to a smaller (larger) binding energy. (see Fig. 6-2). The wound integrals of D1+, $\eta = 1$ and $\eta = 2$ are off the

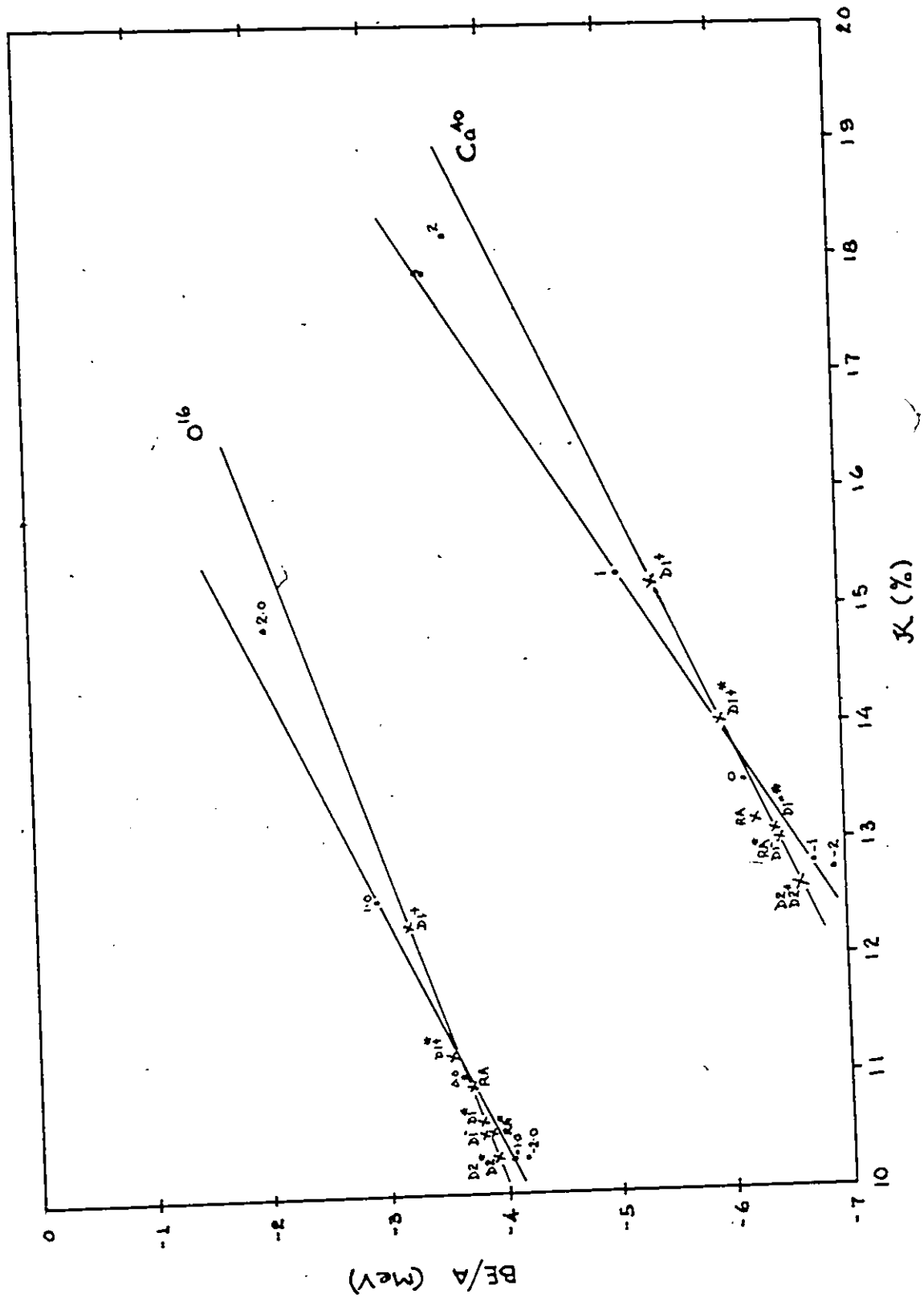

Fig. 6-2 Binding Energies of ^{16}O and ^{40}Ca as functions of the wound integral κ

line slightly, showing that for larger values of κ ($\kappa > 0.12$), the slope becomes somewhat larger.

Further results are now discussed with their relationship to the σ function and to the binding energies investigated.

6.2 The half-shell T matrix $\phi(k,k')$ and the T matrix.

In Fig. 6-3 the half-shell T, $\phi(k,k')$ of nuclear matter has been plotted as a function of k as well as k'. As we can see $\phi(k,k')$ acquires a smaller range when the off-diagonal elements are reduced. This has the effect of making the diagonal T-matrix for low momenta more negative, except for very small k ($k < 0.1$ fm^{-1}), then T matrix elements become very small. This is illustrated in Table 6/4. At $k > 1.78$ fm^{-1}, the diagonal T elements become positive, less so for smaller σ elements. The resulting binding energies of nuclear matter are increased.

From Fig. 6-3 we see that $\phi(k,k')$ decreases slowly with k or k' for large momenta. In Fig. 6-3(a), sharper peaks are shown for increased σ functions. Below 1.5 fm^{-1}, the half-shell T does not respond to off-shell changes.

McCarthy and Davies[71] have shown that for nuclear matter

$$\frac{\partial}{\partial\omega}\langle k|G(\omega)|k\rangle = -\frac{\lambda\kappa}{8\pi^3\rho}^{\dagger} \qquad (6.1)$$

where $\lambda = \hbar^2/m$. Since κ is proportional to $\partial G/\partial\omega$, the derivatives of the T matrix can be correlated to the binding energies. κ_R, the wound

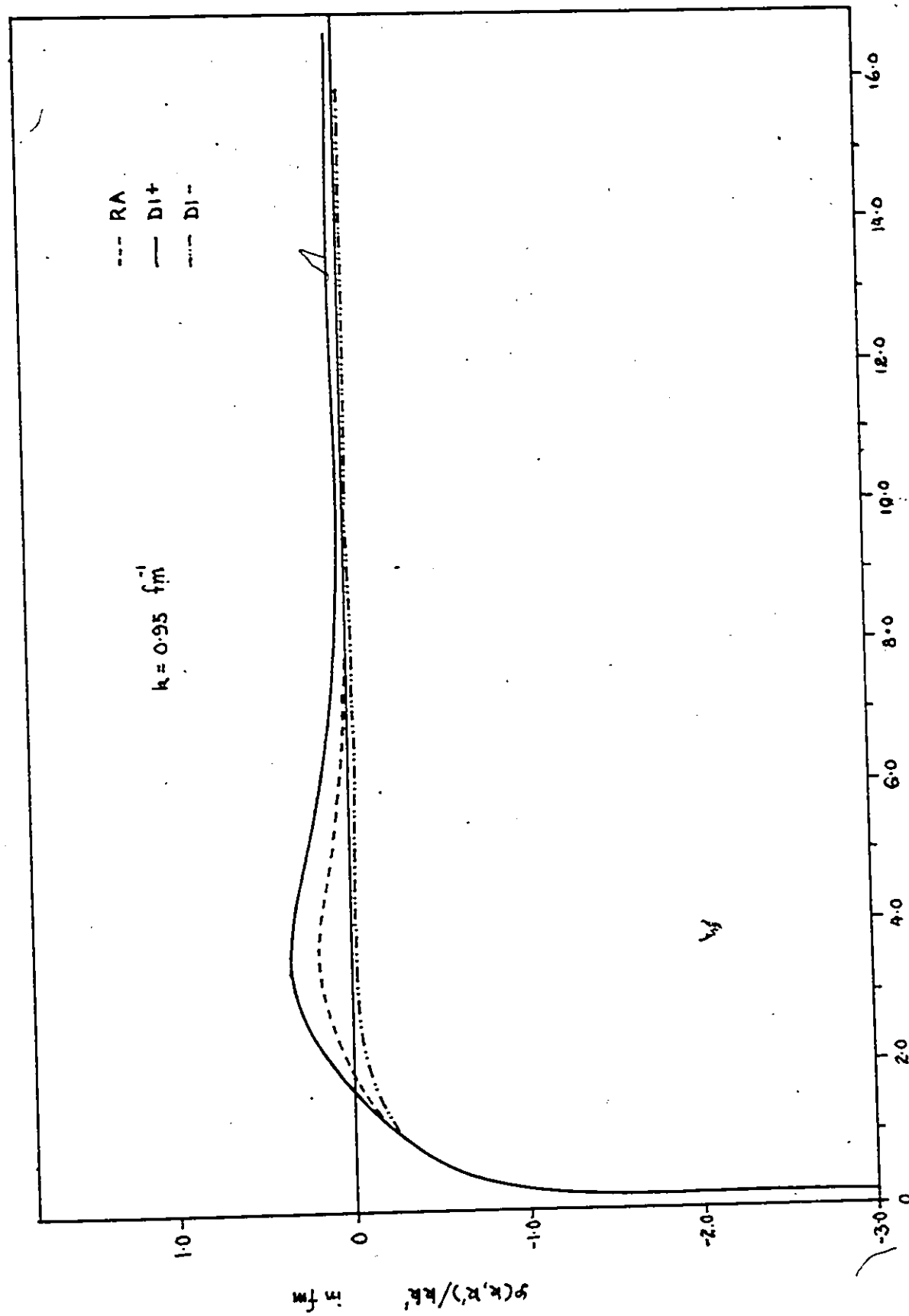

Fig. 6-3 (a) The half-shell T as a function of k'

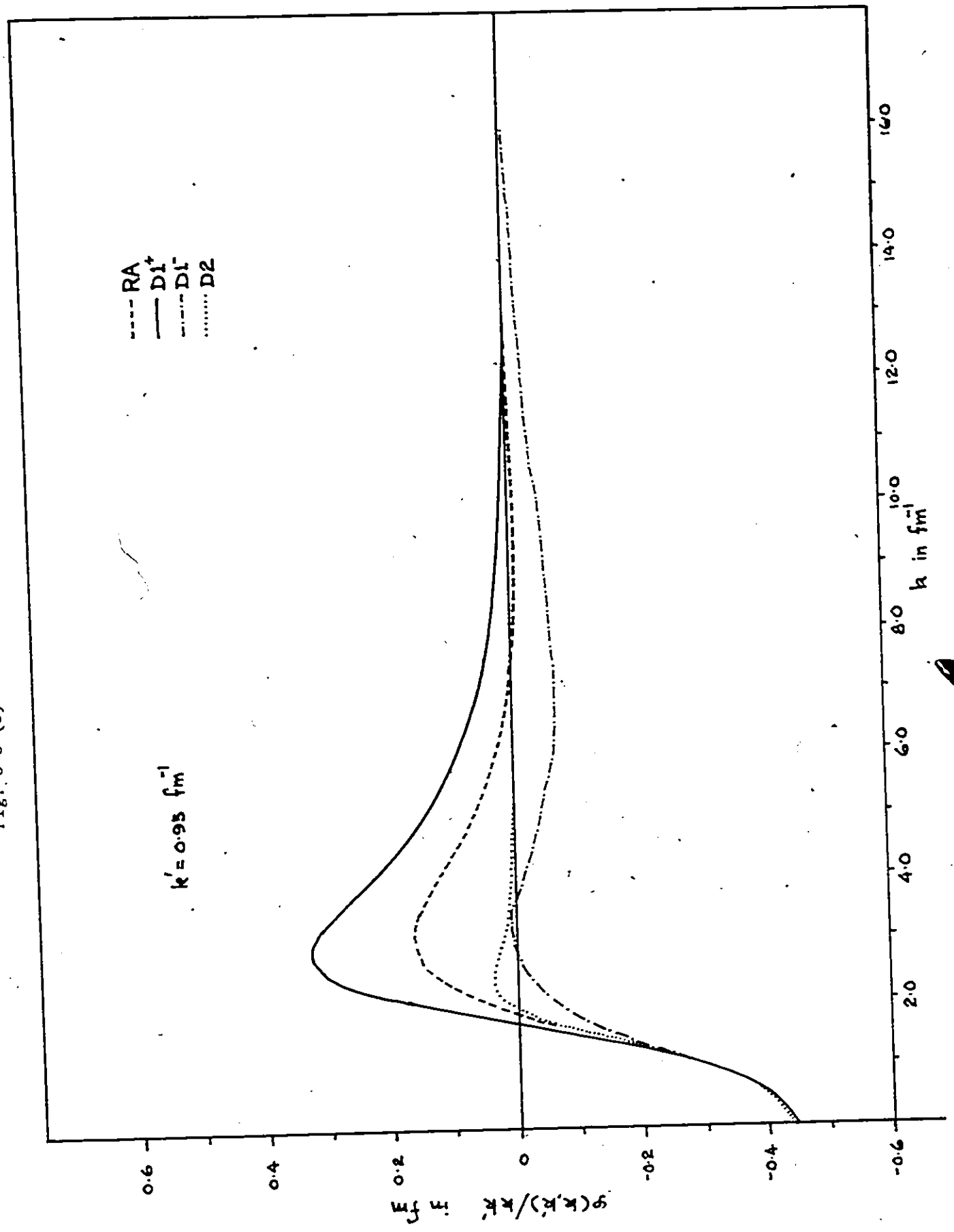

Fig. 6-3 (b) The half-shell T as a function of k

Table 6/4

Nuclear Matter : $^1S_0$ $\langle k|T(\omega)|k'\rangle$ in Units of Fm^{-1}

$k_F = 1.36\ Fm^{-1}$, $k = 1.052\ Fm^{-1}$, $\omega = 97.3$ Mev

$k(Fm^{-1})$	σ_{RA}	$\sigma_{RA}+\sigma_{D1+}$	$\sigma_{RA}+\sigma_{D1-}$	$\sigma_{RA}+\sigma_{D2}$	PRS : $\eta=-2$	$\eta=0$	$\eta=2$
0.00097	-0.0005	-0.0006	-0.0006	-0.0005	-0.0001	-0.0003	-0.0003
0.01247	-0.0072	-0.0080	-0.0076	-0.0071	-0.0014	-0.0041	-0.0037
0.03694	-0.0226	-0.0248	-0.0235	-0.0222	-0.0045	-0.0126	-0.0118
0.07406	-0.0430	-0.0465	-0.0438	-0.0419	-0.0106	-0.0272	-0.0259
0.12347	-0.0707	-0.0750	-0.0700	-0.0678	-0.0255	-0.0535	-0.0517
0.18494	-0.1044	-0.1054	-0.1036	-0.1009	-0.0579	-0.1072	-0.0919
0.25834	-0.1445	-0.1399	-0.1433	-0.1407	-0.0902	-0.1481	-0.1417
0.34481	-0.1892	-0.1756	-0.1885	-0.1859	-0.1176	-0.1932	-0.1875
0.44501	-0.2389	-0.2159	-0.2370	-0.2356	-0.0902	-0.2410	-0.2365
0.56131	-0.2853	-0.2448	-0.2885	-0.2885	-0.1637	-0.2884	-0.2880
0.69724	-0.3342	-0.2805	-0.3377	-0.3412	-0.1740	-0.3305	-0.3388
0.85816	-0.3697	-0.2998	-0.3771	-0.3840	-0.1626	-0.3578	-0.3830
1.05220	-0.3745	-0.2905	-0.3864	-0.3940	-0.1098	-0.3532	-0.4093
1.29175	-0.3170	-0.2189	-0.3391	-0.3270	-0.0174	-0.2868	-0.3974
1.59607	-0.1505	0.0099	-0.2401	-0.1504	-0.2619	-0.1182	-0.3208
1.99616	0.1102	0.0434	-0.1583	0.0395	0.6631	0.1971	-0.1477
2.54415	0.4438	0.1008	0.0887	0.0886	1.1869	0.6680	0.1584
3.33297	0.6672	0.1331	0.0020	0.0507	1.4714	1.1152	0.6483
4.54128	0.4036	0.9713	-0.2077	0.0234	0.4453	0.9222	1.4389
6.54877	0.5800	0.5214	-0.4804	0.0087	-1.2711	-0.0195	1.6817
10.58331	-0.0749	0.2491	-0.4950	-0.0001	0	0	0
18.53877	-0.0450	0.1070	-0.2970	0	0	0	0

integral of the "reference" wave function is given by[6]

$$-\frac{\lambda\kappa_R}{8\pi^3\rho} = \frac{\partial}{\partial\omega}\langle k|T(\omega)|k\rangle \tag{6.2}$$

Equation (2.25) expresses the T-matrix in terms of the half-shell T, i.e.:

$$\langle k'|T(\omega)|k\rangle = \phi(k,k')\cos\delta_o(k) + \int_o^\infty dq\,[(\omega - q^2)^{-1} - P(k^2 - q^2)^{-1}]\,\phi(q,k')\,\phi(q,k) \tag{2.25}$$

If $\phi_{RA}(k,q)$ is the half-shell T-matrix element of σ_{RA} and $\phi_D(k,q)$ that of the distorted σ-functions, differentiating (2.25) for the case of $k = k'$ yields

$$\frac{\partial}{\partial\omega}\langle k|T_{RA}(\omega)|k\rangle = \int_o^\infty q^2 dq\,\phi_{RA}^2(k,q)\,(\omega - q^2)^{-2}$$

and

$$\frac{\partial}{\partial\omega}\langle k|T_D(\omega)|k\rangle = \int_o^\infty q^2\,dq\,\phi_D^2(k,q)\,(\omega - q^2)^{-2} \tag{6.3}$$

If $\Delta k_R^{\,{}^1S_o}$ is the ${}^1S_o$ contribution to the change in the reference wound integral, we have, from eq. (6.2):

$$(\lambda/8\pi^3\rho)\,\Delta k_R^{\,{}^1S_o} = \frac{2}{\pi}\int_o^\infty q^2\,dq[\,\phi_D^2(k,q) - \phi_{RA}^2(k,q)\,](\omega - q^2)^{-2} \tag{6.4}$$

---

† The G matrix elements here are antisymmetrized i.e. $\langle k|G(\omega)|k\rangle \rightarrow \langle\mu\nu|G(\omega)|\mu'\nu' - \nu'\mu'\rangle$, where particles in the single-particle states μ and ν have relative momentum $\vec{k}$ and particles in the states μ' and ν' have relative momentum $\vec{k}'$.

The integrand in Eq. (6.3), D(q) for k = 0.95 fm^{-1} has been plotted as a function of q, for Sauer type distortions in Fig. 6-4. The largest contribution to D(q) comes from q = 2.5 to 5.0 fm^{-1}. D(q) drops to almost zero at about q = 6 fm^{-1} for all distortions. This implies that far off-shell T matrix elements in the region k = 2.5 to 5.0 fm^{-1} are important in accounting for changes in the reference wound integral. These changes are reflected in changes in κ and hence in the binding energies. The wound integral κ_R is proportional to $\partial T(\omega)/\partial\omega$, and $\partial T(\omega)/\partial\omega$ is, in turn, bilinear[1,21] in $\phi(k,k')$. We now have the theoretical justification of the observed correlation between the nuclear matter binding energies and the T matrix. A similar explanation can be applied to ^{16}O and ^{40}Ca. We have shown that the nuclear matter binding energy is sensitive to a large region of the off-shell T-matrix, from k = 2.5 fm^{-1} to k = 5.0 fm^{-1}. Our observations are slightly different from those of Haftel and Tabakin[6] who showed that the far-off-shell elements for $k \gtrsim 6$ fm^{-1} play a significant role in nuclear matter. This is because the Reid potential used in their calculations is not the same as our modified RA potential. Their half-shell T-matrix elements do not show any evidence of decreasing in magnitude up to k = 10 fm^{-1}.

Using σ_{RA} as reference in Fig. 6-3, we observe that σ functions larger than σ_{RA} yield larger $\phi(k,k')$ and vice versa. In Fig. 6-4, increased (decreased) σ diagonal matrix elements yield a positive (negative) deviation of D(q) values resulting in decreased (increased) binding energies of nuclear matter.

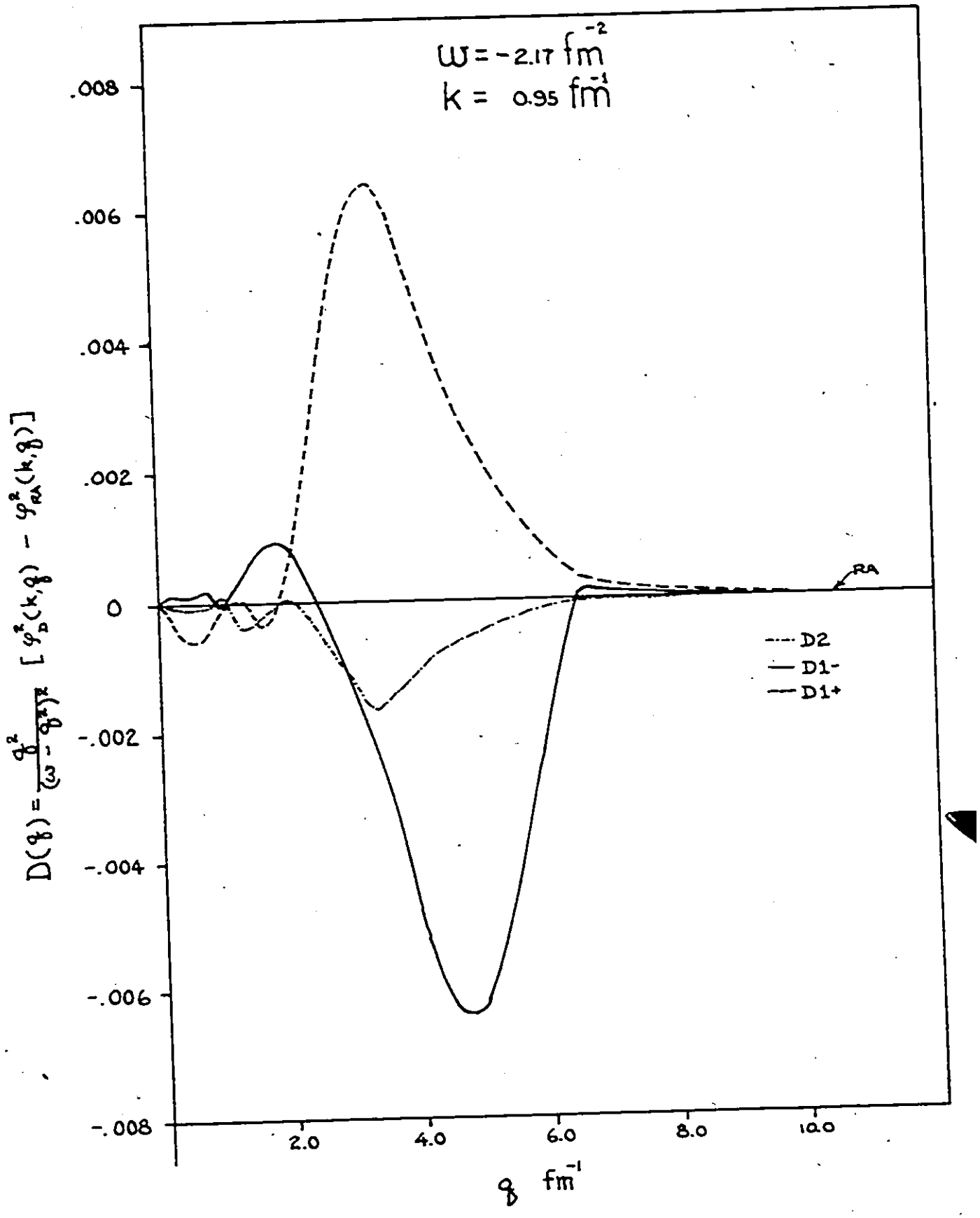

Fig. 6-4 D(q) as a function of q

6.3 The Reaction Matrix

From Table 6/5 where the diagonal G-matrix elements in momentum space $\langle k|G(\omega)|k\rangle$ of nuclear matter are presented for 6k and $\omega(k)$ values, we observe that the sensitivity of the G-matrix elements to variation in ω in the ^1s_o channel is not very great. The variation in the ^1s_o channel is already the most marked. Similarly, the diagonal two-body G-matrix elements of ^{16}O and ^{40}Ca exhibit the same small variation of ω as shown in Tables 6/6 and 6/7. However, the matrix elements decrease in magnitude with increasing negative ω.

In the case of nuclear matter, the G-matrix elements are relatively insensitive to the centre-of-mass momentum $k_{c.m.}$ as the dependence of the diagonal elements on $k_{c.m.}$ is insignificant. The G-matrix is most sensitive to the relative momentum k and it is instructive to consider how the diagonal matrix elements vary with k in Fig. 6-5. The ^1s_o diagonal G matrix element becomes repulsive with increasing k, reaches a maximum at about 2.8 fm^{-1} and then goes to zero at large values of k. Comparison between Table 6/5 and Fig. 6-5 for very low k values ($k < 0.05$ fm^{-1}) reveals that the calculated diagonal G elements are larger than they should be. However, the G matrix elements at such low momenta contribute very little to the binding energy because of small phase space factors. This discrepancy may be due to an error in matrix inversion since a small error in matrix inversion is magnified at such low values of k[65]. Essentially $k^2 \langle k|G(\omega)|k\rangle$ is calculated by matrix inversion. This discrepancy is reflected as a 0.13% difference in the binding energy.

Table 6/5

$\langle k|G(\omega,k)|k\rangle$ in Units of Mev for $^1S_0$ Channel

Case	k in Units of Fm^{-1}					
	0.0316	0.1599	0.3723	0.6549	0.9845	1.2721
σ_{RA}	-19.58	-72.35	-61.38	-44.00	-24.54	-11.28
$+\sigma_{D1+}$	-13.06	-70.32	-56.68	-38.29	-19.59	- 7.24
$+\sigma_{D1-}$	-19.58	-72.61	-62.32	-44.40	-25.45	-12.87
$+\sigma_{D2}$	-26.11	-76.43	-65.00	-46.52	-26.20	-12.54
σ^*_{RA}	-19.58	-73.37	-62.93	-45.08	-25.29	-12.19
$+\sigma_{D1+}$	-13.06	-72.35	-61.94	-41.82	-21.68	- 9.61
$+\sigma_{D1-}$	- 6.53	-73.12	-61.10	-43.97	-25.43	-12.71
$+\sigma_{D2}$	-26.11	-76.43	-65.00	-46.52	-26.20	-12.54
PRS: η =-2	-189.30	-86.88	-65.47	-46.66	-27.36	-14.30
-1	-182.77	-84.84	-64.06	-45.49	-26.54	-13.56
0	-182.77	-80.51	-60.35	-42.13	-23.88	-11.57
1	-182.77	-72.86	-53.77	-36.23	-19.20	- 8.21
2	-169.71	-60.38	-43.52	-27.17	-12.19	- 3.31

Table 6/6

^{16}O : $\langle n|\, G(\omega)\,|n\rangle$ in Units of Mev of $^1S_0$ Channel

N = L = 0

Case	ω Mev	n = 0	n = 1
σ_{RA}	-10	-6.52	-4.80
	-30	-6.44	-4.70
	-60	-6.39	-4.63
	-90	-6.36	-4.58
$+\sigma_{D1+}$	-10	-6.43	-4.19
	-30	-6.30	-3.96
	-60	-6.16	-3.70
	-90	-6.06	-3.46
$+\sigma_{D1-}$	-10	-6.49	-4.96
	-30	-6.39	-4.88
	-60	-6.33	-4.83
	-90	-6.28	-4.81
$+\sigma_{D2}$	-10	-6.55	-4.87
	-30	-6.49	-4.81
	-60	-6.47	-4.79
	-90	-6.46	-4.78
σ^*_{RA}	-10	-6.47	-4.70
	-30	-6.35	-4.59
	-60	-6.25	-4.48
	-90	-6.17	-4.40
$+\sigma_{D1+}$	-10	-6.29	-3.93
	-30	-6.07	-3.64
	-60	-5.80	-3.27
	-90	-5.56	-2.94
$+\sigma_{D1-}$	-10	-6.50	-4.97
	-30	-6.41	-4.89
	-60	-6.36	-4.85
	-90	-6.32	-4.82
$+\sigma_{D2}$	-10	-6.55	-4.87
	-30	-6.49	-4.81
	-60	-6.47	-4.79
	-90	-6.45	-4.78

Table 6/6 (Continued)

Case	ω Mev	n = 0	n = 1
PRS : η=-2.0	-10	-6.74	-5.14
	-30	-6.68	-5.02
	-60	-6.66	-4.93
	-90	-6.65	-4.86
-1.0	-10	-6.64	-4.99
	-30	-6.58	-4.91
	-60	-6.56	-4.87
	-90	-6.56	-4.85
0.0	-10	-6.42	-4.63
	-30	-6.30	-4.52
	-60	-6.19	-4.44
	-90	-6.11	-4.37
1.0	-10	-6.08	-4.04
	-30	-5.82	-3.83
	-60	-5.52	-3.59
	-90	-5.28	-3.39
2.0	-10	-5.60	-3.18
	-30	-5.11	-2.79
	-60	-4.51	-2.28
	-90	-4.01	-1.83

Table 6/7

^{40}Ca : $\langle n|G(\omega)|n\rangle$ in Units of Mev for $^1S_0$ Channel

N = L = 0

Case	ω Mev	n = 0	n = 1	n = 2
σ_{RA}	-10	-5.81	-4.65	-2.82
	-30	-5.76	-4.57	-2.75
	-60	-5.71	-4.50	-2.70
	-90	-5.69	-4.46	-2.66
$+\sigma_{D1+}$	-10	-5.75	-4.18	-2.27
	-30	-5.65	-3.98	-2.13
	-60	-5.54	-3.74	-1.97
	-90	-5.45	-3.54	-1.82
$+\sigma_{D1-}$	-10	-5.78	-4.75	-3.00
	-30	-5.71	-4.67	-2.95
	-60	-5.65	-4.63	-2.92
	-90	-5.61	-4.60	-2.90
$+\sigma_{D2}$	-10	-5.84	-4.71	-2.89
	-30	-5.81	-4.66	-2.85
	-60	-5.79	-4.64	-2.83
	-90	-5.78	-4.63	-2.82
σ^*_{RA}	-10	-5.77	-4.57	-2.67
	-30	-5.68	-4.47	-2.57
	-60	-5.60	-4.38	-2.47
	-90	-5.53	-4.31	-2.39
$+\sigma_{D1+}$	-10	-5.63	-3.98	-1.92
	-30	-5.46	-3.72	-1.71
	-60	-5.23	-3.39	-1.43
	-90	-5.03	-3.10	-1.18
$+\sigma_{D1-}$	-10	-5.80	-4.75	-3.00
	-30	-5.73	-4.68	-2.95
	-60	-5.68	-4.64	-2.92
	-90	-5.65	-4.61	-2.90
$+\sigma_{D2}$	-10	-5.84	-4.71	-2.89
	-30	-5.81	-4.66	-2.85
	-60	-5.79	-4.64	-2.83
	-90	-5.78	-4.63	-2.82

Table 6/φ (Continued)

Case	ω Mev	n = 0	n = 1	n = 2
PRS : n=-2.0	-10	-5.98	-4.91	-3.24
	-30	-5.95	-4.83	-3.15
	-60	-5.94	-4.75	-3.05
	-90	-5.93	-4.69	-3.96
-1.0	-10	-5.90	-4.77	-3.13
	-30	-5.86	-4.71	-3.08
	-60	-5.85	-4.67	-3.04
	-90	-5.85	-4.65	-3.03
0.0	-10	-5.73	-4.46	-2.75
	-30	-5.63	-4.36	-2.69
	-60	-5.54	-4.28	-2.63
	-90	-5.46	-4.22	-2.59
1.0	-10	-5.45	-3.96	-2.09
	-30	-5.23	-3.77	-1.94
	-60	-4.97	-3.54	-1.78
	-90	-4.76	-3.35	-1.63
2.0	-10	-5.06	-3.25	-1.09
	-30	-4.65	-2.88	-0.80
	-60	-4.12	-2.42	-0.42
	-90	-3.68	-2.00	-0.06

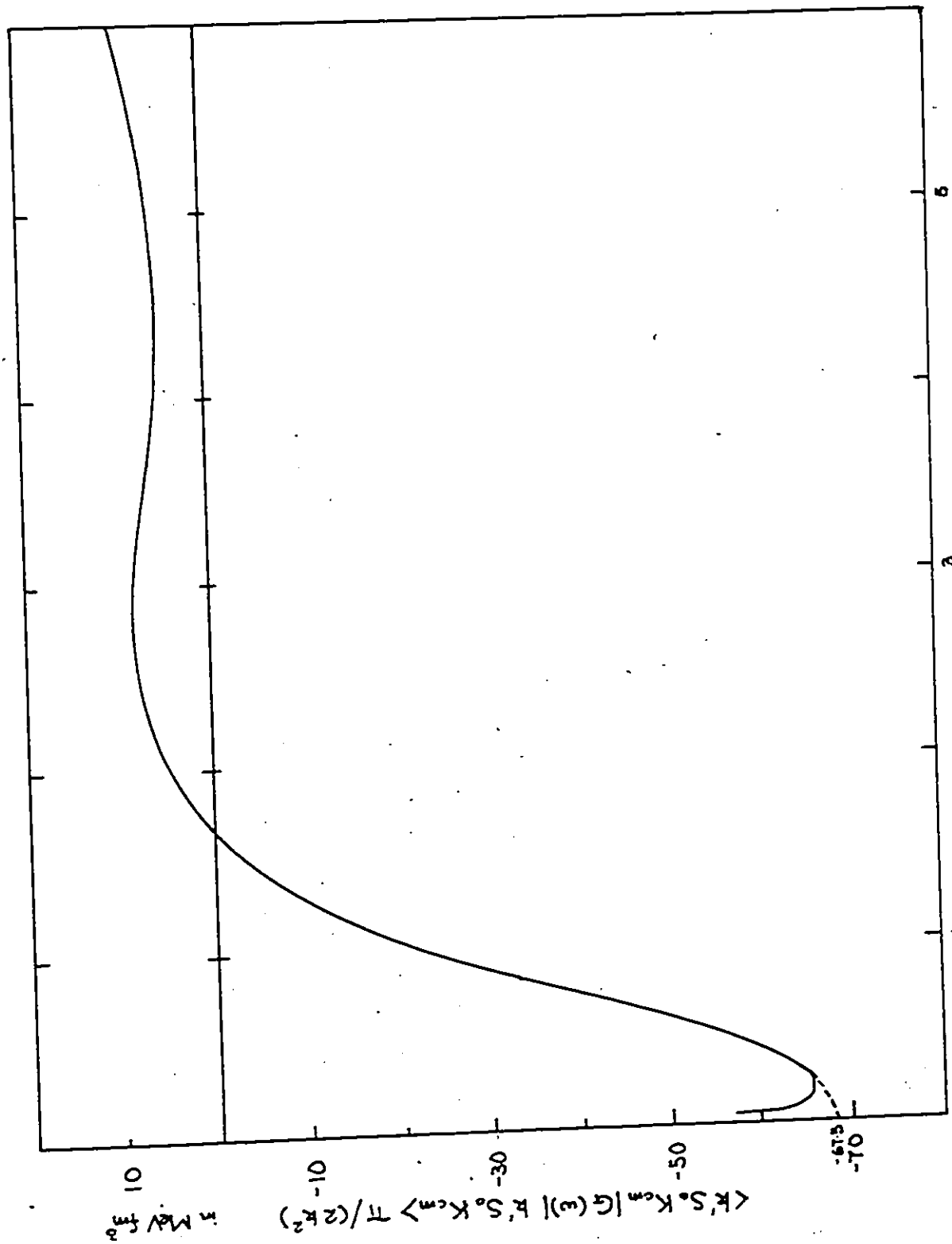

Fig. 6-5 The nuclear matter Reaction matrix in momentum space as a function of k

The G-matrices of the finite nuclei are basically direct transforms of the nuclear matter G-matrix to the harmonic oscillator basis. Tables 6/6 and 6/7 show that the sensitivity of the two-body G-matrix increases with n. This is because states with higher n have more kinetic energy on the average and see more of the core. The matrix elements $\langle n|G|n\rangle$ decrease in magnitude with increasing n.

Next, we will examine the behaviour of the G-matrix with off-shell effects. For nuclear matter, smaller σ functions (D1-, D2, more negative η values) yield larger diagonal matrix elements and hence, more binding. Larger σ functions (D1+ and increasing +η values) correspond to smaller G-matrix elements resulting in a loss of binding. The same trends are observed in the $\langle n|G|n\rangle$ matrices of ^{16}O and ^{40}Ca. In all cases, $\sigma_{RA} + \sigma_{D2}$ and $\sigma_{RA}^* + \sigma_{D2}$ have identical G-matrix elements. The distortion D2 has such a large distorting effect that the difference between σ_{RA} and σ_{RA}^* due to different high-energy phase-shift behaviour is overshadowed. Consistent with our previous observation regarding $\Delta_o(k,r)$, D1-* yields smaller reaction matrix elements than σ_{RA}^* for $k < 0.65$ fm^{-1}. This accounts for decreased binding energies in nuclear matter, ^{16}O and ^{40}Ca, contrary to expectations.

Since phase-shifts with two different high-energy forms have been used in this study, i.e. RA and RA*, we can investigate the sensitivity of the G-matrix to high-energy phase-shifts. In Fig. 5-1, RA* has its minimum in phase shifts pushed further down, corresponding to increased repulsion. The G-matrix elements of σ_{RA}^* become less attractive and more repulsive as they should, resulting in a loss of binding as seen from Table 6/2. This observation applies to the nuclear matter

as well as the two finite nuclei. For nuclear matter the change in G-matrix elements is hardly discernible at small k, up to about 1.0 fm^{-1}. It starts becoming more appreciable at higher values of k. For ^{16}O and ^{40}Ca, this change in numbers is small, though increasing with larger n. This is consistent with the fact that at lower k, which are of relevance to nuclear matter as well as finite nuclei calculations, the unknown high-energy phase-shift plays an insignificant part.

This is reflected in the binding energies listed in Table 6/8 which includes results calculated by Kao[77], Sprung[76], Mukhopadkyay[45], Haftel and Takabin[70]. The discrepancy between the Kao and Sprung numbers using the same potential is much greater than that obtained by changing the high energy phase-shift behaviour.

6.4 The Wave Function $\psi_o^{(+)}(k,r)$

The wave function $\psi_o^{(+)}(k,r)$ associated with each σ-function has been examined. Actually, the real function $w_o(k,r)$ was calculated. It is related to $\psi_o^{(+)}(k,r)$ through the definition

$$w_o(k,r) = e^{-i\delta_o(k)} kr\, \psi_o^{(+)}(k,r), \tag{4.23}$$

which in the PRS formalism is given by

$$w_o(k,r) = \Delta_o(k,r) + \sin(kr + \delta_o) \tag{6.5}$$

For the Sauer type σ-functions, $w_o(k,r)$ is calculated from the half-shell

Table 6/8

Dependence of Binding Energies on High Energy Behaviour of Phase Shifts

High Energy Behaviour	Binding Energy of Nuclear Matter in Mev	Binding Energy of ^{16}O in Mev	Binding Energy of ^{40}Ca in Mev
RA	-10.89	-3.72	-6.22
RA*	-11.31	-3.86	-6.45
Kao (Reid Soft Core)	-14.30	—	—
Sprung (Reid Soft Core)	-11.76	—	—
Mukhopadhyay	-11.64	—	—
Haftel and Tabakin (Reid Yukawa Core)	- 9.86	—	—

T matrix elements $\phi(k,k')$, i.e.:

$$w_o(k,r) = \cos\delta_o(k) \sin kr + P \int_0^\infty dk' \sin(k'r)(k^2 - k'^2)^{-1} \phi(k,k') \tag{6.6}$$

Since the PRS wave functions are not orthogonal, the results of Eqs. (6.5) and (6.6) cannot be treated on the same footing. To find out if the orthogonalization procedure will change results appreciably, the PRS wave functions have been calculated using both expressions. For small r values, the wave functions cannot be distinguished. For r near the matching point (R = 1.43 fm) the difference is about 2%. The graphs of $\Delta_o(k,r)$ versus r are indistinguishable except for slight differences at the right hand boundary at about 1.4 fm.

When $\eta \leq -2.2$, the value of $w_o(k,r)$ in Eq. (6.5) is observed to have an amplitude larger than the free wave function $\sin(kr + \delta_o)$. An extra node occurs in the function $w_o(k,r)$ when $\eta \geq 0.7$. Imposing the additional constraint discussed in Chapter IV, i.e. that the wave function be well-balanced, posses no extra nodes and have an amplitude less than that of the external free wave function, the wave functions in the region $+0.7 \leq \eta \leq -2.2$ and therefore the corresponding σ-functions are rejected. $w_o(k,r)$ is plotted as a function of r in Fig. 6-6.

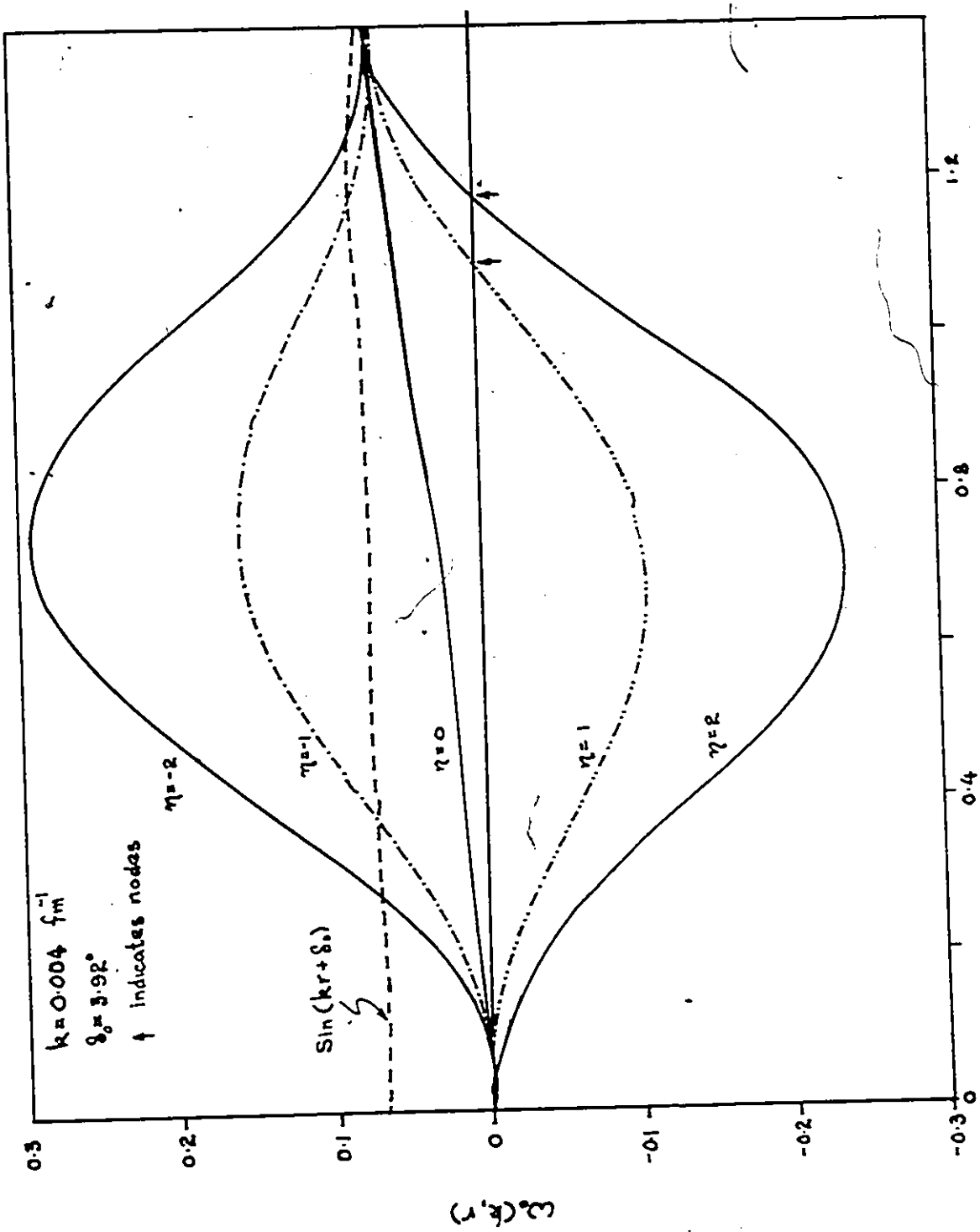

Fig. 6-6 The wave function $w_0(k,r)$ as a function of r

6.5 The Difference Integral

In order to explore the relationship between the wound integral, κ or binding energy and either the σ-function, or the difference function $\Delta_o(k,r)$, we have defined a 'difference integral' I, for the $\ell = 0$ states.

$$I(k,R) = 4\pi \int_0^R \Delta_o^2(k,r)\, dr \tag{6.7}$$

Table 6/2 list values of I(k,R) for R = 1.43 fm and k = 1.052 fm^{-1} for various σ-functions. Fig. 6-7 shows I(k,R) as a function of binding energies for ^{16}O, ^{40}Ca and nuclear matter. An interesting and unexpected relationship can be observed. Those difference integrals obtained from the PRS polynomial form of $\Delta_o(k,r)$ all lie on a smooth curve while those for the distortions D1+ lie on or very near this curve. By transposing Figs. 6-1 (a) - (c) and examining the shapes of $\Delta_o(k,r)$, we found that the PRS results, by definition, have the same slope at the origin, i.e. $\Delta_o'(k,o)$. The distortions D1+ have this same slope while the other distortions have different slopes. RA and RA* have the same slopes and D1- D2 and D2* have almost identical slopes. The exception is D1-* which yields a positive $\Delta_o'(k,o)$. In the PRS one-parameter model, it is assumed that

$$\Delta_o'(k,o) = -k \cos \delta_o(k) \tag{4.20}$$

which is valid for a local potential, with a very small wave function at short distances. Apparently, among the Sauer type distortions, only D1+ fits this assumption.

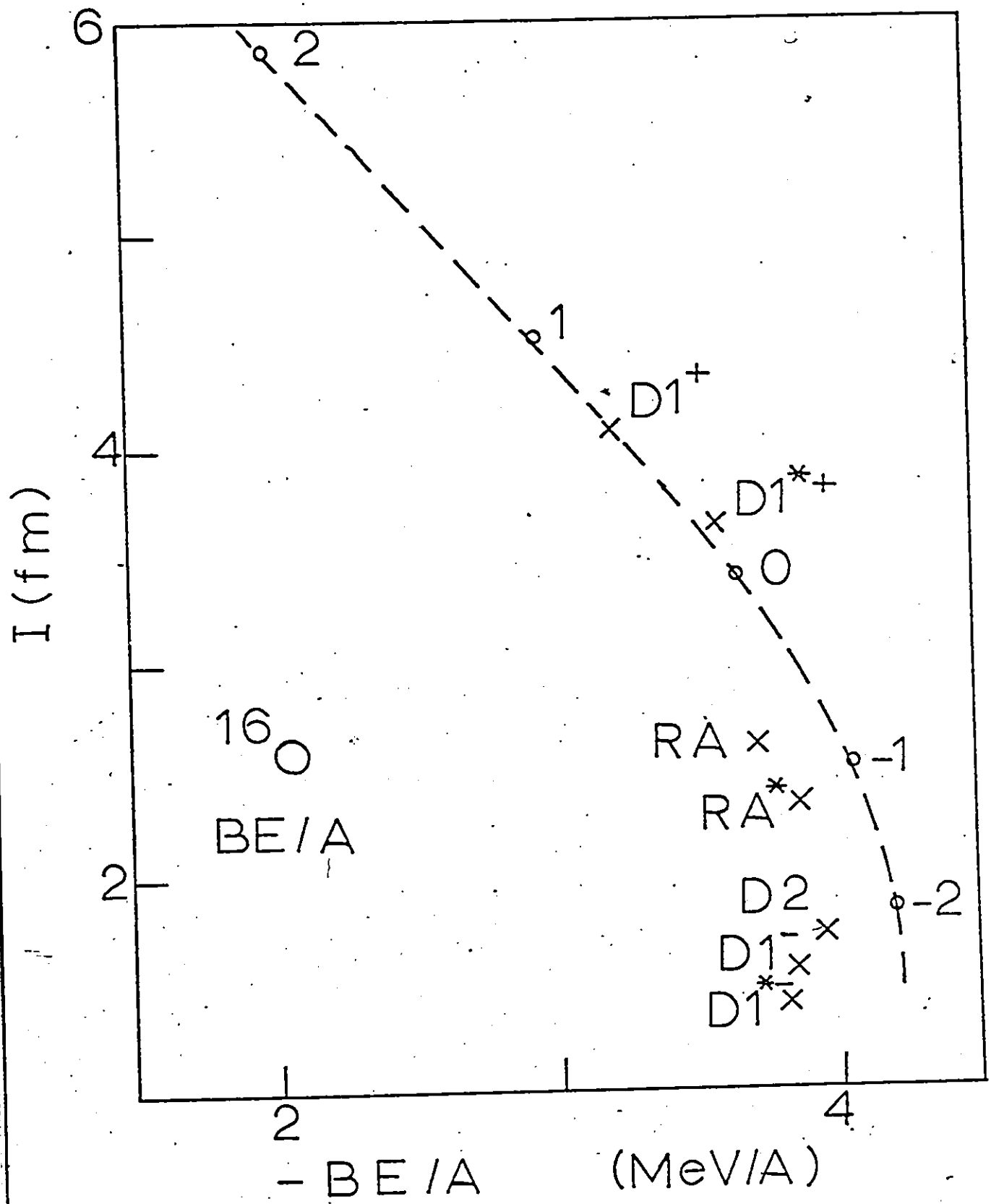

Fig. 6-7(a)The difference integral I(k,R) for ^{16}O.

k = 1.052 fm^{-1} and R = 1.43 fm.

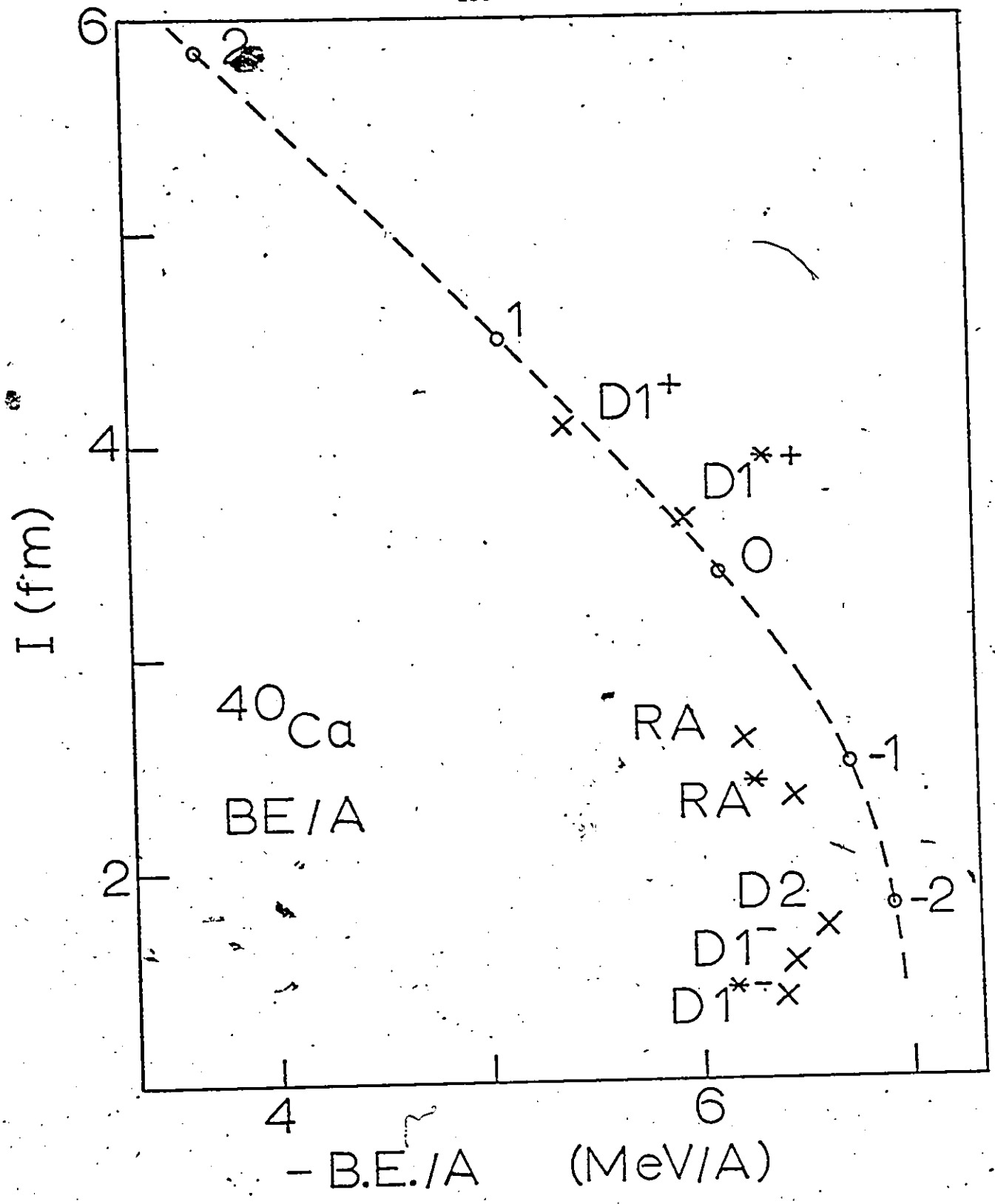

Fig. 6-7 (b) The difference integral I(k,R) for ^{40}Ca.

k = 1.052 fm^{-1} and R = 1.43fm.

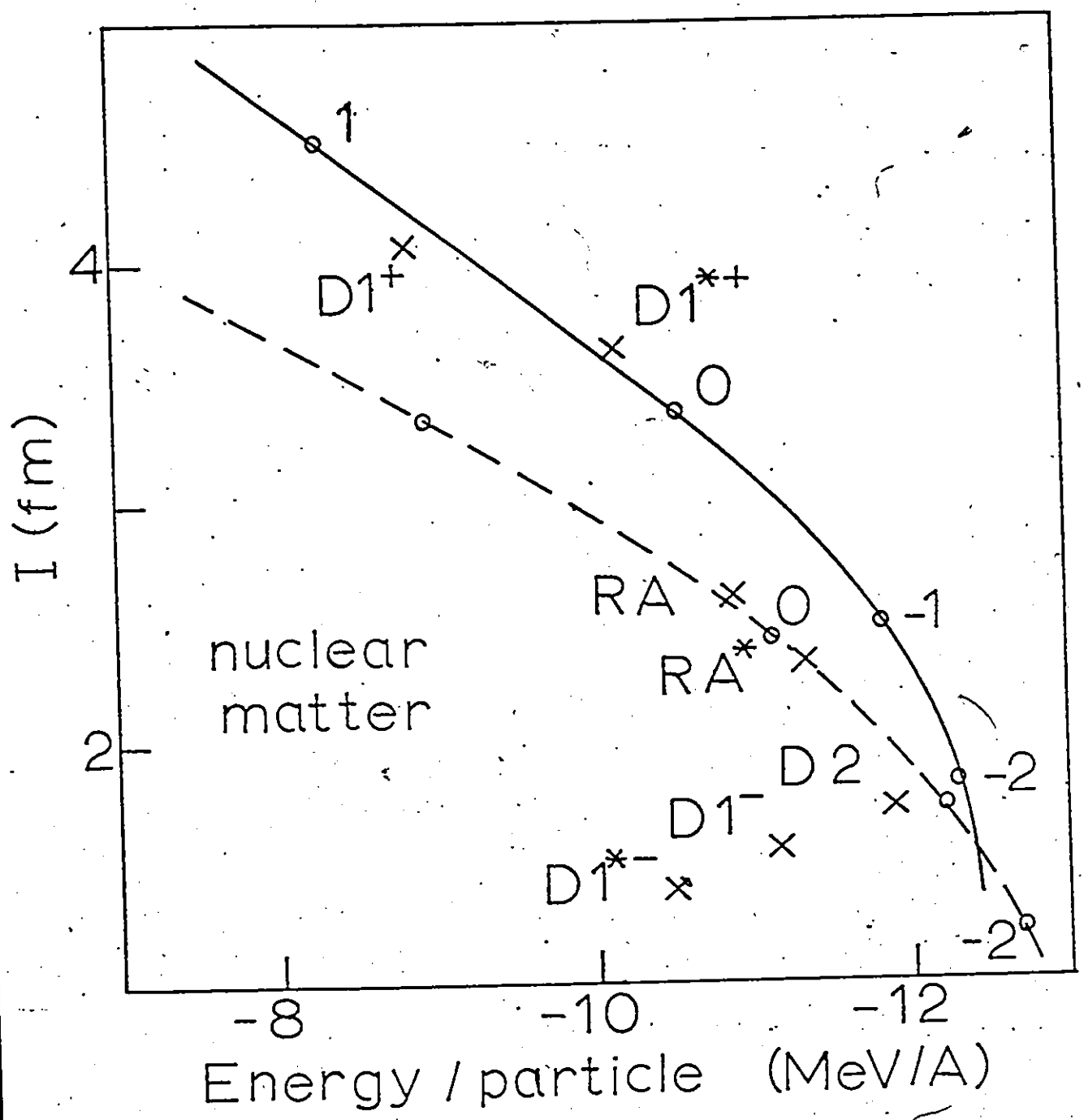

Fig. 6-7 (c) The difference integral I(k,R) for nuclear matter. k = 1.052 fm^{-1} and R = 1.43 fm.

We have restricted η to be in the range $0.7 \geq \eta \geq -2.2$; this would imply, by extrapolation from Fig. 6-7, that I should be restricted to $4.2 > I > 1.7$. However, σ_{D1-} and $\sigma_{D1-}{}^*$ have $I < 1.7$ but are acceptable. It appears therefore that the acceptable values of I also depend on the slope $\Delta_o'(k,o)$. To establish this dependence, we examined the complete expression of $\Delta_o'(k,o)$ given by Eq. (4.21), i.e.:

$$\Delta_o'(k,o) = k/|f_o(k)| \int - k \cos \delta_o(k)$$

$$= w_o'(k,o) - k \cos \delta_o(k) \qquad (4.21)$$

where

$$f_o(k) = \exp\left(-\frac{2}{\pi} \int_0^\infty dq \, \frac{\delta_o(q)}{q - k + i\varepsilon}\right) \qquad (4.22)$$

is the S-wave Jost function. The wave functions associated with σ_{RA} were examined and the values of $\Delta_o'(k,o)$ calculated from them for $k < 2.0$ fm^{-1}. Then the Jost function $f_o(k)$ was extracted using Eq. (4.21) and displayed in Fig. 6-8. A least square fit was made to this curve using Chebyshev polynomial expansion. (see Appendix C). This fit was then used in Eq. (4.21) to calculate the difference function $\Delta_o(k,r)$ and then the difference integral I. σ-functions for the five η values, and corresponding to this new $\Delta_o'(k,r)$, were generated. The procedures for the construction of the T matrix, and for the computation of the binding energies of nuclear matter described in section 5.3 were repeated. The resulting binding energies are shown by the dashed curve in Fig. 6-7(c). This curve passes very close to the points associated with σ_{RA} and $\sigma_{RA}{}^*$, consistent with the observations made from Fig. 6-1 (b), (c).

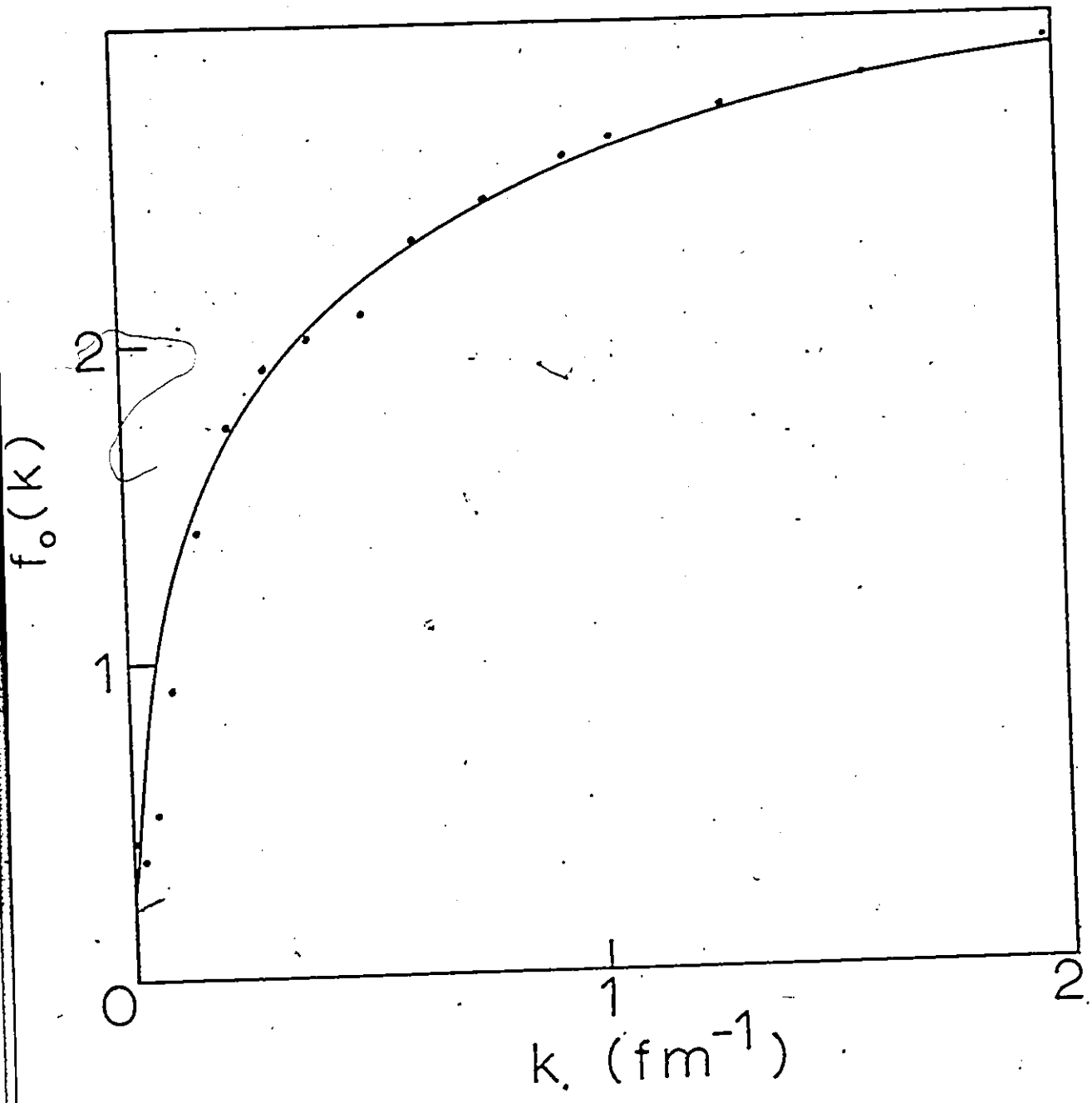

Fig. 6-8 The Jost function $f_0(k)$ associated with σ_{RA}

Portions of these calculations for I and the binding energies have been carried out at other k-values less than 2.0 fm^{-1}, with similar results being obtained. Two different slopes were used:

$$\Delta'_o(k,o) = \frac{k}{|f_M(k)|} - k \cos \delta_o(k), \tag{6.8}$$

and

$$\Delta'_o(k,o) = \frac{k}{|f_{HC}(k)|} - k \cos \delta_o(k) \tag{6.9}$$

Appendix D gives the forms of $f_M(k)$ and $f_{HC}(k)$. The resulting curves of I vs. B.E. for nuclear matter calculated from these different Jost functions were all markedly different from the original PRS calculation indicating the sensitivity of these results to the form of $\Delta'_o(k,o)$. Table 6/9 gives the nuclear matter binding energies calculated from $f_M(k)$ and $f_{HC}(k)$.

To investigate how the effective range parameters are changed by different distortions and different boundary conditions of Δ_o, the scattering length a_o for each of the slopes $\Delta'_o(k,o)$ discussed and for each η value was calculated. (See Appendix E for the procedure). Table 6/10 lists these scattering lengths for different η values.

a_o is seen to change by a minimal amount, thus assuming that the σ-function in the low energy region remains unchanged.

We have observed earlier that wave functions associated with $\eta \geq 0.7$ should be rejected. Plots of I vs. BE/A imply that the $\sigma_{RA} + \sigma_{D1+}$ results should also be excluded, consistent with the observation that an extra node occurs in the wave function of this particular

Table 6/9

Nuclear Matter Binding Energy for Different Slopes of the Difference Function, $\Delta_0'(k,0)$

$\Delta_0'(k,0)$	n	-BE/A (Mev)
Chebyshev fit to $f_0(k)$ of σ_{RA}	-2.0	12.76
	0.0	11.11
	1.0	8.91
	2.0	5.54
Chebyshev fit to $f_0(k)$ of $\sigma_{RA}+\sigma_{D1-}$	-2.0	12.01
	0.0	10.19
	2.0	2.32

Table 6/10

Scattering Length a_0 for Different Slopes $\Delta_0'(k,0)$

$\Delta_0'(k,0)$	n	a_o (Fm)
$-k\cos\delta_0(k)$	-2.0	-16.800
	-1.0	-16.854
	0.0	-16.845
	1.0	-16.843
	2.0	-16.845
$\frac{k}{\lvert f_M(k)\rvert} - k\cos\delta_0(k)$	-2.0	-16.992
	-1.0	-16.987
	0.0	-16.987
	1.0	-16.990
	2.0	-16.986
$\frac{k}{\lvert f_{HC}(k)\rvert} - k\cos\delta_0(k)$	-2.0	-16.885
	-1.0	-16.887
	0.0	-16.887
	1.0	-16.889
	2.0	-16.888

distortion. Of course, the range of allowed wave functions and corresponding σ-functions shifts according to the different assumptions made for $\Delta_o'(k,o)$.

CHAPTER VII DISCUSSION AND CONCLUSIONS

There are strong arguments favoring the construction of the T-matrix directly from nuclear data, rather than the construction of a phenomenological potential model. However, the main problem is to impose constraints on the full T-matrix, limiting its form. By studying the off-shell behaviour of the T-matrix, one can establish some sort of constraints. Off-shell variations have been generated in the T-matrix and the subsequent nuclear structure results investigated. In this study, the T-matrix in the ^1s_o channel has been our focal point.

To create off-shell changes in the two-nucleon interaction through the ^1s_o T-matrix, there is the approach of Baranger et al. The symmetric part of the T-matrix is defined by the σ-function. Too much freedom is allowed in the forms of σ and it is difficult to impose sufficient constraints on it directly from physical observations. The alternative approach of starting from a model wave function $\psi_o^{(+)}(k,r)$ or difference function $\Delta_o(k,r)$ utilizes the information that the long-range tail of the potential is well known and given by the on-energy-shell part of T. The interior form of the wave function is controlled by the off-shell part of the T and needs to be specified. Certain conditions can be imposed on the interior wave function. It must match smoothly to the exterior wave function, it must have an amplitude less than that of the free wave function and it must not possess any extra nodes. The last two conditions are additional and reasonable assumptions. The

form of the interior wave function is therefore limited. Its uncertainty is expressed in the parameterized model of $\Delta_o(k,r)$, i.e. in η and the boundary conditions at r = 0 (values of $w'_o(k,o)$ and $w''_o(k,o)$; $w'_o(k,o)$ is a function of the high-energy phase shift and $w''_o(k,o)$) a function of the short-range non-locality of the interaction.

In this study, the best points of both approaches were incorporated to construct the fully off-shell T-matrix and to eliminate as much freedom as possible. In our approach the half-shell T from PRS can be used to construct the σ-function which then serves as a foundation on which the full T-matrix is constructed. Nuclear matter and finite nuclei (^{16}O, ^{40}Ca) calculations were performed using σ-functions of Sauer-type distortions and σ-functions derived from the interior wave function model.

Dependence of the structure results on off-shell behaviour of the two-body interaction is very marked and highly important. The amount of variation exceeds that which exists among calculations based on the same potential but using different calculational techniques. The effect of the high-energy phase shifts is small compared to the off-shell effects. Sensitivity of the results to off-shell changes increases with density, therefore the largest variations were found in nuclear matter. The range of variation of the interior wave function σ is larger than the Sauer type σ functions. Repulsive-attractive effects are consistently evident in every stage of the results, i.e.:

Large(small) off-diagonal σ-matrix elements → more(less) negative $\Delta_o(k,r)$ → large(small) $\phi(k,k')$ → small(large) diagonal G-matrix

elements → small(large) binding energies → large(small) wound k → repulsion(attractive).

We have observed that the binding energy is sensitive to a large region of far-off-shell T-matrix elements, e.g. k = 2.5 to 5.0 fm^{-1} for nuclear matter.

Finally, there is an interesting link between the wave function and the binding energies of nuclei and nuclear matter, manifested in the difference integral I. For fixed boundary conditions, there is a smooth relationship between I and the binding energies. Only part of this curve contains wave functions which are physically acceptable, allowing the corresponding σ functions to be rejected.

This approach places considerable restrictions on the permitted form of σ, and can be applied to any σ-function in general. To investigate how the limits in the range of allowed σ-functions change with the assumptions on the boundary conditions, the following mechanics can be employed. The wave functions associated with a σ-function of a particular local potential and the values of $\Delta'_o(k,r)$ are computed. From these, the Jost function $f_o(k)$ is extracted according to Eq. (4.21) which is the form of $\Delta'_o(k,o)$ assumed for a purely local potential. A fit is made to $f_o(k)$. Then $\Delta_o(k,o)$ and hence I can be calculated from the analytic expression of $\Delta'_o(k,o)$. The σ-functions of the different η values are generated, enabling the T-matrix to be constructed. Binding energies of nuclear matter are computed from each σ-function and the I vs. BE/A curve should pass through the point associated with the potential. Setting up this particular boundary condition of $\Delta'_o(k,o)$, the nuclear matter binding

energy and difference integrals of any unitary transformed σ-function can be calculated. The points associated with different distortions are checked against the allowed section of the curve. The σ-functions are then rejected or accepted on the basis of the established constraints for those particular boundary conditions.

To further limit the form of σ, it will be necessary to study processes involving higher interaction energies than are involved in binding energy calculations. The proton-proton bremsstrahlung can be very useful in providing information far off the energy-shell.

In another perspective, field-theoretic information can be built into models of σ(k,k'). Field theoretic models and NN peripheral phase shifts have suggested that the NN interaction is approximately local at large distances. It would be highly desirable to be able to control explicitly the range and degree of non-locality in the underlying interaction associated with a particular σ-function. Any variation in σ(k,k') due to different degrees of non-locality in the interaction can then be detected and separated. Information about the range and strength of the local parts of the NN interaction suggest roughly, Yukawa potentials with appropriate spin and isospin dependence describing the exchange of single pi- and omega-mesons. The range and strengths are determined by empirical mesons and coupling constants. Yukawa potentials of the form

$$V(r) \sim \int_{2m_\pi}^{\infty} \eta(\mu)\, d\mu\, \frac{e}{r}^{-\mu r} \qquad (7.1)$$

are suggested by the two-pion exchange processes. In Eq. (7.1), the

appropriate spin and isospin factors have been omitted. In the crucial region $2m_\pi < \mu < 4m_\pi$, $\eta(u)$ can be determined from analytic continuations of the πN and the $\pi\pi$ elastic scattering data. These features of the NN interaction due to field-theoretic considerations should be exploited to reduce the freedom in $\sigma(k,k')$. The analytical properties of Eq. (7.1) can be studied to parameterize $\sigma(k,k')$ in such a way that its known analytic properties in complex kk'-space can be explicitly displayed. The σ-function can then be constrained to reproduce the known one- and two-pion exchange discontinuities. The freedom in the off-shell T-matrix becomes greatly reduced. The above discussion represents an entirely different approach to that of Baranger et al.[1].

In the approach of Baranger et al.[1], which was adopted in the present study, only the partial-wave T-matrix without a bound state was considered. Haftel[21] has extended this work to include a bound state. In this case, one must include information on the binding energy and bound-state wave function as well as the scattering phase shifts. These forms of the off-shell T-matrix are too complex and too arbitrary for direct use in nuclear physics calculations. In particular, the off-shell arbitrariness contained in the off-diagonal parts of ϕ is mixed in with the diagonal part which contains the on-shell information. The T-matrix should have a form which allows the off-shell part to be varied at will with the on-shell part kept explicitly fixed. Amado[79] has suggested writing the off-shell two-body T-matrix in terms of a T-matrix that is correct on-shell, i.e. giving the exact phase shifts and bound states on-shell, plus a term that vanishes on-shell and affects only the off-shell behaviour. In order to include a bound state, a model

potential V_m is introduced. It has the same bound-state energy and wave function as the full amplitude, as well as the same scattering phase. One can then write for the general off-shell T-matrix.

$$\langle k'|T(\omega)|k\rangle = \langle k'|T_m(\omega)|k\rangle + C(k', k;\omega) \tag{7.2}$$

where T_m is the off-shell T-matrix for V_m and C is the correction term. C vanishes on shell. The existence of any number of bound states is of no concern as long as they are fully contained in T_m. If $\phi_m(k,k')$ is the half-shell function of V_m and satisfies the condition

$$\phi_m(k,k) = \phi(k,k) \tag{7.3}$$

C can be written as

$$C(k', k;\omega) = (k^2 - k'^2)\,\Delta(k,k')\cos\delta(k)$$

$$+ \int_0^\infty dq \left(\frac{1}{\omega - q^2} - P\frac{1}{k^2 - q^2}\right)$$

$$\left[\phi_m(q,k')\,\Delta(q,k)(q^2 - k^2) + (q^2 - k'^2)\Delta(q,k')\phi_m(q,k)\right.$$

$$\left. + (q^2 - k'^2)(q^2 - k^2)\Delta(q,k')\,\Delta(q,k)\right], \tag{7.4}$$

and $\phi(k,k')$ as

$$\phi(k,k') = \phi_m(k,k') + (k^2 - k'^2)\,\Delta(k,k') \tag{7.5}$$

$\Delta(k,k')$ is parametrized so that off-shell effects can be controlled. The model T-matrix is chosen so that it can be easy to use in any nuclear

physics application under study. The precise way to parametrize Δ and to handle C remains to be pursued.

As we can see, more and more avenues are being sought to explore constraints on the off-shell T-matrix and to provide easier, more accurate means of generating off-shell variations. It is felt that the present study can be useful as a preliminary investigation, raising some interesting questions which will hopefully stimulate further interest.

APPENDIX A ^1s_o TABAKIN POTENTIAL[66]

The analytic expression for the half-shell T-matrix element $\phi(k,k')$ for the potential

$$V(k,k') = \frac{2}{\pi} \lambda[-g(k)g(k') + h(k)h(k')] \tag{A.1}$$

is given by

$$\phi(k,k') = -(2k'/\pi) \sin \delta_o(k) \frac{\{ g(k')A(k) - h(k')B(k) \}}{\{ g(k)A(k) - h(k)B(k) \}} \tag{A.2}$$

The phase shift $\delta_o(k)$ is determined by

$$\tan \delta_o(k)/k = g(k)A(k) - h(k)B(k) \tag{A.3}$$

where

$$g(k) = \gamma(a^2 + k^2)^{-1} \tag{A.4}$$

$$h(k) = \beta\{[b^2 + (k - d)^2] [b^2 + (k + d)^2]\}^{-1} \tag{A.5}$$

$$G(k) = [a^2 - k^2)] g^2(k)/2a \tag{A.6}$$

$$\begin{aligned} H(k) = {} & [(5b^6 - 3d^6 + 7b^4 d^2 - d^4 b^2)/k^2 \\ & + (b^2 + d^2)^4/k^4 - k^2(5b^2 + d^2) + 3d^4 \\ & + 15b^4 + 2d^2b^2] h_o^2(k)/16b^3 \end{aligned} \tag{A.7}$$

$$\begin{aligned} M(k) = {} & \frac{g(k)h(k)}{2b[d^2 + (a + b)^2]} \{-k^2(d^2 + b^2 + 2ab) \\ & + a^2(d^2 + b^2)^2/k^2 + (d^2 + b^2)^2 + a(2b - a)(d^2 + b^2) + 4a^2b^2\} \end{aligned} \tag{A.8}$$

$$A(k) = \{g(k)[1 + H(k^2)] - h(k)M(k^2)\}\{[1 - G(k^2)][1 + H(k^2)] + M(k^2)^2\}^{-1} \quad (A.9)$$

$$B(k) = \{h(k)[1 - G(k^2)] + g(k)M(k^2)\}\{[1 - G(k^2)][1 + H(k^2)] + M(k^2)^2\}^{-1} \quad (A.10)$$

$$\gamma^2 = V_\gamma a/\pi \quad (A.11)$$

$$\beta^2 = V_\beta b/\pi \quad (A.12)$$

The parameters used are:

V_γ = 115.9 MeV, a^{-1} = 0.834 fm,

V_β = 235.6 MeV, b^{-1} = 0.801 fm,

d^{-1} = 0.694 fm, π = 41.472

APPENDIX B SIX-POINT GAUSSIAN INTEGRATION OF $\int_0^{k_F} F(k)dk$

Equation (5.26) gives

$$k = c \tan \pi/4 \,(1 + x) \tag{5.26}$$

from which one gets $x = -1$ when $k = 0$. Inversely, for $k = k_F$, we get:

$$x = z - 1 \qquad \text{where } z = 4/\pi \tan^{-1}(k_F/c) \tag{B.1}$$

We can therefore write

$$\int_0^{k_F} F(k)dk = c\pi/4 \int_{-1}^{x} F\,[c \tan \pi/4(1 + y)][1 + \tan^2 \pi/4 (1 + y)]\, dy \tag{B.2}$$

Gauss' formula for integration between an arbitrary interval is given as

$$\int_a^b F(y)dy = \frac{b - a}{2} \sum_{i=1}^{n} w_i F(y_i) \tag{B.3}$$

where

$$y_i = \left(\frac{b - a}{2}\right) x_i + \left(\frac{b + a}{2}\right) \tag{B.4}$$

x_i and w_i for $n = 6$ are given in Table 5/1. Applying Gauss' approximation to (B.2) we obtain

$$\int_0^{k_F} F(k)dk = c\pi/4 \,\frac{a}{2} \sum_{i=1}^{6} F[c \tan \pi/4(1 + y_i)][1 + \tan^2 \pi/4(1 + y_i)]w_i \tag{B.5}$$

where

$$y_i = \left(\frac{x + 1}{2}\right) x_i + \left(\frac{x - 1}{2}\right) \qquad (B.6)$$

$$= \frac{a}{2} x_i + \left(\frac{a - 2}{2}\right)$$

Hence,

$$k_i = c \tan \pi/4 \ (1 + y_i)$$

$$= c \tan \pi/4 \left\{ \frac{a}{2} \left[1 + x_i\right]\right\} \qquad (B.7)$$

Finally,

$$\int_0^{k_F} F(k)\,dk = c\pi/4 \ \frac{a}{2} \sum_{i=1}^{6} F(k_i) \ (1 + k_i^2/c^2) w_i \qquad (B.8)$$

when

$k_F = 1.36 fm^{-1}$ k_i is given by (B.7) to be

$$k_i = c \tan \pi/4 \ [0.596(1 + x_i)] \qquad (B.9)$$

APPENDIX C CHEBYSHEV SERIES

A least square fit was made to the Jost function $f_o(k)$ using the Chebyshev polynomial expansion. The Chebyshev polynomials T(x) are defined by

$$T_n(x) = \cos (n \cos^{-1} x) \tag{C.1}$$

For example,

$$T_o(x) = \cos 0 = 1 \tag{C.2}$$

$$T_1(x) = \cos (\cos^{-1} x) = x \tag{C.3}$$

$$T_2(x) = \cos (2 \cos^{-1} x) = 2x^2 - 1 \tag{C.4}$$

and so forth. The recursion relationship is

$$T_{n+1}(x) = 2xT_n(x) - T_{n-1}(x) \tag{C.5}$$

Any properly behaved function f(x) can be expressed as Chebyshev series,

$$f(x) = \tfrac{1}{2}c_o + \sum_{n=1}^{\infty} c_n T_n(x) \tag{C.6}$$

where the coefficients c_n are given by

$$c_n = \frac{2}{\pi} \int_{-1}^{1} \frac{f(x)\, T_n(x)\, dx}{\sqrt{1 - x^2}} \tag{C.7}$$

APPENDIX D THE JOST FUNCTIONS $f_M(k)$ and $f_{HC}(k)$

The Jost function $f_M(k)$ is used to calculate $\Delta'_o(k,o)$ in

$$\Delta'_o(k,o) = \frac{k}{|f_M(k)|} - k \cos \delta_o(k) \tag{D.1}$$

where

$$f_M(k) = e^{\zeta/2} \Gamma(B) \zeta^{A-B} / \Gamma(A) \tag{D.2}$$

$$\zeta = 2V_o^{\frac{1}{2}} b e^{c/b} \tag{D.3}$$

$$|\Gamma(B)|^2 = \frac{2\pi kb}{\sinh (2\pi kb)} \tag{D.4}$$

$$\Gamma(B) = \Gamma(1 - 2ikb) \tag{D.5}$$

$$|\zeta^{A-B}| = \zeta^{-\frac{1}{2}} \sqrt{v_o} b \tag{D.6}$$

and

$$\Gamma(A) = \Gamma[\tfrac{1}{2}(1 - 2ikb) - V_o^{\frac{1}{2}} b] \tag{D.7}$$

The following data was used:

$$V_o = 43.05 \text{ MeV}, \quad b = 0.4722 \text{ fm}, \quad c = 1.0112 \text{ fm}.$$

Another fit to $f_o(k)$ of σ_{RA} that was employed to calculate $\Delta'_o(k,o)$ was:

$$f_{HC}(k) = [\kappa^2 \cos^2 \kappa b + k^2 \sin^2 \kappa b]^{\frac{1}{2}} \tag{D.8}$$

where

$$\kappa = (V_o + k^2)^{\frac{1}{2}} \tag{D.9}$$

with

$$V_o = 17.84 \text{ MeV}, \quad b = 2.306 \text{ fm}, \quad c = 0.1372 \text{ fm}.$$

The parameters for the Morse potential are:

$$V_o = 43.05 \text{ MeV}, \quad b = 0.4722 \text{ fm}, \quad c = 1.0112 \text{ fm}.$$

The Jost function for the hard-core potential turns out to be

$$f_{HC}(k) = e^{ik(b + c)} [\kappa \cos \kappa b - \kappa ik \sin \kappa b] \tag{D.11}$$

where

$$\kappa = (V_o + k^2)^{\frac{1}{2}} \tag{D.12}$$

Therefore

$$|f_{HC}(k)| = [\kappa^2 \cos^2 \kappa b + k^2 \sin^2 \kappa b]^{\frac{1}{2}} \tag{D.13}$$

The parameters for the hard-core potential are:

$$V_o = 17.84 \text{ MeV}, \quad b = 2.306 \text{ fm}, \quad c = 0.1372 \text{ fm}.$$

APPENDIX E DETERMINATION OF THE SCATTERING LENGTH a_o IN THE PRS APPROACH

In the PRS, the integral $I_n = \int_o^R \Delta_o(k,r)\,dr$ can be expanded as:

$$I_n = \int_o^R \Delta_o(k,r)\,dr \underset{k\to o}{\to} -\frac{1}{140}\,\eta R^7 + \frac{1}{10}\,R^2\,\Delta_o'(k,r) + \frac{1}{120}\,R^3\,\Delta_o''(k,r) + \beta k + (\gamma + \tfrac{1}{2}R)a_o k + \cdots$$

$$= \alpha + \beta k + \gamma a_o k \qquad (E.1)$$

In the initial case, i.e. $\Delta_o'(k,o) = -k\cos\delta_o(k) \to -k$

and $\Delta_o''(k,o) = k^2 \sin\delta_o(k) \to -k^3 a_o \to 0$, (E.2)

we have

$$I_n \underset{k\to o}{\to} -\frac{1}{140}\,\eta R^7 + (\beta - \frac{1}{10}R^2)k + (\gamma + \tfrac{1}{2}R)a_o k + \cdots \qquad (E.3)$$

where

$$\alpha = \tfrac{1}{2}R(a_o k) - \frac{1}{10}R^2 k - \frac{1}{140}\eta R^7 \qquad (E.4)$$

$$\beta = \tfrac{1}{2}AR - \frac{1}{10}CR^2 + \frac{1}{120}R^4 V(R) \qquad (E.5)$$

$$\gamma = R\left[\tfrac{1}{2}C + \frac{2}{5}DR - \frac{1}{120}R^2 V(R)\right] \qquad (E.6)$$

For the Reid potential,

$$V(R) = \sum_\beta G_\beta \frac{e^{-\beta\mu R}}{\mu R} \qquad (E.7)$$

$$A = \frac{1}{\mu}\sum_\beta G_\beta \frac{e^{-\beta\mu R}}{(\beta\mu)^2} \qquad (E.8)$$

$$C = -\frac{1}{\mu}\sum_{\beta} G_{\beta} \frac{e^{-\beta\mu R}}{(\beta\mu)} \tag{E.9}$$

$$D = \frac{1}{\mu}\sum_{\beta} G_{\beta} E_1(\beta\mu R) \tag{E.10}$$

(see Eq. (5.10))

These can be easily computed and thereby giving γ and β.

Regrouping so that

$$I_n = b_o + b_1 k \tag{E.11}$$

and

$$b_1 = \beta' + \gamma' a_o, \tag{E.12}$$

one obtains

$$\beta' = \beta - \frac{1}{10} R^2 \tag{E.13}$$

$$\gamma' = \gamma + \tfrac{1}{2}R \tag{E.14}$$

For R = 1.43 fm, we have found that

$$\beta' = -0.615939, \quad \gamma' = 0.883587.$$

For the Morse potential, $\frac{1}{|f_M(k)|}$ can be expanded as:

$$\frac{1}{|f_M(k)|} = e^{-\zeta/2}\, \zeta^{\frac{1}{2} + \sqrt{V_o}b}\, |\Gamma(\tfrac{1}{2} - \sqrt{V_o}b)| \{ 1 + \frac{\pi^2 b^2}{3} k^2 - \tfrac{1}{2} \left(\frac{b}{\frac{1}{2} - \sqrt{V_o}b}\right)^2 k^2 \ldots\ldots \}$$

$$= G_M [\, 1 + \Delta k^2 + \ldots\ldots \,] \tag{E.15}$$

where

$$G_M = e^{-\zeta/2}\, \zeta^{\frac{1}{2} + \sqrt{V_o}b} = 7.094$$

Therefore

$$\Delta_o'(k,o) = \frac{k}{|f_M(k)|} - k \cos \delta_o(k)$$

$$\underset{k\to o}{\to} G_M [k + \Delta k^3 + ...] - k$$

$$\to (G_M - 1)k. \qquad \text{(E.16)}$$

In Eq. (E.12), we now have

$$\beta' = [\beta + \frac{1}{10} R^2 (G_M - 1)] \qquad \text{(E.17)}$$

For the hard-core potential, $\frac{1}{|f_{HC}(k)|}$ is expanded to be

$$\frac{1}{|f_{HC}(k)|} = \frac{1}{\sqrt{V_o} \cos(\sqrt{V_o} b)} \cdot [1 - \frac{\sqrt{V_o} b \sin(\sqrt{V_o} b) \cos(\sqrt{V_o} b)}{2V_o \cos^2(\sqrt{V_o} b)} k^2$$

$$+ O(k^4) = G_{HC} [1 - \Delta k^2 ....] \qquad \text{(E.18)}$$

Therefore

$$\Delta_o'(k,o) = \frac{k}{|f_{HC}(k)|} - k \cos \delta_o(k)$$

$$\underset{k\to o}{\to} G_{HC} [k - \Delta k^3 .....] - k$$

$$\underset{k\to o}{\to} (G_{HC} - 1) k \qquad \text{(E.19)}$$

and

$$\beta' = [\beta + \frac{1}{10} R^2 (G_{HC} - 1)] \qquad \text{(E.20)}$$

where

$$G_{HC} = 26.56$$

For linear regression, we can equate

$$b_1 = \frac{\Sigma k_i In_i - \Sigma k_i \Sigma In_i/4}{\Sigma k_i^2 - (\Sigma k_i)^2/4} \qquad (E.21)$$

and compute a_o using Eq. (E.12) from the integrals In.

BIBLIOGRAPHY

1- M. Baranger, B. Giraud, S.K. Mukhopahgyay, and P.U. Sauer, Nucl. Phys. A138 (1969) 1.

2- P. Marmier & E. Sheldon "Physics of Nuclei and Particles" (Academic Press, Inc. 1970).

3- L.D. Faddeev, JETP (Sov. Phys.) 12 (1961) 1014.

4- P. Signell, Ref. 2; M.K. Banerjee, C. Levinson, M. Shuster, and D. Zollman Phys. Rev. C3, (1971) 509.

5- E.F. Redish, C.J. Stephenson, Jr., and G.M. Lerner, Phys. Rev. C2 (1970) 1665.

6- F. Coester, S. Cohen, B. Day, C.M. Vincent, Phys. Rev. C1 (1970) 769.

7- M.I. Haftel and F. Tabakin, Phys. Rev. C3 (1971) 921.

8- C.W. Wong and T. Sawada, Ann. of Phys. 72 (1972) 107.

9- P.U. Sauer, Phys. Rev. Lett. 32 (1974) 626.

10- P.U. Sauer, Phys. Rev. C 11 (1975) 1786.

11- K.A. Brueckner, Phys. Rev. 96 (1954) 508.

12- R.E. Peierls, Proc. Int. Conf. on Nuclear Structure, Kingston, Canada, 1960 (Univ. of Toronto Press, 1960) p. 14

13- A. Kallio, Phys. Lett. 18 (1965) 51.

14- J.P. Elliott, H.A. Mavromatis and E.A. Sanderson, Phys. Lett. 24B (1967) 358.

15- D. Koltun, Phys. Rev. Lett. 19 (1967) 910.

16- J.P. Elliott, A.D. Jackson, H.A. Mavromatis, E.A. Sanderson and B. Singh, Nucl. Phys. A121 (1968) 241.

17- A.H. Cromer and M.I. Sobel, Phys. Rev. 152 (1966) 1351.

18- S. Kahana and E. Tomusiak, Nucl. Phys. 71 (1965) 402.

19- M. Razavy and R.J.W. Hodgson, Nucl. Phys. A149 (1970) 65.

20- M.J. Reiner, Phys. Rev. Letts. 32 (1974) 236.

21- M.I. Haftel, Phys. Rev. Letts. 25 (1970) 120.

22- W. Van Dijk and M. Razavy, Nucl. Phys. A159 (1970) 161.

23- K.L. Kowalski, J.E. Monahan, C.M. Shakin and R.M. Thaler, Phys. Rev. C3 (1971) 1146.

24- P.U. Sauer, Nucl. Phys. A150 (1970) 467

P.U. Sauer, Nucl. Phys. A170 (1971) 497.

25- P.U. Sauer, Ann. Phys. (N.Y.) 80 (1973) 242.

26- H.S. Picker, Edward F. Redish and G.J. Stephenson, Jr., Phys. Rev. C4 (1971) 287; Phys. Rev. C8 (1973) 2495.

27- D.M. Brink, Theory of Nuclear Structure, Trieste Lectures 1969, (Vienna 1970) p. 13.

28- M. Srivastava and D.W.L. Sprung, Nucl. Phys. A149 (1970) 113.

29- M.K. Srivastava, Nucl. Phys. A157 (1970) 61.

30- H. Fiedeldey, Nucl. Phys. A135 (1969) 353.

31- J.E. Monahan, C.M. Shakin and R.M. Thaler, Phys. Rev. C4 (1971) 43.

32- W. Van Dijk and D. Kiang, Nucl. Phys. A181 (1972) 106.

33- M.I. Haftel, E. Lambert and P.U. Sauer, Nucl. Phys. A192 (1972) 225.

34- E.P. Harper, Y.E. Kim and A. Tubis, Phys. Rev. C6 (1972) 1601.

35- E. Hadjimichael and A.D. Jackson, Nucl. Phys. A180 (1972) 217.

36- H.C. Pradhan, P.U. Sauer and J.P. Vary, Phys. Rev. C6 (1972) 407.

37- J.P. Vary, Phys. Rev. C7 (1973) 521.

38- M.I. Haftel, Phys. Rev. C7 (1973) 80.

39- I.R. Afnan and F.J.D. Serduke, Phys. Lett. 44B (1973) 143.

40- H. Fiedeldey, Nuovo Cimento Lett. 9 (1974) 301.

41- M.J. McGurk and H. De Groot, Nucl. Phys. A231 (1974) 233.

42- M.K. Srivastava, Nucl. Phys. A221 (1974) 183.

43- A.W. Thomas and I.R. Afnan, Phys. Lett. 55B (1975) 425.

44- W. Van Dijk and M. Razavy, Nucl. Phys. A204 (1973) 412.

45- P.U. Sauer and J.A. Tjon, Nucl. Phys. A216 (1973) 541.

46- M.L. Goldberger and K.M. Watson, Collision Theory, (Wiley, New York, 1964).

47- M.K. Srivastava and D.W.L. Sprung, "Off-Shell Behavior of the Nucleon-Nucleon Interaction" in Advances in Nuclear Physics, vol. 8 (1975).

48- T.R. Mongan, Phys. Rev. 184 (1969) 1888.

49- H.A. Bethe and J. Goldstone, Proc. Roy. Soc. A238 (1957) 531.

50- T.R. Mongan, Off-energy-shell partial wave amplitudes.

51- K.A. Brueckner and C.A. Levinson, Phys. Rev. 97 (1955) 1344.

52- K.A. Brueckner, "Theory of Nuclear Structure" in The Many Body Problem (Université de Grenoble 1958.)

53- J. Goldstone, Proc. Roy. Soc., A239 (1957) 267.

54- P.U. Sauer, "Parametrization of the ^1S_o Two Nucleon Transition Matrix" Lab. for Nuclear Science and Dept. of Physics, MIT.

55- K.L. Kowalski and D. Feldman, J. Math. Phys. 2 (1961) 499
K.L. Kowalski and D. Feldman, J. Math. Phys. 4 (1963) 507.

56- G. Breit, Rev. Mod. Phys. 34 (1962) 766.

57- T. Fulton and P. Schwed, Phys. Rev. 115 (1959) 973
H.P. Noyes, Phys. Rev. Lett. 15 (1965) 538.

58- M.G. Fuda, Phys. Rev. C1 (1970) 1910.

59- E.M. Henley, "Charge independence and charge symmetry of nuclear forces" in Isopin in Nuclear Physics, D.H. Wilkinson ed.(North-Holland Publishing Co. 1969.)

60- A. Messiah, Quantum Mechanics (Interscience Publishers, Inc, New York, 1962), Vol. II.

61- M. Bolsterli, Phys. Rev. 182 (1969) 1095.

62- V.G. Neudatchin, J.T. Obukhovsky, V.I. Kukulin, and N.F. Golovanova, Phys. Rev. C11 (1975) 128.

63- K. McVoy, L. Heller and M. Bolsterli, Rev. Med. Phys. 39 (1967) 245.

64 Handbook of Mathematical Functions, edited by M. Abramowitz and I.A. Stegun. (Dover Publications, Inc., New York).

65- S.K. Mukhopadhyay, Ph.D. Thesis "Two Nucleon Reaction Matrix off the Energy-shell" 1970.

66- F. Tabakin, Ann. Phys. (N.Y.) 30 (1964) 51.

67- H.A. Bethe, B.H. Brandow and A.G. Petschek, Phys. Rev. 129 (1963) 225.

68- K.A. Brueckner and J.L. Gammel, Phys. Rev. 109 (1958) 1023.

69- H.S. Kohler and R.J. McCarthy, Nucl. Phys. A106 (1967) 313.

70- M.I. Haftel and F. Tabakin, Nucl. Phys. A158 (1970) 1.

71- R.J. McCarthy and K.T.R. Davies, Phys. Rev. C1 (1970) 1644.

72- K.T.R. Davies, S.J. Krieger and M. Baranger, Nucl. Phys. 84 (1966) 545.

73- R.J.W. Hodgson, Computer Phys. Communications 11 (1976) 113.

74- T.A. Brody and M. Moshinsky, Tables of Transformation Brackets Monografias del Instituto de Fisica, Mexico 1960.

75- C. Bloch and A. Messiah, Nucl. Phys. 39 (1962) 95.

76- D.W.L. Sprung, Invited paper at the International Conference on Atomic Masses, Winnipeg, August 1967.

77- H.W. Kao, Thesis.

78- P.M. Morse, Phys. Rev. 34 (1929) 57.

79- R.D. Amado, Phys. Rev. C2 (1970) 2439.

80- R. V. Reid, Ann. of Phys. (N.Y.) 50 (1968) 411.

81- T. Hamada and I. D. Johnston, Nucl. Phys. 34 (1962) 382.

82- E. L. Lomon and H. Feshbach, Ann. of Phys. (N.Y.) 48 (1968) 94

83- R. De Tourreil and D. W. L. Sprung, Nucl. Phys. A201 (1973) 193.